NASA-CR-159486
PWA-5615-3

NASA

STRAIN GAGE SYSTEM EVALUATION PROGRAM
FINAL REPORT

by

G. W. Dolleris, H. J. Mazur, and E. Kokoszka, Jr.

UNITED TECHNOLOGIES CORPORATION
PRATT & WHITNEY AIRCRAFT GROUP
COMMERCIAL PRODUCTS DIVISION

March 1979

Prepared for

NATIONAL AERONAUTICS AND SPACE ADMINISTRATION

Lewis Research Center
Contract NAS3-20298

PRATT & WHITNEY AIRCRAFT GROUP
Commercial Products Division

East Hartford, Connecticut 06108

T-10d

In reply please refer to:
GWD:BA - Eng. 2B
PWA-5615-3

March 23, 1979

To: National Aeronautics and Space Administration
Lewis Research Center
21000 Brookpark Road
Cleveland, Ohio 44135

Attention: Mr. John E. Dilley
Contract Section D
MS 500-305

Subject: Submittal of Final Report for the Strain Gage System Evaluation Program

Reference: (1) Contract NAS3-20298

(2) Letter: J. E. Dilley (NASA) to G. W. Dolleris (P&WA) dated January 24, 1979 (Ref. 1442)

Gentlemen:

The subject report has been modified in accordance with the Reference (2) letter and is being distributed in accordance with the contract requirements and the distribution list enclosed with the referenced letter.

Submittal of this report completes the requirements of the work under the Reference (1) contract.

Sincerely yours,

UNITED TECHNOLOGIES CORPORATION
Pratt & Whitney Aircraft Group
Commercial Products Division

George W. Dolleris
Program Manager

cc: Air Force Plant Representative Office
Pratt & Whitney Aircraft Group
East Hartford, Connecticut 06108

National Aeronautics and Space Administration
Lewis Research Center
21000 Brookpark Road
Cleveland, Ohio 44135
Attn: Mr. Raymond Holanda, Project Manager, MS 77-1

TABLE OF CONTENTS

TABLE OF CONTENTS (Continued)

LIST OF ILLUSTRATIONS

LIST OF TABLES

SECTION 1.0

SUMMARY

A two-phase, 25-month program was conducted to determine the reliability of various strain gage systems when applied to rotating compressor blades in aircraft gas turbine engines. A particular objective of the program was to identify those systems offering the highest reliability in the gas turbine engine environment. The work was conducted under National Aeronautics and Space Administration Contract NAS3-20298.

In Phase I, a survey of current technology strain gage systems was conducted. On the basis of this survey, those systems that appeared capable of meeting the program goals were identified. These systems were then reviewed by NASA and a total of seven systems were selected for testing.

Three different strain gage coating combinations were used. Two systems used flame-sprayed Rokide H or HT rod as the precoat and overcoat material and two systems used Plasmalloy 331-M powder. The other three systems used the Rokide H or HT rod as the precoat and overcoat, and used Bean H cement as an attachment coat for the gage and leadwires.

Two strain gage wires were used. Five systems used Nichrome V strain gages and two systems used platinum-8 percent tungsten gages.

Two leadwire materials were used. Five systems used Chromel P 36-gage lead wire and two systems used platinum-10 percent nickel 36-gage wire.

Three blade-to-disk jump wires were tested. One type, stranded nickel-plated copper wire with Kapton/Teflon insulation, was used only on four first stage systems. Its use was restricted to the first stage because of temperature limitations. Another type, bare 36-gage Chromel P wire, was used only on three third-stage systems. A third type, 28-gage Chromel/-Alumel duplex wire in Fiberglas/-asbestos insulation, was used on the remainder of the systems on both stages.

Testing was conducted on a NASA-owned F100 fan module. In preparation for the test, this module was disassembled, and the first- and third-stage blades were removed. Sixty of these blades were instrumented with strain gages with one gage per blade. Twenty of the blades were instrumented by NASA and forty by Pratt & Whitney Aircraft. The fan module was then reassembled for testing by NASA.

Testing and evaluation was conducted under Phase II. The fan module was mounted on F100 Engine 026 and the test program was run concurrent with an afterburner rumble test program at the NASA Lewis Research Center. Following testing, the fan module was returned to Pratt & Whitney Aircraft for a post-test examination.

A total of 19 of the 60 strain gages failed during 62 hours of engine operation, for a 68-percent survival rate. This is considered acceptable for a program of this duration.

Of the 19 failures, 16 occurred at blade-to-disk leadwire jumps (84 percent), two at a leadwire splice (11 percent), and one at a gage splice (5 percent).

Erosion was severe on the concave surface of the first stage blades, but no gage failures were attributed to erosion damage. Results indicated that Rokide rod, used as a precoat and overcoat, was the best material used in gage installations with respect to erosion resistance. Gages and leadwires should be located away from high erosion areas, if possible.

Erosion patches were used to evaluate the erosion characteristics of several materials and combinations. The combination of flame-sprayed aluminum oxide rod or powder coated with GA-60 epoxy cement proved to be highly erosion resistant.

Materials for this evaluation were chosen to withstand 316°C, eliminating the use of epoxy cements for gage installations. During testing, however, a maximum temperature of only 250°C was encountered. No temperature-related problems occurred.

G-loading reached about 40 kG for approximately 60 percent of the running time. No failures were attributed to this cause.

Strain levels were estimated to be in the 0 to $\pm$ 300 microstrain range, a value well within the endurance limit of these gage installations. No failures related to high stress levels were observed.

Jump failures were primarily attributed to the inadvertent coating of bare wire jumps with the epoxy cement used to secure the leadwires, and to the unexpected wicking of this cement by the asbestos-insulated jumps, reducing their flexibility.

Stranded 36-gage, nickel-plated copper wire with Teflon/Kapton insulation performed well as a jump material. Its use was limited by temperature to the first stage. The other jump materials performed well when not contaminated by epoxy cement.

SECTION 2.0

INTRODUCTION

An important part of any gas turbine engine development program is the determination of the operating vibratory stress characteristics of the blades and disks. Included is determination of the effects of speed and other operating parameters on the stress levels and frequencies of vibration to ensure that the blades and disks do not operate in regions of dangerously high levels of vibratory stress. The entire operating range of the engine must be surveyed to ensure safe operation.

The most practical method of determining these operating vibratory stress characteristics on compressor and turbine stages is to instrument the blades and disks with electric resistance strain gages attached directly to the parts. Leadwires from the gages are then routed out of the compressor or turbine assembly through a rotating data transmitting system to electronic monitoring and recording instrumentation. However, considerable difficulty has been encountered in satisfactorily implementing this approach because of the effect on the strain gage systems of the extremely hostile environment commonly encountered in such testing. Frequently, the result is system failure long before the test program can be completed, with consequent costly delays associated with re-instrumenting and re-building the engines and rigs.

The program described herein was undertaken with the following specific objectives:

1. To determine the state-of-the-art of strain gage systems for application to rotating compressor blades in aircraft gas turbine engines,

2. To identify those systems having the highest reliability, and

3. To identify failure mechanisms as a guide to future research and development efforts.

A goal of 90 percent reliability for a test of 50 hours duration was selected.

The following section, Section 3, describes the basic technical approach pursued for the program. This is followed in Section 4 by a description of the candidate strain gage systems and identification of the systems selected for evaluation in the subject program. Installation, test, and evaluation results are discussed in Section 5, and conclusions and recommendations are presented in Section 6. Detailed tabular data and photographs are presented in the appendices.

SECTION 3.0

TECHNICAL APPROACH

The program was conducted in two phases. In Phase I, strain gage system technology was reviewed, and the more promising systems were selected and applied to a test fan module. In Phase II, the fan module was tested in an F100 engine. The strain gage systems were then studied and evaluated.

In Phase I, Task 1, Pratt & Whitney Aircraft surveyed the state of current technology of compressor blade strain gage systems and selected the systems that appeared to be capable of meeting or approaching the performance goal of 90-percent reliability in fifty hours of operation under typical gas turbine engine environmental conditions. The selection involved consideration of the basic components of strain gage systems capable of being fabricated in a reproducible manner.

The results of the Phase I, Task 1 work were reviewed jointly by NASA and Pratt & Whitney Aircraft personnel in Phase I, Task 2. On the basis of this review, five strain gage systems were selected for installation by Pratt & Whitney Aircraft and two strain gage systems were selected for installation by NASA. In addition, it was decided to install erosion patches on some blades to evaluate erosion effects. A sequence and schedule was established for the strain gage and erosion patch installations.

In Phase I, Task 3, Pratt & Whitney Aircraft disassembled the F100 fan module and delivered 20 blades to NASA. NASA then installed the blade portion of their two strain gage systems and erosion patches on these blades and returned them to Pratt & Whitney Aircraft.

In Phase I, Task 4, Pratt & Whitney Aircraft installed their five strain gage system types and erosion patches on forty blades. The fan module was then reassembled with all seven systems and delivered to NASA for testing.

Phase II, Task 1, consisted of testing the instrumented fan module in a full scale F100 engine (Engine 026). Testing was conducted by NASA in conjunction with an afterburner rumble program.

The Phase II, Task 2, post-test examination was conducted by Pratt & Whitney Aircraft after disassembling the fan module. Each strain gage system and erosion patch was examined and its condition documented. The results were correlated with the test data obtained in Phase II, Task 1. The disassembled module was then packaged and returned to NASA.

Contract reporting was provided under Phase II, Task 3.

SECTION 4.0

SELECTION OF STRAIN GAGE SYSTEM CANDIDATES

4.1 TECHNOLOGY EVALUATION

A complete strain gage system consists of a surface preparation, bond coat, precoat, gage, lead-wire, splicing, attachment coat, overcoat, jumps, and trunk leads, as shown in Figure 1. There are a number of possible choices of material and techniques for each of these elements and selection of the appropriate material and techniques is based on consideration of the operating environment and gage location.

The operating conditions and related considerations used for the subject program were as follows:

(1) The compressor inlet gas temperature was assumed to be in the 177° to 316°C range with a minimum of 10 start-ups and shutdowns. The gas temperature for the shutdown portion of the cycle was assumed to be in the -18 to 65°C range. These selections were based on the fact that system durability depends on the length of time spent at elevated temperatures. Strain gage systems are subjected to differential thermal strains that are proprotional to both the temperature and the difference between expansion rates of the compressor blades and the strain gage system components. These strains can cause delamination, strain gage and weld joint

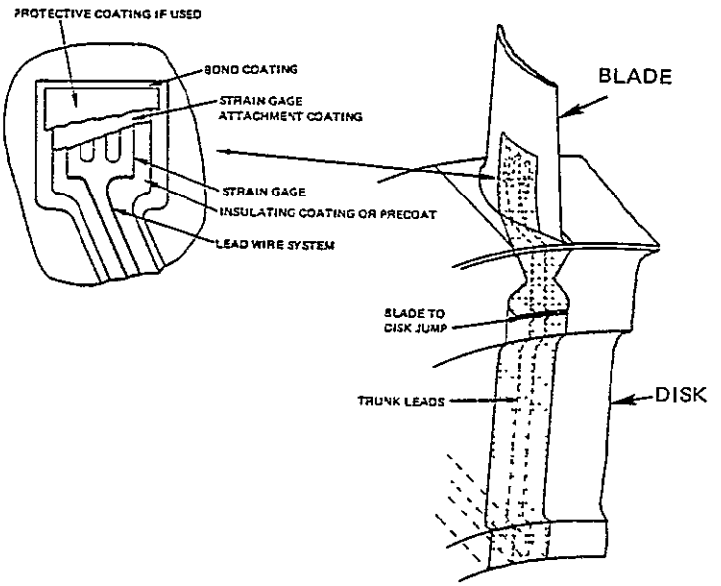

Figure 1 Typical Strain Gage Installation - A complete strain gage system consists of a surface preparation, bond coat, precoat, gage, lead-wire, splicing, overcoat, jumps, and trunk leads.

failures, and strain gage sensitivity changes.

(2) The compressor stage inlet total pressure was assumed to be in the 10130 to 202650 N/m^2 range.

(3) The rotational speed of the compressor was assumed to be such that the strain gages would be subjected to steady-state g-loadings up to 50,000 g with 50 percent of the running time at g-loadings above 40,000 g. High g-loading can cause separation of strain gage systems from the blade surface, failure of unsupported jumps, lead wire separation from the rotor, and shorting of leadwire conductors through the insulation.

(4) A specific range of overall compressor vibration was not specified (although vibration was monitored during the test program using accelerometers capable of measuring up to 10 g's in any or all axes over a frequency range of 100 to 300 Hz.) Fatigue failure of strain gage and leadwire joints can be caused by high blade vibration.

(5) The strain gages were required to withstand a minimum of 25 compressor accelerations and decelerations between idle and maximum speed since fatigue failure can also be caused by repeated speed cycling of the compressor. Thermal shock occurs when the compressor is rapidly accelerated and decelerated and this thermal shock can cause delamination and flaking of the coating.

(6) Erosion conditions were not specified, but it was recognized that erosion resistance is required because of the erosive particles present in many test facilities as a result of dirt and rust entrained in the inlet flow. (The test program included erosion patches to monitor the erosion sensitivity of candidate materials.)

To provide a basis for making these selections, the initial effort conducted under the contract consisted of an evaluation of available strain gage technology. Candidates for evaluation were selected on the basis of Pratt & Whitney Aircraft experience and by consultations with Mr. Peter K. Stein of Stein Engineering Services and Mr. Stephen P. Wnuk, Jr., of Hitec Corporation, both recognized leaders in strain gage instrumentation technology.

The evaluation was divided into several major areas, namely:

1. Surface Preparation
2. Bond Coatings
3. Precoats
4. Gages
5. Gage Splices
6. Attachment Coating and Over coat
7. Leadwire
8. Jump and Splice Area
9. Trunk Leads

The results of this evaluation for each of these areas are discussed in the following paragraphs.

4.1.1 Surface Preparation

The cements used to bond strain gages to the parent material require some type of surface preparation. For some low temperature applications, cleaning the surface with solvents only may be practical. However, in most cases, and particularly for high temperature applications, the surface must be degreased and roughened, in addition to being cleaned with a solvent.

Degreasing - All new parts should be degreased and baked before grit blasting. The process for titanium parts consists of baking the parts for 20 to 30 minutes at 10°C above the planned test temperature or 200°C, whichever is higher.

Surface Roughening - Grit blasting is then used to clean and roughen the surface that will be instrumented. The abrasive is forcibly propelled using a stream of high-pressure air. Depending on the type of abrasive, the process either rearranges or removes the surface material.

The type of abrasive used depends on the requirements of the operations and the hardness of the material being blasted. Aluminum oxide abrasives provide the best surface preparation for most metals, but certain groups of hard materials require the use of silicon carbide to yield a satisfactory surface. Both preparations provide an excellent bonding surface for aluminum oxide flame spray precoats.

The desired surface finish is achieved by selecting the appropriate grit size, impingement angle, and pressure. The following surface preparations are commonly used for titanium, nickel, and nickel-steel alloys:

A. #30 grit Al_2O_3 when using flame sprayed precoats of aluminum oxide. This results in a surface finish with a roughness of 3.00 micrometers, rms.

B. #60 grit Al_2O_3 when using ceramic cement precoats and epoxies. This results in a surface finish with a roughness of 5.00 micrometers, rms.

C. #120 grit Al_2O_3 when using nickel-aluminum bond coats and epoxies. This results in a surface finish with a roughness of 9.50 micrometers, rms.

Correct air pressure is one of the most important grit blasting parameters. For aluminum oxide and silicon carbide abrasives, the air pressure is typically in the range of 2 to 3.4 atm. These pressures are somewhat lower than those for other commonly used abrasives because of the superior cutting characteristics of the aluminum oxide and silicon carbide materials. The value actually selected is, in part, dependent on the type of blasting equipment being used.

The angle at which the abrasive strikes the part is also important. For maximum cutting rate and roughness, which is desirable for adhesion and bonding, a 45° impingement angle is used. At this angle, the fast cutting abilities of manufactured abrasives enable the individual particles to penetrate, suitably roughening the

surface, and removing minute particles of dirt and contaminants. It is the elimination of these small particles that enhances the bonding of the various coatings.

Finally, to obtain the most uniform results, the distance between the blasting nozzle and the part should be controlled. Generally, a distance of 15 to 30 cm is used.

Cleaning - The selection of the best solvent obviously depends on the particular material being cleaned. Typical solvents used for gas turbine engine hardware are acetone, alcohol, and methyl ethyl ketone.

4.1.2 Bond Coatings

Bond coatings improve adherence and are particularly important for applications where grit blasting is difficult or impractical. In theory, the bond coating can be applied directly to a clean surface; however, Pratt & Whitney Aircraft experience indicates that the surface should be roughened to achieve maximum bond strength.

Two types of bond coatings are in general use: Metco 450 (nickel-aluminum powder) and Metco 443 (nickel-chromium-aluminum powder). The manufacturer recommends that Metco 450 material be used for applications up to 815°C, while Metco 443 material is recommended for use up to 982°C. Pratt & Whitney Aircraft experience indicates that these temperatures are conservative. Higher temperature operation has been successful, but excessive temperatures result in oxidation. Of the two materials, Pratt & Whitney Aircraft experience has demonstrated that Metco 443 is more difficult to flame spray. Improper flame spraying results in poor bonding to the parent material.

Certain application procedures should be adhered to when flame spraying a Metco bond coating. The surface to be coated should be kept clean and should be roughened, if possible, to increase the bond strength. This may be accomplished by cross-hatching the surface with aluminum oxide grit paper or grit blasting with #120 grit aluminum oxide and then cleaning the surface with a solvent.

A properly applied coating should be approximately 0.05 to 0.07 mm thick and have a surface finish equivalent to a surface grit blasted with #30 grit aluminum oxide.

Metco bond coatings have been found to degrade the fatigue life of some parent metals. Testing of titanium airfoils has indicated that a 20 percent reduction in fatigue life might occur. However, these tests did include a precoat of aluminum oxide in addition to the Metco 443 bond coating, precluding clear identification of the effects of the Metco bond coating alone.

Two other comments should be made concerning Metco coatings. First, the coatings are generally very difficult to remove. Grinding or machining is the most effective technique for coating removal. Secondly, the coatings are subject to contamination, requiring that additional gage installation steps

be performed immediately following application of the Metco coating.

In deciding whether or not a bond coating is to be used, it should be remembered that the use of a bond coating or the addition of any material to the airfoil may affect the frequency response of the airfoil.

4.1.3 Precoats

The study of precoats was limited to ceramic cements and flame sprayed aluminum oxides. Epoxy and polyimide cements were considered but eliminated early in the program. The epoxy cements were eliminated because of their inability to meet the program requirement of operating at a temperature of 316°C for periods up to fifty hours. Polyimide cements could survive the 316°C temperature but were rejected because they are extremely difficult to use and Pratt & Whitney Aircraft's limited experience with these materials indicated that successful results might not be obtained for this program.

Ceramic Cements - Ceramic cements considered were SermeTel P-1 and PBX, BLH CER-1000 and 1200, Bean H, and Micro-Measurements GA-100. The criteria used to determine the suitability of each of these products included ease of application, type and ease of curing, fatigue strength, electrical resistance at high temperature, and tolerance to thermal shock. P-1 was considered as good as, or better than, the other ceramic cements in all of these categories, and as a result was given primary consideration.

Flame Sprayed Aluminum Oxides - Flame sprayed aluminum oxides are considered to be superior to the ceramic cements in erosion resistance and are capable of 1 percent elongation, as compared with 1/2 percent for the ceramic cements. In addition, flame sprayed installations have the advantage of not requiring a bake cycle to cure the cement. Commonly used flame sprayed materials are Plasmadyne Plasmalloy 331-M aluminum oxide powder and Rokide Type S, Type H, or Type HT aluminum oxide rod.

The Plasmadyne powder has good insulation properties up to 760°C, and good bonding properties up to 982°C. It also offers good thermal shock resistance and good erosion properties up to this temperature. It has the added benefit of being easier to apply than the other candidates because of the lighter weight and smaller size of the Hitec flame spraying equipment used.

The Rokide S rod is best suited for use below 537°C. It has qualities similar to the Plasmadyne system but is more difficult to use.

The Rokide H or HT rod is suitable for use up to 982°C and offers greater resistance to erosion than the Plasmadyne powder or the Rokide S rod.

Some technicians find the Rokide rod more difficult to apply than the Plasmadyne powder. There are several types of Rokide flame spray systems, including a fixed system with a spray booth and a portable unit for parts that are

not amenable to spraying in a booth. However, the Rokide spray gun is heavier and even the portable system is not as convenient as the Hitec powder flame spray system. In addition, the Rokide equipment must be continually serviced to maintain good quality and operation of the equipment requires a more experienced technician.

It should be noted that both the ceramic cements and the flame sprayed aluminum oxide materials are susceptible to moisture absorption and contamination. Once application has been started, the parts should be completed as soon as possible to avoid contamination and subsequent delamination.

A complete summary of bonding materials is presented in Table I.

4.1.4 Gages

Strain gages are categorized by type (wire or foil), size, and strain sensing material.

Type - Although foil gages may be installed using flame spray or ceramic cements, they are not recommended procedures because the large conductor area that must be coated results in poor gage bonding. For this reason, the current study was restricted to wire wound gages.

Size - Strain gages come in various shapes and sizes. The selection is usually dependent on the location and size of the part being tested.

Typical gage materials can be drawn into wires with diameters in the range of 0.001 cm to 0.0025 cm, permitting strain gages with a grid size down to 0.080 cm in length to be produced.

Strain Sensing Material - Platinum-tungsten and nickel-chrome wires are commonly used for winding high temperature dynamic strain gages.

Platinum-tungsten has a high gage factor (4 or better), but is non-linear in high strain fields. Past experience has also indicated that the fatigue life of platinum-tungsten wire is significantly reduced when installed on a parent metal with a different coefficient of thermal expansion. Although this does not present a problem for titanium components, another gage material would be more suitable for nickel base steels. At Pratt & Whitney Aircraft, platinum-tungsten gages are generally used only for very high temperature applications between 760°C and 982°C.

Three types of nickel-chrome wire alloys are available commercially for strain gage applications. These are Evanohm S, Karma, and Nichrome V. Material compositions for these products are presented in Table II.

The compositions of Karma and Evanohm S are very similar and they may be considered to be essentially equivalent products. Both Evanohm S and Nichrome V have performed well in the past for Pratt & Whitney Aircraft.

4.1.5 Gage Splice

The leadwire-to-strain gage attachment area is critical to the durability of a strain gage

TABLE I

SUMMARY OF BONDING MATERIAL CANDIDATES

Name	Type	Temperature Limit for 50 Hours (°C)	Normal Use
INORGANIC MATERIALS			
Serma Bond	Ceramic Cement	816	Strain gages and leadwires
CER1200	Ceramic Cement	816	Strain gages and leadwires
M-Bond GA-100	Ceramic Cement	704	Strain gages and leadwires
Rokide S	Al_2O_3 Flame Spray	538	Strain gages and leadwires
Rokide H	Al_2O_3 Flame Spray	982	Strain gages and leadwires
Plasmalloy 331-M	Al_2O_3 Flame Spray	538	Strain gages and leadwires
Metco 450	Nickel-Aluminum	927	Surface protection from oxidation and spot welding
Metco 443	Nickel-Chromium-Aluminum	982	Substitute for grit blasting
ORGANIC MATERIALS			
EPY 400-600	Epoxy	260	Strain gages and leadwires
M-Bond GA-60	Epoxy	260	Strain gages and leadwires
Mithra 200	Epoxy	260	Strain gages and leadwires
PLD-700	Polyimide	316	Strain gages and leadwires
M-Bond 600	Epoxy	260	Strain gages
M-Bond 610	Epoxy	260	Strain gages

TABLE II

COMPOSITION OF CANDIDATE STRAIN GAGE MATERIALS

	Evanohm S	Karma	Nichrome V
Nickel(%)	75	73	80
Chromium(%)	20	20	20
Copper and Aluminum(%)	5		
Iron and Aluminum(%)		7	

system. In addition to the problem of attaching two metallurgically different wires of different sizes, the junction must withstand strains similar to those being measured. Large wire is desirable from the standpoint of handling, welding, and electrical resistance, while small wire is desirable from the bonding and routing standpoint.

A wide variety of techniques have been used to attach the leadwire or ribbon to the strain gage wire. Specific techniques evaluated at Pratt & Whitney Aircraft have included various combinations of tweezer (capacitance discharge) welds, soldering, and brazing. The best results to date have been obtained using a parallel gap welder. The leads are attached by crossing the gage wire and the leadwire and welding the two together. This technique has consistently produced the most reliable splices.

4.1.6 Attachment Coating and Overcoat

After the strain gage and extension leadwires are positioned, the strain gage attachment coating is applied to encapsulate and bond the gage to the precoat. Usually, the same material as the precoat is used. However, composite installations can be used if the gage environment permits such use. A ceramic cement bond coat would be used for the gage and leadwire between a flamesprayed precoat and overcoat. It is particularly important when applying any attachment coating to avoid excessive buildup of material because this will adversely affect the aerodynamic and aeroelastic performance of the engine component and could cause premature failure of the strain gage system.

When choosing an attachment coating, the primary considerations are adherence ability, thickness, and erosion resistance. The primary candidates considered in this study were:

1. Bean Type H Cement
2. SermeTel P-1 Cement
3. Plasmadyne Plasmalloy 331-M Aluminum Oxide Powder

4. Rokide H Aluminum Oxide Rod

5. Rokide S Aluminum Oxide Rod

Bean type H cement is a pre-mixed ceramic cement which employs aluminum phosphate as a binder. It has found wide acceptance for the application of high temperature strain gages and thermocouples. The cement may also be used as a general purpose ceramic coating to improve oxidation resistance of metals at temperatures up to 880°C. It has very good electrical insulating properties at temperatures up to 982°C.

SermeTel P-1 cement is a fully inorganic cement for use in severe environmental conditions. This material is supplied in a two-component mix to extend the life of the material prior to use. It bonds well to most metals, has a low shrinkage factor, and has a low thermal expansion coefficient. SermeTel P-1 can be applied in a very thin coating, resulting in a total installation thickness of only 0.4 mm. However, this material is not as durable with respect to erosion as a flame sprayed coating and requires a minimum cure cycle of 316°C. SermeTel P-1 has the advantage of not being as susceptible to surface contamination as the aluminum oxide flame sprayed coatings.

Plasmadyne 331-M powder is an aluminum oxide material for flame spraying. It is 99.53 percent aluminum oxide, 0.04 percent silicon oxide, 0.01 percent iron oxide, and 0.33 percent sodium oxide. The Plasmadyne Plasmalloy 331-M aluminum oxide powder also can be applied in a very thin coating, resulting in a total installation thickness of 0.4 mm. However, contamination of the precoating caused by the environment, handling, or tape residue can cause delamination between the precoating and the attachment coating. The parts must, therefore, be handled carefully and once an installation has been started, it should be completed as soon as possible. It is recommended for gages and leadwork at temperatures up to 760°C in areas that are not subject to extreme erosion.

Rokide, a trademark of the Norton Company, is an aluminum oxide material supplied in rod form for flame spraying. Rokide S rod is composed of 98 percent aluminum oxide, 0.58 percent silicon oxide, and 1.42 percent of other materials. It is recommended for gages and leadwork at temperatures below 540°C. Rokide H rod is composed of 97 percent aluminum oxide, 2.5 percent silicon oxide, and 0.5 percent of other materials. BLH Electronics sells H rod and recommends its use up to 760°C. Hitec sells Rokide rod as HT rod with a composition of 98 percent aluminum oxide and 2 percent silicon oxide. Rokide H and HT rod has been used successfully at Pratt & Whitney Aircraft at temperatures up to 982°C.

The Rokide H, HT, and S aluminum oxide rod materials are much more difficult to use than powder and more technician experience is required if a total installation thickness of 0.4 mm is to be achieved.

The same contamination problems that exist with the Plasmadyne

powder exist with Rokide. Once the installation has been started, it should be completed without delay, with emphasis placed on keeping the parts clean and the installation thin.

4.1.7 Leadwire System

Failure in the leadwire system is a major cause of strain gage system malfunctions in gas turbine engine tests. The difficulties result from the need to compromise between the leadwire structural requirements and the engine aerodynamic and aeroelastic restrictions. These compromises vary among the airfoils, platforms, and blade roots because of the differences in hardware reoperation needed, performance considerations, blade-to-disk movement, and stress concentrations produced by hardware reoperation and strap welding.

Small leadwires must be used in the airstream to minimize the effects of the installation on the airfoil resonant frequencies and aerodynamic characteristics. The wire should also have good fatigue strength and low electrical resistance. Three types of leadwires were suggested: Chromel P, Nichrome V, and platinum-nickel. Pratt & Whitney Aircraft uses Chromel P almost exclusively for high temperature dynamic strain gage systems.

Uninsulated 36 gage Chromel P wire has good fatigue life characteristics, can be spliced to the gage with relative ease, and can be soldered, brazed, or resistance welded to trunk leads for routing out of the engine. The electrical resistance is approximately 0.590 ohm/cm. Forty gage uninsulated wire provides a smaller installation thickness, but the resistance is much higher (1.44 ohm/cm). Although the resistance of the 36 gage material is substantially higher than that of such alternate materials as nickel clad copper (0.0032 ohm/cm), nickel (0.065 ohm/cm), or Alumel (0.23 ohm/cm), these alternate materials have poor fatigue resistance at elevated temperatures.

Nichrome V has the same desirable fatigue resistance as Chromel P and is also easily attached to both the gage and the trunk leads. However, this material has an electrical resistance of approximately 0.92 ohm/cm for 36-gage wire. If the installation requires long leads, desensitization of the strain gage can become significant.

Platinum-nickel wire is still in the testing phase but laboratory test results and actual engine test results at Pratt & Whitney Aircraft indicate that its fatigue life is superior to that of both Chromel P and Nichrome V wire. The use of convoluted or sinusoidally formed wire also offers the potential of improving fatigue life.

4.1.8 Jump/Splice Area

A very critical area for leadwire routing is the attachment of the blade to the disk. If the blade must be free to move, small jumps of unbonded wire must be used to allow for this movement. The wire must tolerate the consequent bending, and unbonded wire in a high acceleration g field can cause peel failures in adjacent bonding material. These bare wire jumps are also very vulnerable to

erosion and foreign object damage. In some cases where erosion is a serious problem or blade movement is large, unusual leadwire schemes have been used. Many of the problems associated with bare wire jumps can be eliminated through the use of slotting and strap welding techniques, which then permit the use of Fiberglas-insulated wire or sheathed wires.

Pratt & Whitney Aircraft has generally taken a conservative approach in solving this problem and has used uninsulated 36-gage wire to make this jump. Uninsulated wire is required because the ceramic cements do not have adequate strength to hold the larger Fiberglas insulated wires or sheathed wires to the hardware during high g loading.

Consultation with Messrs S. P. Wnuk and P. K. Stein has indicated that other major strain gage installers use some type of slotting or welding technique to hold the leadwires in place. This permits the use of larger, more durable wires. Pratt & Whitney Aircraft has investigated some of these approaches in aircraft engine applications. The major objection to using such devices as slots or straps is that they require changes or modifications to the engine parts that reduce their operating lives.

4.1.9 Trunk Leads

Trunk leads are used to carry the strain gage signals from the leadwires to the front compressor hub. Once out of the high temperature portion of the compressor, alternate insulation materials offering higher durability can be used. Typical materials for this application include Fiberglas and polyimide. It is still important to accommodate high g loading, and, therefore, care must be taken to route the trunk leads along inside surfaces where the bonding system will be in compression.

In the case of low-pressure compressor work, the trunk leads are stranded nickel-plated copper alloy 32 gage wire with Kapton/-Teflon insulation. This wire is sufficiently flexible to facilitate routing and is also capable of withstanding the low-pressure compressor environment if adequately supported.

Splices are occasionally required in the trunk lead system, and where these occur, adequate support and protection must be provided.

It should be noted that the temperatures in the low-presssure compressor are sufficiently low to permit the use of epoxy cements to secure the trunk leads.

A complete manufacturers summary is presented in Appendix G listing those items and materials that were considered as candidates or used in actual system installations.

4.2 SYSTEM SELECTION

The selection process began by defining the individual components of a strain gage system. The various possible materials that could be used to fabricate each component were ranked in order of estimated reliability based on an F100 fan application. Temperature, pressure, g level, erosion, stress level, size, time, and vibration characteristics all influenced the

selection process. The resulting ranking is shown in Table III.

The selection of specific systems was based on the reasoning that the largest uncertainty of component reliability was in the coatings and the jumps. These two components varied from system to system for the five systems selected to be installed by Pratt & Whitney Aircraft. Two systems were selected by NASA to be installed with additional component variation, although several of the components did remain the same. A total of seven systems were selected and these are summarized in Table IV.

The strain gages were mounted on both the first and third stages for a satisfactory evaluation. The first stage was included to provide an environment subject to erosion and to permit evaluation at relatively low pressures. The third stage was chosen because this stage operates at the highest temperature conditions in the fan. The distribution of the strain gage systems among the blades and stages is shown in Appendix F. Only one gage was installed on each blade to maximize reliability and minimize fabrication problems. Twenty gages were mounted on the first stage and forty on the third stage.

The locations chosen for strain gage placement were the above-shroud, maximum thickness, convex side, and the above-shroud, trailing edge, concave side. Only two locations were chosen to minimize the number of variables involved in this test. The locations chosen are typical of those currently used in test programs. The locations are shown in Figures 2 and 3.

Erosion patches designed to monitor the erosion characteristics of the gas stream and to determine the erosion resistance characteristics of various materials were selected and installed at the locations shown in Appendix F. NASA installed several erosion patches on the first stage blades in the shape of typical gage installations. Pratt & Whitney Aircraft installed erosion patches on some of the instrumented blades on the side opposite the gage systems. This resulted in patches being installed on both sides of the blades as shown in Figures 4 and 5. In general, the patches were made with ceramic cement as well as aluminum oxides except for three epoxy installations. The plan provided that if any other promising materials were found, they would be added to the group. The patches were scattered over a wide variety of locations on the blades to get a complete map of erosion patterns.

TABLE III

STRAIN GAGE SYSTEM COMPONENTS RANKED IN ORDER OF PERFORMANCE FOR F100 FAN APPLICATIONS

Surface Preparation

1. Grit blasting - #120 grit Al_2O_3

Bond Coating

1. Metco 450

Precoating

1. Rokide H (or HT) rod
2. Plasmalloy 331-M powder
3. Rokide S rod
4. SermeTel P-1 ceramic cement

Gage Wire

1. Nichrome V
2. Evanohm S - Karma
3. Platinum-Tungsten

Gage Size

0.79 cm x 0.24 cm
BLH HT-1212-2A - 0.32 cm x 0.16 cm
BLH HT-1212-5A - 0.79 cm x 0.24 cm

Attachment Coating and Overcoat

1. Rokide H (or HT) rod*
2. Plasmalloy 331-M powder*
3. Rokide S rod*
4. SermeTel P-1 ceramic cement
5. Bean H Cement

Leadwire

1. Chromel P (35 gage)
2. Platinum - 10 percent Nickel
   (36 gage with BLH HT-1212-5A strain gage)
   (40 gage with BLH HT-1212-2A strain gage)
3. Nichrome V (36 gage)

Blade-to-Disk Jump (First Stage)

1. Stranded nickel-plated copper - 32 gage - Kapton/Teflon insulation

2. Chromel/Alumel - 28 gage duplex - Fiberglas/Asbestos Insulation

Blade-to-Disk Jump (Third Stage)

1. Chromel/Alumel - 28 gage duplex - Fiberglas/Asbestos Insulation
2. Chromel P (35 gage)
3. Chromel/Alumel 34-gage, mineral-insulated, metal-sheathed wire

* In composite installations, a ceramic cement such as Bean H is also used in the gage attachment process. The cement is used as a finish coat in the precoat and as an attachment coat for the gage and leads prior to application of an overcoat.

TABLE IV

SELECTED STRAIN GAGE SYSTEMS

COMPONENT	STRAIN GAGE SYSTEM						
	P&WA SYSTEMS					NASA SYSTEMS	
	1	2	3	4	5	6	7
Surface Preparation	Grit Blast-#120 grit Al_2O_3	Same as 1	Same as 1	Same as 1	Same as 1	Same as 1	Same as 1
Bond Coating	Metco 450	Same as 1	Same as 1	Same as 1	Same as 1	Same as 1	Same as 1
Precoat and Overcoat	Flame sprayed Rokide H (or HT) rod	Same as 1	Flame sprayed Plasmalloy 331-M powder	Same as 3	Same as 1 with Bean H cement	Same as 5	Same as 5
Strain Gage Wire	Nichrome V - P&WA Wound 0.79 cm x 0.24 cm	Same as 1	Same as 1	Same as 1	Same as 1	Platinum Tungsten BLH HT-1212-5A at Location A BLH HT-1212-2A at Location B	Same as 6
Lead Wire	Chromel P 36 gage	Same as 1	Same as 1	Same as 1	Same as 1	PT-Ni 36 gage	PT-Ni (40 gage on first stage and 36 gage on third stage)
Blade-to-Disk Jump (first-stage)	Stranded Nickel-Plated Copper-32 gage- Kapton/ Teflon insulation	Chromel/Alumel 28 gage duplex-Fiberglas/Asbestos insulation	Same as 1	Same as 2	Same as 1	Same as 2	Same as 1
Blade-to-Disk Jump (third-stage)	Chromel/Alumel 28 gage duplex Fiberglas/Asbestos insulation	Chromel P 36-gage	Same as 1	Same as 2	Same as 1	Same as 1	Same as 2

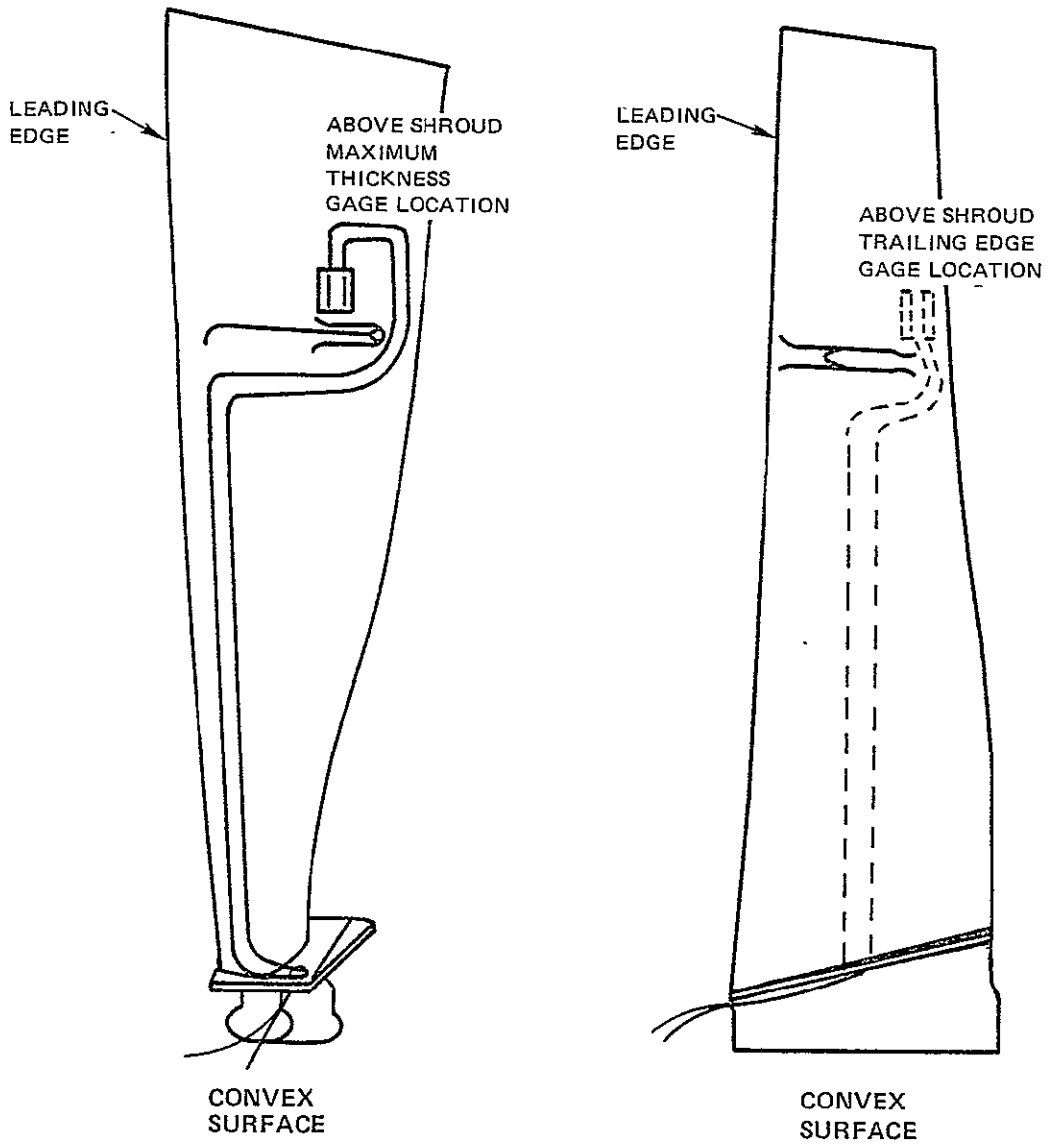

Figure 2 Strain Gage and Leadwire Locations for First-Stage Blades - Only two locations, both representative of typical mounting points currently used in test programs, were chosen to minimize the number of variables involved in this test.

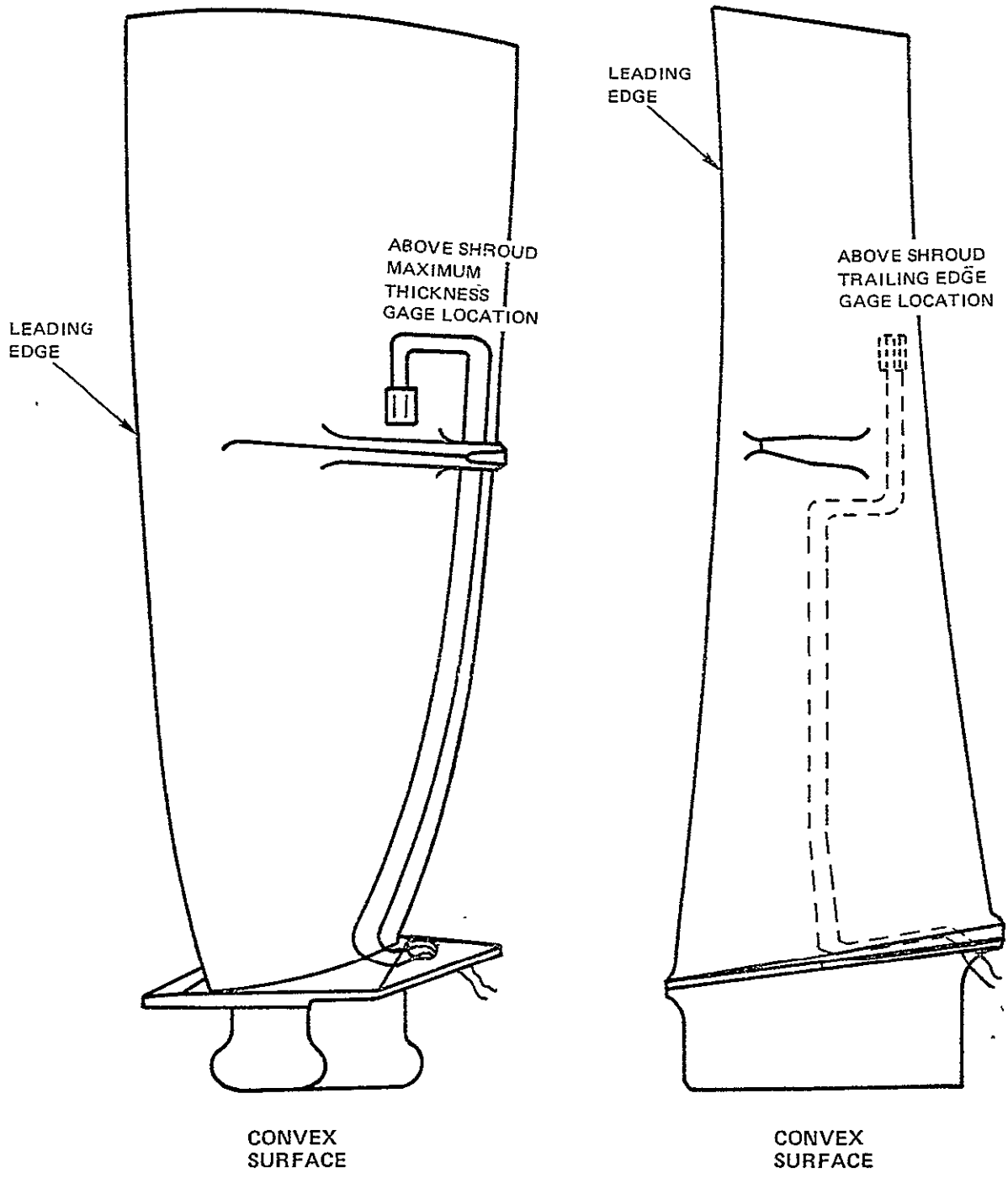

Figure 3 Strain Gage and Leadwire Locations for Third-Stage Blades - Third-stage blade installations were essentially identical to the first-stage blade installations.

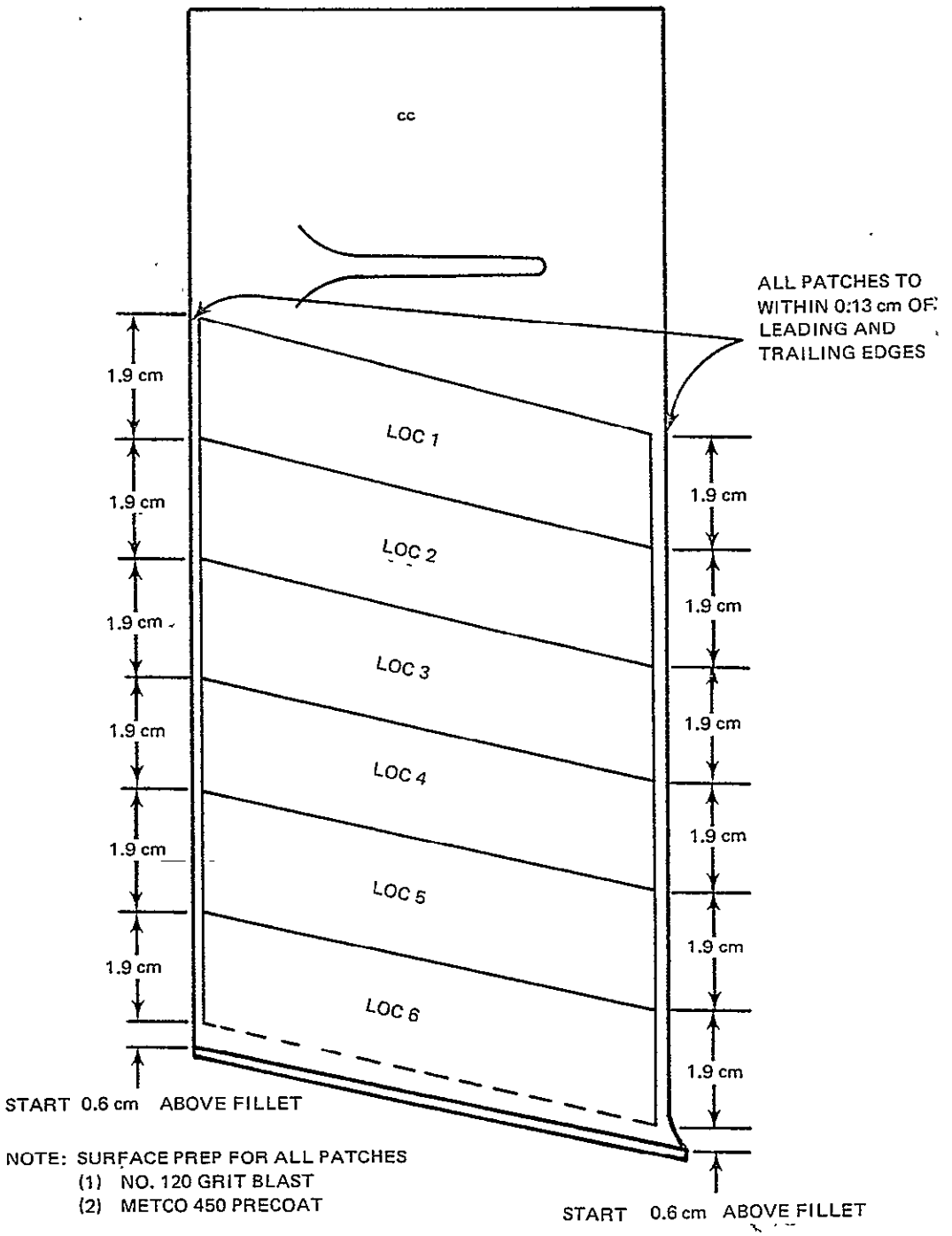

Figure 4 Pratt & Whitney Aircraft Erosion Patch Installations for First-Stage Blades - The patches were installed in strips with a surface preparation consisting of grit blasting with #120 grit followed by a Metco 450 precoat. The patches are described in detail in Appendix E.

SKETCH #2

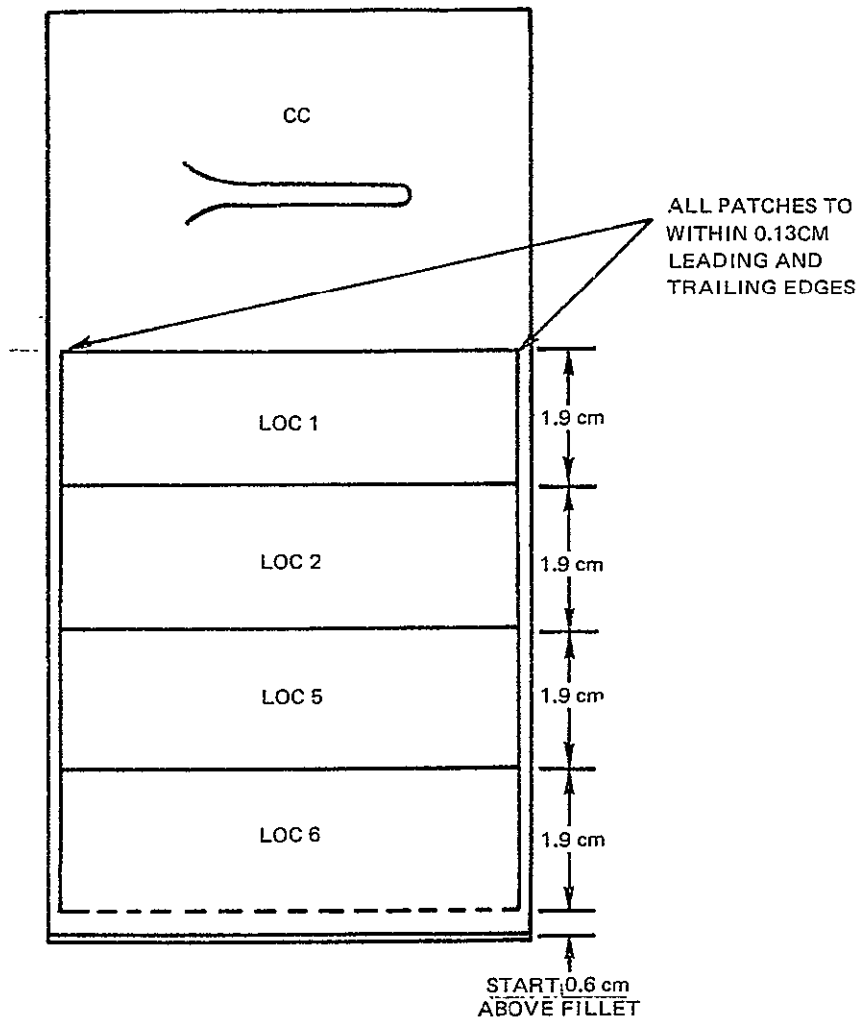

NOTE: SURFACE PREP FOR ALL PATCHES
(1) NO. 120 GRIT BLAST
(2) METCO 450 PRE-COAT

Figure 5 Pratt & Whitney Aircraft Erosion Patch Installations for Third-Stage Blades - The procedure used for the third-stage blades was identical to that for the first-stage blades. The patches are described in detail in Appendix E.

SECTION 5.0

INSTALLATION, TEST, EVALUATION

5.1 STRAIN GAGE AND EROSION PATCH INSTALLATION

5.1.1 Strain Gage Application Procedure for Pratt & Whitney Aircraft Installations

Each system used the same general strain gage application procedure. Each system used a common surface preparation, bond coating, strain gage wire installation, and leadwire installation. Variations occurred in the precoat, attachment coat, overcoat, and blade-to-disk jumps.

Surface Preparation - For all systems installed by Pratt & Whitney Aircraft, the hardware was baked at 340°C for 30 minutes to remove any oil contaminants.

Airfoil thickness measurements were then taken at various locations identified through templates using calipers and a dial indicator. The locations for thickness measurements are shown in Figures 6 and 7. The dimensions were recorded on a summary sheet.

The strain gage and leadwire areas were then masked using 3M #470 yellow pressure sensitive tape. These areas were then grit blasted using #120 grit aluminum oxide and blown clean with dry nitrogen.

Final inspection following the surface preparation procedure consisted of inspection under a microscope to verify that the proper surface preparation had been performed, and airfoil thickness measurements using the same procedures mentioned previously.

Bond Coating - Bond coatings were applied to all systems. BLH Rokide tape was used to mask the area around the gage and the leadwire area in preparation for application of the Metco 450 precoat. The tape exposed an area approximately 0.25 cm smaller in each direction than the grit blasted area. A 0.05 to 0.07 mm thick coating of Metco 450 was then applied to the masked area.

Inspection consisted of both microscopic examination to verify that an even coat had been applied, and airfoil thickness measurements.

Precoating - In preparation for precoating, the gage and leadwire areas were masked using BLH Rokide tape. The masking overlapped the Metco 450 bond coating by at least 0.13 cm.

Systems 1, 2, and 5 were coated using flame sprayed Rokide HT rod to produce a 0.05 to 0.07 mm thick coating. The coating was then inspected under a microscope to verify that a uniform coating of adequate thickness had been achieved. In addition, airfoil thickness measurements were again taken.

The precoat for Systems 3 and 4 were similar to those for Systems 1 and 2 except that flame sprayed Plasmalloy 331-M powder was used instead of flame sprayed Rokide HT rod.

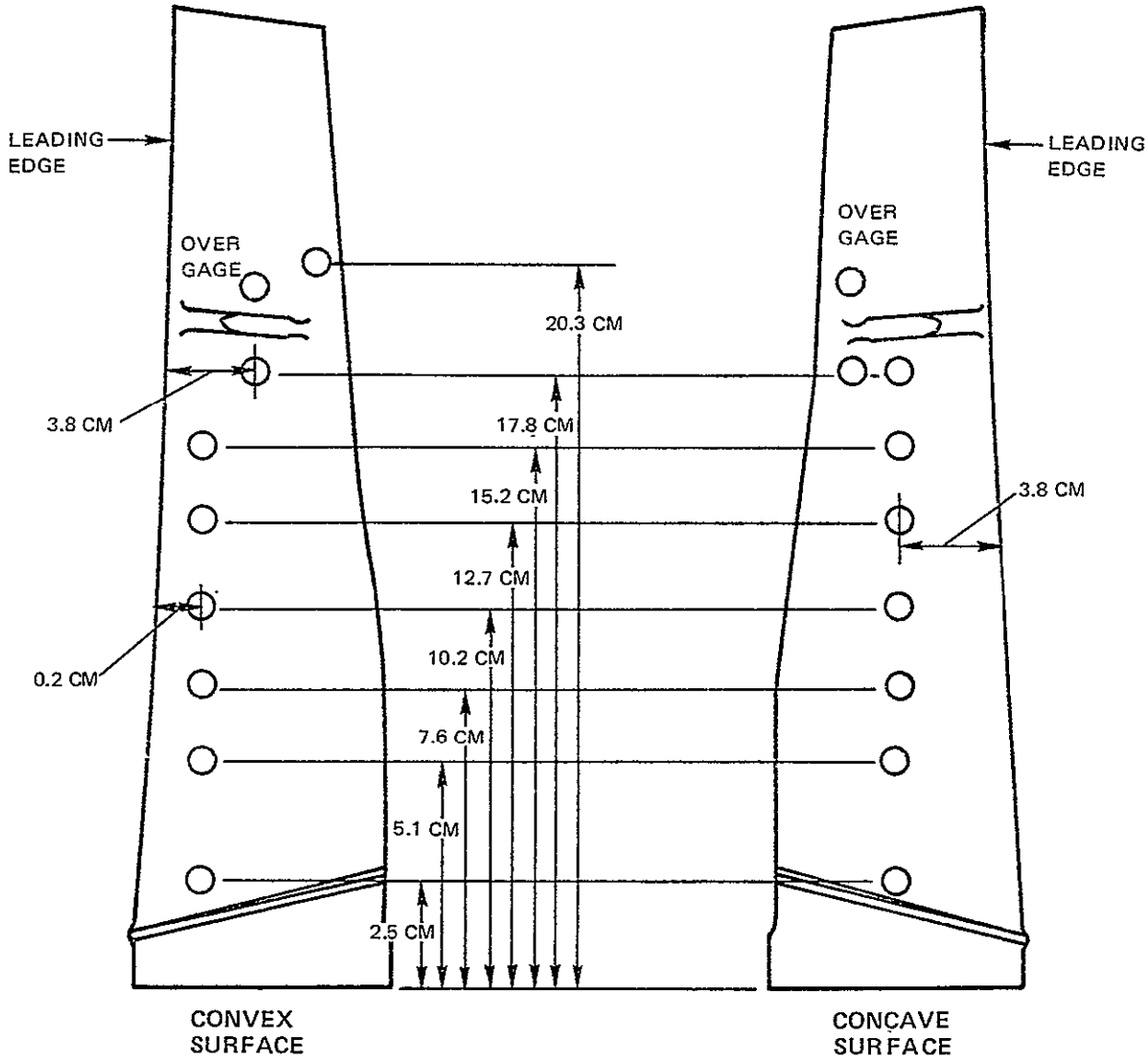

Figure 6 Locations for Thickness Measurements for the First Stage - Airfoil thickness measurements were then taken at various locations identified through templates using calipers and a dial indicator.

Strain Gage Wire Installation - All strain gages installed by Pratt & Whitney Aircraft were wound using 0.0019 cm diameter Nichrome V wire. The winding produced a grid size of 0.79 cm x 0.24 cm. A standard leadwire configuration was used, and is shown in Figure 8. The strain gage was then taped in position with BLH tape and inspected with a microscope to ensure that the gage was in intimate contact with the precoat.

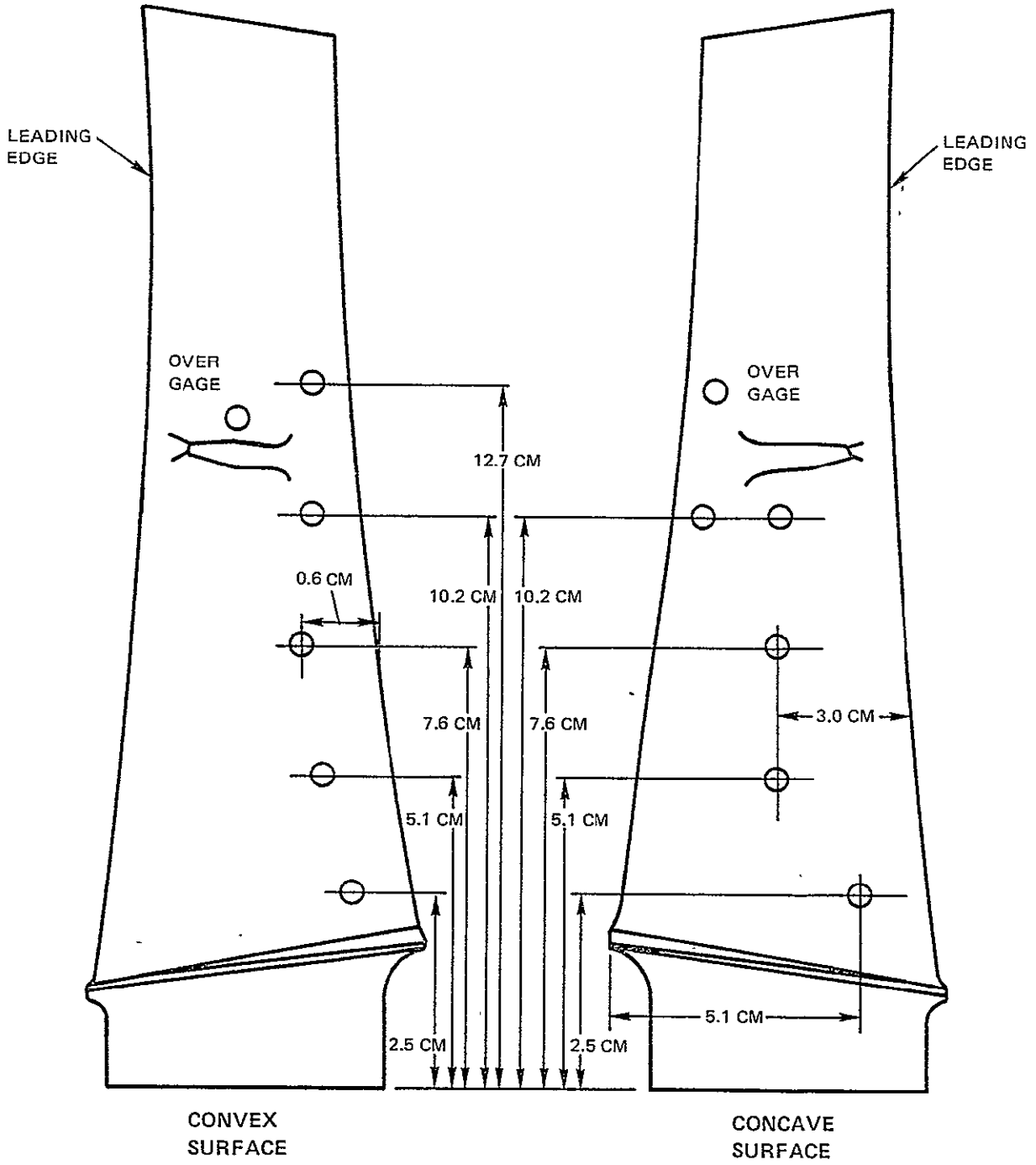

Figure 7 Locations for Thickness Measurements for the Third Stage

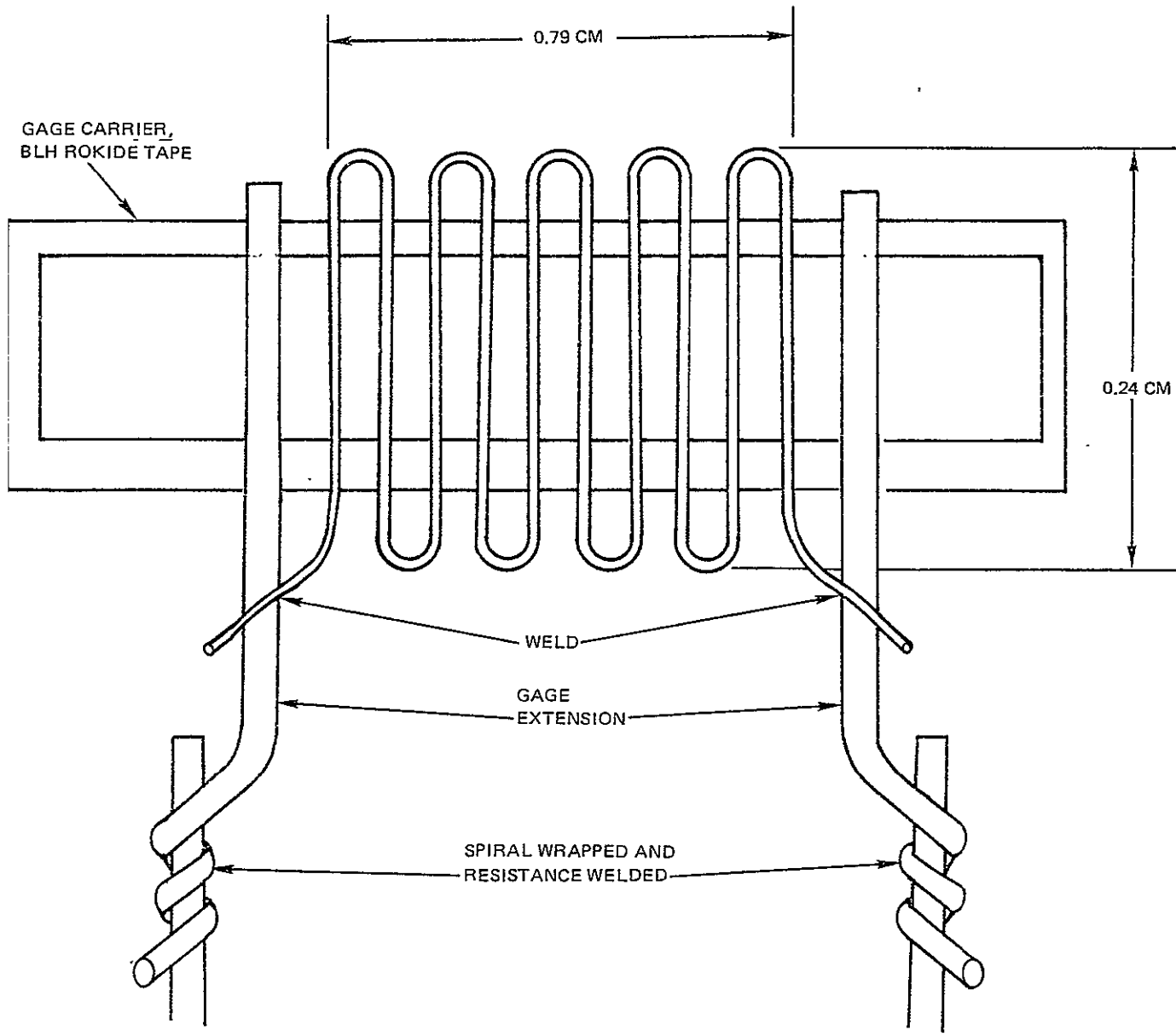

Figure 8 Strain Gage Winding Pattern for Pratt & Whitney Aircraft Installed Gages - The winding produced a grid size of 0.79 cm x 0.24 cm in a standard leadwire configuration.

Attachment Coating and Overcoat - For Systems 1 through 4, areas where overspray could occur were masked using BLH Rokide tape. A tack coat of flame sprayed Rokide HT rod was then applied thick enough to just cover the gage wire. The tape carrier was then removed and the gage installation inspected under a microscope for damage and to ensure that the gage wire was in contact with the precoat. Any tape residue was removed with tweezers. If no damage was found, the gage area was remasked and a final coat of flame sprayed Rokide HT rod was applied. If damage was observed, the installation was removed by grit blasting down to the bond coat and the installation was then repeated. The final coat was then

inspected under a microscope to make sure that there were no cracks or crevices in the coating.

For System 5, a thin coat of Bean type H ceramic cement was applied to the exposed strain gage grid area. The cement was allowed to air dry for 30 minutes. The installation was then baked at 65°C for 10 minutes and allowed to cool. The tape carrier was then removed, and the gage installation inspected for damage and proper grid positioning. The installation was then baked at 65°C for 30 minutes followed by baking at 343°C for 1 hour and cooling to at least 150°C prior to removal from the oven. Another coating of Bean H cement was then applied using the same application and curing procedure to fill in the area masked by the gage carrier tape during the previous application. The installation was then checked under a microscope.

Following application of the overcoat, final airfoil thickness measurements were taken and recorded for all 5 gage system types. A gage resistance check was also made. A change of 2 to 3 ohms was expected while a change of 4 ohms or more was indicative of thermal or mechanical damage to the gage wire. Consequently, if the resistance after installation differed by more than 4 ohms from the value recorded before the gage was installed, the entire installation was replaced.

Leadwire Installation - The leadwire was attached to the gage extension by spiral-wrapping and resistance welding. Thirty-six gage Chromel P wire was used. The leads were secured to the precoat using 0.25 cm wide Rokide tape strips at intervals of 0.25 cm. The tape was 0.13 cm narrower than the precoated area. The installation was then inspected under a microscope to make sure that the leadwires were in intimate contact with the precoat.

For Systems 1 through 4, a tack coat of flame sprayed Rokide HT rod 0.05 to 0.07 mm thick was applied to the leadwork. The Rokide tape was then removed and the tack coat inspected under a microscope to verify that the leads were in intimate contact with the precoat and that all tape residue had been removed. Any jagged or overlapping edges were removed. The area was then remasked with the tape overlapping the tack coated area by 0.13 cm. A final fill-in and overcoat of Rokide rod 0.05 to 0.07 mm thick was then applied.

For System 5, a thin coat of Bean H cement was applied to the leadwork between the Rokide tape strips and allowed to air dry for 30 minutes. The installation was then baked at 65°C for 10 minutes and allowed to cool. The Rokide tape strips were then removed and the installation baked for 30 minutes at 65°C followed by 1 hour at 343°C. The installation was allowed to cool to at least 65°C before it was removed from the oven. The installation was then inspected to verify that the leads were in contact with the precoat. A fill-in coating of Bean H was not applied. The area was then remasked using Rokide tape. The tape enclosed an area 0.13 cm narrower than the precoat but did not approach the Bean cement. A final thin fill-in and overcoat of flame sprayed Rokide rod was then

applied over the entire installation.

Final Inspection and Dressing - The final installations for all systems were then inspected under a microscope for voids or cracks. Airfoil thickness measurements were again taken. Maximum allowable installation thickness was 0.046 cm. An aluminum oxide dressing stick was then used to smooth out nonuniformities and reduce the overall thickness to 0.046 cm if required. Installations that could not be dressed to this thickness limit were replaced. A final thickness measurement was recorded and the blade was stored in plastic for protection pending installation into the disk.

5.1.2 Strain Gage Application Procedure for NASA Installations

Systems 6 and 7 were installed by NASA personnel. The same general strain gage installation procedure was used for both systems, including the surface preparation, bond coating, precoating, overcoating, and strain gage installation. However, the leadwire and blade-to-disk jumps differed between the two systems.

Surface Preparation - The blades from both stages were cleaned with a solvent and a degreaser. They were then baked in the oven at 370°C for 1 hour and cleaned again with a solvent.

The gage and leadwire areas were then masked using Scotch 470 pressure sensitive tape. These areas were then grit blasted with 120 grit aluminum oxide at a distance of 10 to 15 cm at an angle of 45 degrees. The blades were then cleaned with a neutralizer and distilled water and blown dry with nitrogen gas.

Bond Coating - The blades were then remasked using Fluorolin 404 tape outlining the gage and leadwire area. A Metco 450 bond coat was then applied to the masked area by the flame spray process. Holding the nozzle at 15 to 20 cm above the blade, a 0.05 to 0.07 mm thick coating was applied.

Precoat - The blade was once again remasked outlining the gage and leadwire area with Fluorolin 404 tape. A 0.05 to 0.07 mm base coat of Rokide H rod was applied by the flame spray process with the nozzle held 15 to 20 cm above the part. The base coat of Rokide H rod was then primed with a thin layer of Bean H cement mixed with water to produce a coating approximately 0.03 mm thick. A paint brush was used to apply the cement. The part was then air dryed for 15 minutes at room temperature.

Strain Gage Installation - NASA used BLH HT 1212 platinum 8 percent tungsten gages. These gages were applied to the blades by using tape strips. The leadwires were then spliced to the gages. Both 40 and 36 gage platinum 10 percent nickel leadwires were used. The leads were spliced by overlapping the gage leads by 0.16 cm (side by side) and then spot welding the leads in three places with a miniature tweezer-type custom-made welder. The leads are then taped in place along the airfoil.

Attachment Coating and Overcoat - A thin layer of Bean H cement was

applied between the strips of tape on the gage and the strips of tape on the leadwires. This is noteworthy in NASA's installation because both the gage and leadwire areas were coated at the same time. The cement was then allowed to air dry for 15 minutes and then oven set for 20 minutes at 82°C. The tape strips were then removed and a thin layer of Bean H cement applied to the uncoated strips. The entire assembly was then air dryed and oven cured for 1 hour at 315°C.

A final coat of Rokide H rod was applied to the gage and leadwire area by the flame spray process to a thickness of 0.07 to 0.13 mm. An effort was made to minimize the overall thickness of the installation and keep it between 0.25 and 0.46 mm. Thickness measurements were made using a Brown and Sharpe dial indicator Model 8241-941. This instrument was specially made for the measurement of strain gage installations.

The blades were protected and then shipped to Pratt & Whitney Aircraft for installation into the rotors.

5.1.3 Blade-to-Disk Jump Application Procedure on First Stage

The first step in making the blade-to-disk jumps was the application of a precoat of GA-60 epoxy cement to the blade instrumentation lead-through holes in the blade platform and to the underside of the platform. The leadwire that had been spliced to the gage and routed down the airfoil was routed through the blade lead-through holes to the underside of the platform. Here they were spliced to the wire used to jump from the blades to the first stage disk. The holes were then potted with ceramic cement.

Systems 1, 3, 5, and 7 were spliced to 32-gage stranded nickel-plated copper alloy wire with Kapton/Teflon insulation. High temperature solder (309°C) was used to make the splice. This solder material is an Alpha solder with an energized resin core. The core permits excellent tinning and ease of soldering and is compatible with all materials soldered in the program.

Systems 2, 4, and 6 were spliced to 28-gage Chromel/Alumel duplex wire insulated with Fiberglas/-asbestos. Below the splices, the leads were routed to within 0.46 cm of the leading edge and secured using GA-60 epoxy cement. The individual blade assemblies were then baked at 180°C for 2 hours to cure the cement. The blades were then installed in the rotor.

The first stage rotor had been previously prepared to receive the leadwork. Both leadwire type jumps were made from the underside of the blade platform to the disk, as shown in Figure 9. In making the jumps, 0.16 cm of slack was left to allow for blade movement and deflections caused by "g" loading. Once on the disk, the leads were secured using MicroMeasurements GA-60 epoxy cement.

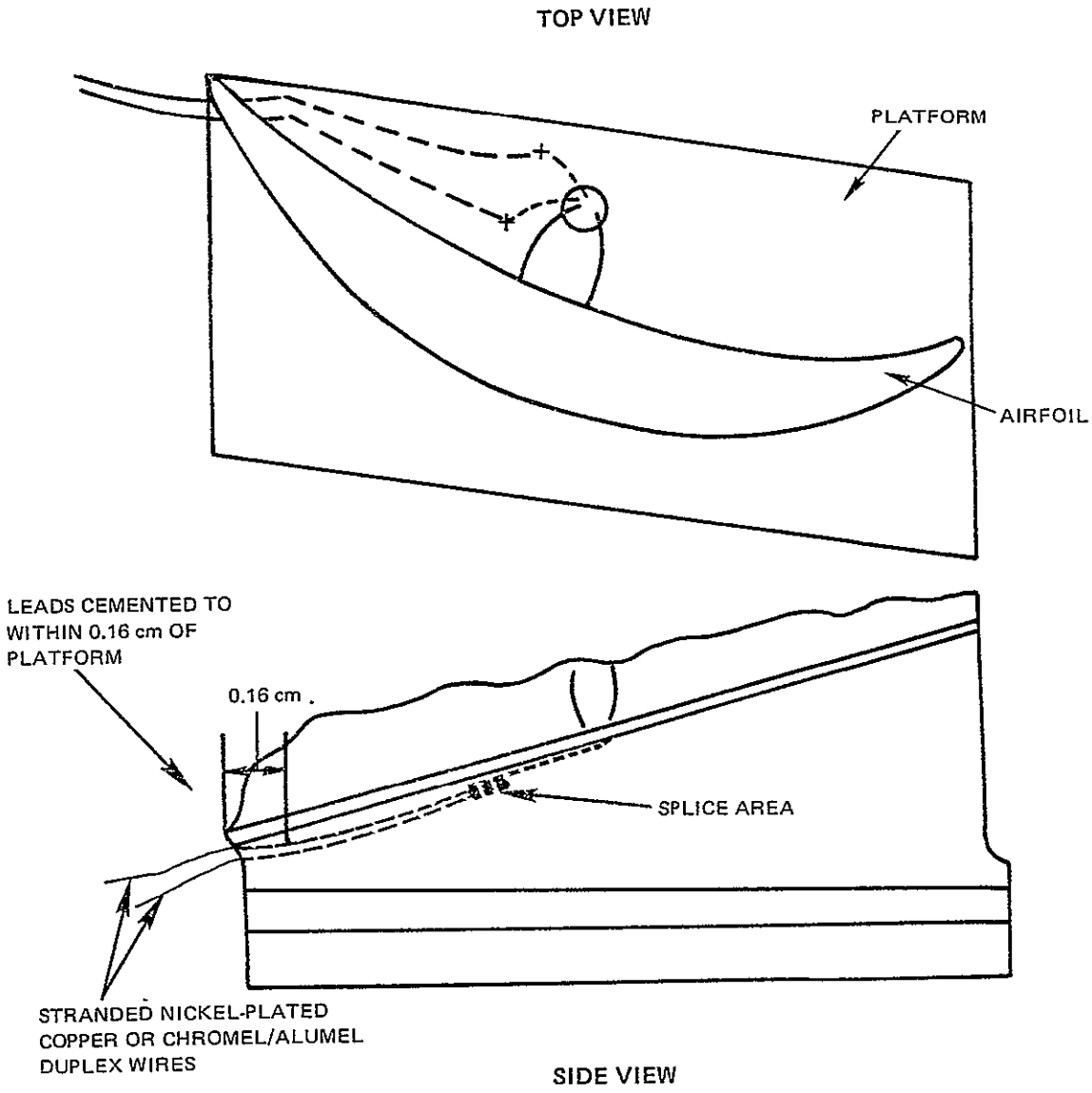

Figure 9 First-Stage Leadwire Jump Scheme - Both leadwire jumps were made from the underside of the blade platform to the disk leaving a little slack to allow for blade movement and deflections from "g" loading.

5.1.4 Blade-to-Disk Jump Application Procedure on Third Stage

All of the third stage blades had holes drilled in the rear of the platforms to allow for leadwire routing. The blades with gages installed by Pratt & Whitney Aircraft had a precoat of GA-100 ceramic cement applied to the root, while the blades with gages installed by NASA had a precoat of SermeTel P-1 ceramic cement applied. After all the airfoil leads were brought through the

holes to the splice area at the blade root, the holes were potted with a slurry of GA-100 ceramic cement and Fybex, added to increase cement body, and baked at 180°C for 1 hour. The installation scheme is shown in Figure 10.

Pratt & Whitney Aircraft Systems 1, 3, 5 and NASA System 6 were spliced to 28-gage Chromel/Alumel duplex wire in a specified precoated area. In routing the leadwires and making the splices, it was important to maintain certain tolerances since the splice had to fit within the slot in the blade retainer that covers a portion of the blade root. A 0.25 by 0.76 cm piece of titanium strap material 0.008 cm thick was tack welded over the Chromel/-Alumel duplex wire to secure it to the blade root. The splice was overcoated with GA-100 ceramic cement, and a final overcoat of GA-60 epoxy cement was applied.

Pratt & Whitney Aircraft Systems 2 and 4 were not spliced. The 36 gage Chromel P wire from the airfoil was routed through the hole in the platform, and continued down the blade root. The leads were routed to match the slots provided in the blade retainer. The leads were secured to the root using GA-100 ceramic cement. They were then baked to cure the cement.

For the NASA System 7, the 36 gage platinum-nickel wire was routed through the holes in the platform and spliced to 36 gage, Chromel P wire on the SP-1 precoat area under the platform. The leads were then routed down the blade root to match the slots in the blade retainer. The splices and leads were secured using GA-100 ceramic cement.

All the blades were then installed in the rotor. In an effort to reduce blade movement, red RTV silicone rubber was initially installed between the root of the blade and the disk. However, this technique was found to be unsatisfactory in reducing blade movement because the RTV was not firm enough when cured. Consequently, Mylar shims were placed under the blade roots. GA-60 epoxy cement was then flowed around the shims. This approach provided good control of the blade-disk relative movement.

The jumps to the disk were then made. The 28 gage Chromel/Alumel duplex wire was routed straight down from the blade root to the disk, leaving 0.16 cm of uncemented lead on either side of the jump. SP-1 ceramic cement was used to secure the leads once on the disk. The 36 gage Chromel wire had a small 0.08 cm radius loop formed in the wire to provide strain relief. In all cases, the 28 gage Chromel/Alumel duplex wire and the 36 gage Chromel P wire were spliced to pre-routed 36 gage Chromel P wires on the web of the disk secured with SP-1 ceramic cement. The splices were covered with GA-100 ceramic cement. An overcoat of GA-60 epoxy cement was applied to the entire installation.

The remaining leadwork to the slip ring was not considered part of the system evaluation. Four special wire guides were designed and constructed to support the 28 gage Chromel/Alumel leadwire between the third stage disk bore and the outside surface of the second stage disk hub, as shown in Figure A-5 in Appendix A. This routing scheme was unique to the

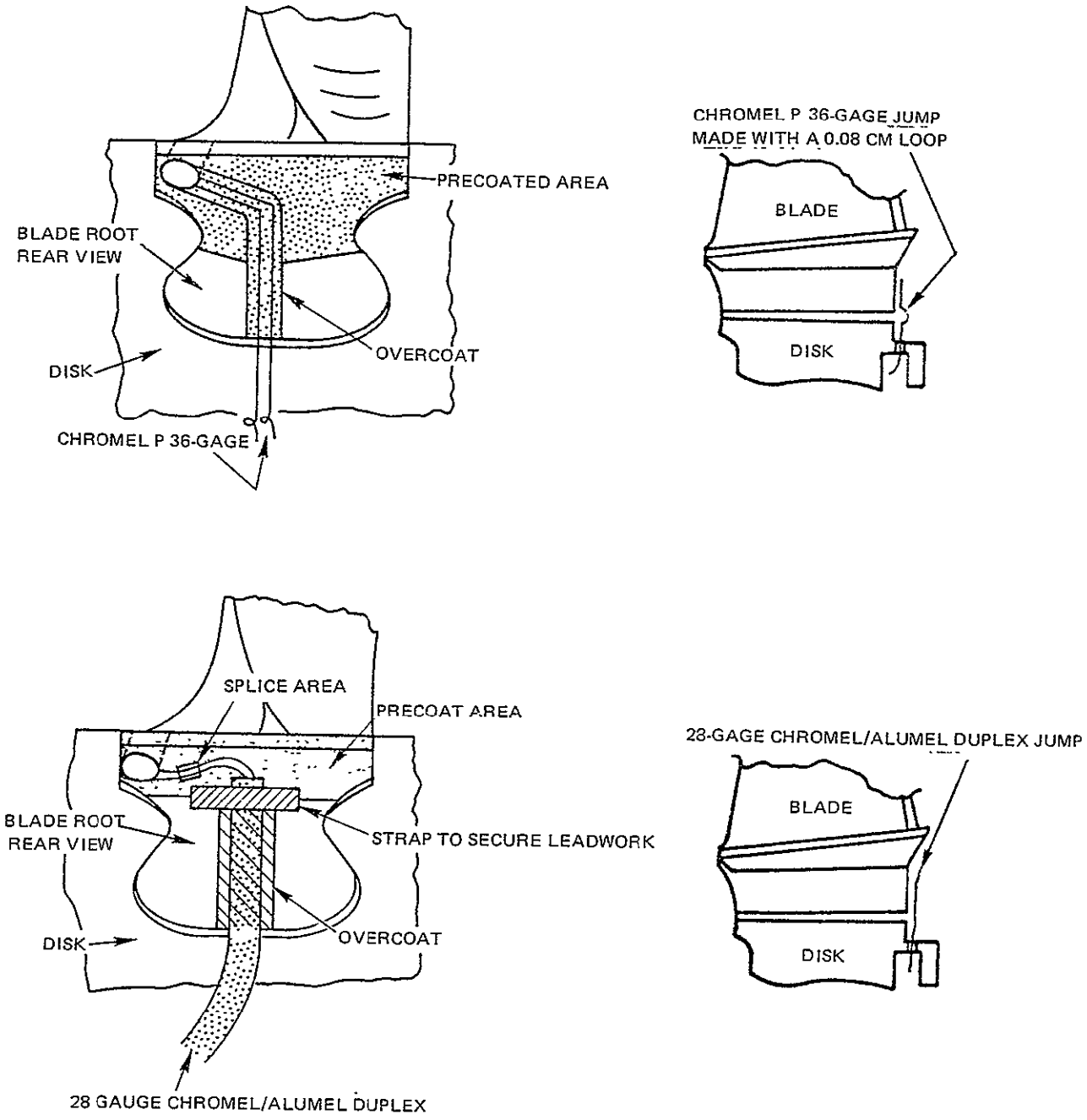

Figure 10 Third-Stage Leadwire Jump Scheme - In the third stage, the leadwires were routed through holes in the blade roots, potted with a slurry of GA-100 ceramic cement and Fybex, and baked at 176°C for 1 hour.

F100 engine and was included to prevent secondary failures.

5.1.5 Erosion Patch Installation Procedure for Pratt & Whitney Aircraft Installations

Pratt & Whitney Aircraft installed several types of erosion patches on the first and third stage blades. Eleven different patch material combinations were installed on the concave surfaces of four first stage and eight third stage blades. Strips of six materials were installed on the first stage and strips of four materials were installed on the third stage. These installations are shown in Figures 4 and 5 and described in Appendix E.

Surface Preparation - The initial step of the installation involved marking off and preparing the surface for the patches. On both stages, this area extended in the chordal direction from 0.13 cm from the leading edge to 0.13 cm from the trailing edge. In the radial direction, the area extended from a line 0.6 cm above the platform fillet outwards 11.4 cm on the first-stage blades and 7.6 cm on the third-stage blades. Strips 1.9 cm wide were then measured off along the span to outline the individual patch installation sites.

Airfoil thickness measurements were taken at 25 percent and 75 percent chordal locations for each of these strips.

For all but two of the blades from each stage, the patch area was masked with 3M #470 yellow pressure sensitive tape and grit blasted using #120 grit aluminum oxide, after which it was blown clean with dry nitrogen. The airfoils were then inspected to verify that the desired surface cleanliness and finish had been achieved.

For the two remaining blades from each stage, the entire concave surface was grit blasted with #60 grit aluminum oxide except for a 0.64 cm strip around the shroud and platform fillet and a 0.13 cm strip around the edge of the airfoil.

Bond Coating - A bond coating was applied to the grit blasted areas for all blades except those that were grit blasted over the entire concave surface. BLH Rokide tape was used to mask the erosion patch areas, after which a 0.05 to 0.07 mm thick coating of Metco 450 material was applied. The areas were then inspected to verify that an even coat had been obtained.

Overcoat - A different material sample was applied to each of the 1.9 cm strips. The material samples were alternated through the various strip locations on the different blades to expose each material to each erosion environment. The patch materials that were evaluated on the first and third stages were:

1. Various thicknesses of Rokide HT rod. (First and third stages)

2. A coat of Rokide HT rod overcoated with GA-60 epoxy cement. (First and third stages)

3. A coat of Rokide HT rod overcoated with Bean H ceramic cement followed by an overcoat of Rokide HT rod. (First and third stages)

4. A coat of Plasmalloy 331-M aluminum oxide powder. (First and third stages)

5. A coat of Plasmalloy 331-M aluminum oxide powder overcoated with GA-60 epoxy cement. (First and third stages)

6. Two coats of GA-60 epoxy cement. (First and third stages)

7. Two coats of GA-60 epoxy cement covered with two layers of 0.07 mm Fiberglas cloth. (First and third stages)

8. A coat of PLD polyimide cement. (Third stage)

9. A coat of Plasmalloy 331-M aluminum oxide powder overcoated with PLD polyimide cement. (Third stage)

10. A coat of PLD polyimide cement covered with 0.07 mm Fiberglas cloth. (Third stage)

11. A coat of Rokide HT rod overcoated with PLD polyimide cement. (Third stage)

Of the four blades that had the entire concave surface grit blasted, one from each stage had a 0.07 mm coat of SP-1 ceramic cement applied and the other had a 0.07 mm coat of Bean H ceramic cement applied to the entire concave surface.

After all the patches were installed, airfoil thickness measurements were taken at 25 percent and 75 percent chordal locations for each strip area, and the total thickness of the erosion patch was then calculated on the basis of the initial uncoated airfoil thickness measurements.

5.1.6 Erosion Patch Installation Procedure for NASA Installations.

NASA installed erosion patches on both sides of the first stage blades in the form of typical strain gage system installations. The surfaces were grit blasted and, in some cases, a Metco 450 bond coat was applied. Details of the installations are presented in Appendix E. The patch materials applied were as follows:

1. A coat of M-Bond 610 epoxy cement.

2. A 0.17 mm coat of Rokide HT rod.

3. A 0.17 mm coat of Metco 105 aluminum oxide powder.

4. A 0.17 mm coat of Bean H ceramic cement.

5. A 0.17 mm coat of PBX ceramic cement.

6. A 0.17 mm coat of Rokide H rod overcoated with Bean H ceramic cement.

7. A 0.17 mm coat of Metco 105 aluminum oxide powder overcoated with Bean H ceramic cement.

8. A 0.25 mm coat of Rokide H rod.

9. A 0.25 mm coat of Metco 105 aluminum oxide powder.

10. A 0.35 mm coat of Rokide H rod.

11. A 0.35 mm coat of Metco 105 aluminum oxide powder.

5.2 TEST PROCEDURE

5.2.1 Engine Test Procedure

The running schedule of the strain gage system evaluation program is shown in Table V. The "Cumulative Cycles" column includes any cycle from stop to at least windmilling speed (about 2000 RPM) and back to stop. Most cycles went to higher speeds at idle (5000 RPM) or running conditions (8,000 to 10,000 RPM). Total running time for the test was 62.4 hours.

Figure 11 shows the operating points for the engine during the program. Point 1 is the operating condition for checkout runs with ambient inlet conditions. Points 2 to 8 are the conditions for the main program with inlet temperatures of -13.3°C, -28.8°C and -41°C. Points 9 and 10 are the operating conditions for an inlet temperature of about 115°C. This inlet temperature resulted in a third-stage inlet temperature of approximately 250°C. These conditions were held for 30 minutes and then repeated again. Because testing was conducted concurrent with a NASA afterburner rumble test, the test program differed in some respects from the original plan, primarily with respect to inlet temperature. Only one high temperature run was achieved.

Strain gage data were monitored and tape recorded during the test. In all, approximately 20 to 25 hours of strain gage data signals were recorded. These data were recorded on magnetic tape at a tape speed of 3 3/4 in/sec with short sections at 15 in/sec to extend the frequency response. Gages were generally scanned sequentially at about 5 seconds per gage in the normal mode, although occasionally individual gages were recorded for longer periods to observe changing conditions. The details of the recording and monitoring equipment are shown in Appendix D.

Several operational problems were encountered during the test program. During the first four test runs, oil leakage from the front bearing and seals around the slip ring installation resulted in an unusual amount of oil being sprayed on all the internal surfaces of the engine. Inspection at the end of the fourth run revealed that the front of the first stage fan blades, including the strain gage installations, were coated with a film of oil. The slip ring was removed for the next three runs to work on this problem. This resulted in a seven-hour gap in the recorded tapes. The oil leakage problems were solved after the fifth run. During this time, the slip ring was checked and found to have six open channels, all of which had been good at the start of the program. Consequently, a new slip ring was substituted and used for the remainder of the program. Dynamic tests were performed on this slip ring before installation and after teardown and verified that the slip ring functioned properly.

An additional problem was noise on the strain gage signals. The noise first occurred when the new slip ring was installed and the fan

TABLE V

TEST LOG FOR F-100 026 ENGINE
WITH 034 STRAIN-GAGED FAN

	Cumulative Times (Hours:Minutes)				
Date	Windmill Operation	Idle and Above	Total Time	Afterburner Lit	Cumulative Cycles
2/11/78	0:33	0:06	0:39	0:00	3
2/15/78	0:58	0:21	1:19	0:00	5
2/17/78	1:26	0:39	2:05	0:00	7
2/24/78	2:08	1:56	4:04	0:00	13
3/09/78*	2:48	3:45	6:35	0:00	18
3/11/78*	2:59	4:01	7:00	0:00	19
3/14/78*	3:24	7:04	10:28	0:00	21
3/16/78	4:02	8:53	12:55	0:00	25
3/18/78	5:11	12:42	17:53	0:33	27
3/21/78	5:17	18:02	23:19	2:20	28
3/23/78	5:26	23:41	29:07	5:10	29
3/28/78	5:38	28:41	34:19	7:39	31
3/31/78	5:53	34:11	40:05	10:20	32
4/04/78	6:12	40:07	46:20	12:40	34
4/19/78	6:50	40:54	47:45	12:40	36
4/20/78	7:44	44:46	52:31	12:40	37
4/22/78	8:00	49:49	57:49	12:40	38
4/25/78	8:44	53:51	62:35	12:40	41

*Slip ring removed for evaluation and replacement

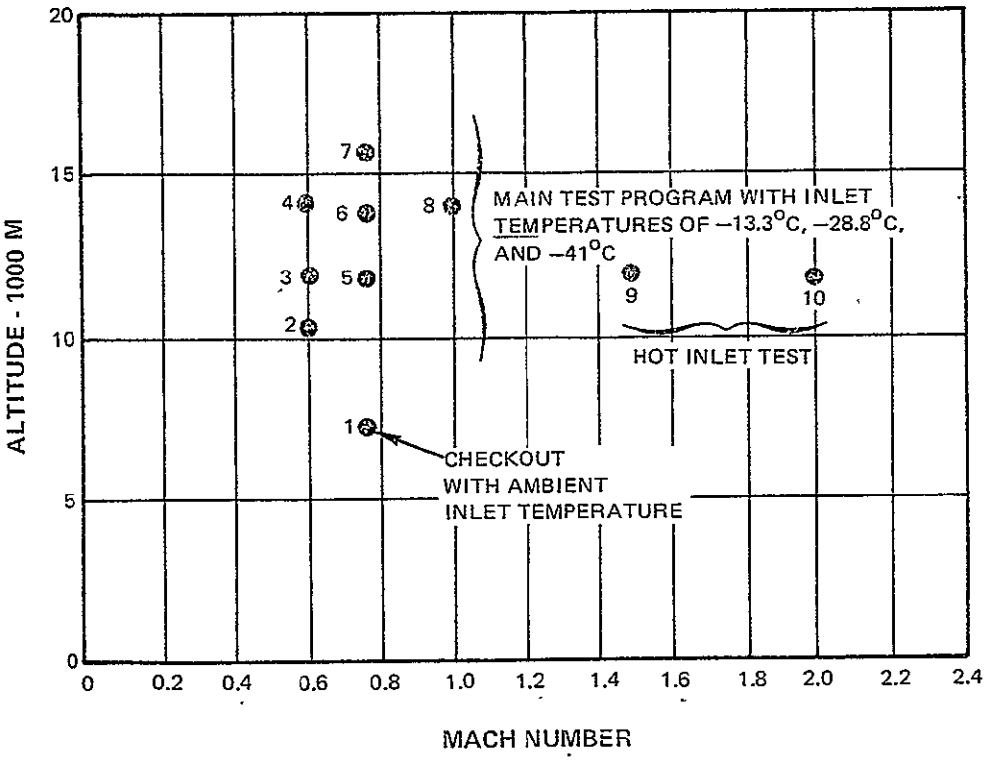

Figure 11 Engine Test Operating Conditions - The program was designed with an initial series of checkout runs, a series with inlet temperatures of approximately -13°C, -28°C, and -41°C, and two high-temperature inlet points.

speed sensing was moved from the slip ring speed pick-ups to the fan case eddy current sensor. The gage signal would become assymetrical, increase in magnitude, and change randomly. No noise was observed when the gages were unpowered. Although the slip ring was suspected, checkout after the test did not detect any problems.

A spectrum analysis of the gage signals was performed. This analysis showed that peaks at engine order frequency and its multiples were the major components of the signals at both noisy and quiet conditions.

It should be noted that the slip ring had a high transient vibration when traveling through the 5000 to 6000 RPM speed range. High vibration levels also occurred during the hot run. The vibration at these conditions exceeded the allowable limits and therefore limited the maximum temperature level attainable.

Three compressor stalls occurred during the hot run after the completion of the second thermal cycle. In addition, several afterburner blowouts occurred during the afterburner phase of the program.

5.2.2 Strain Gage Evaluation Procedure

The fan module was returned to Pratt & Whitney Aircraft and systematically disassembled and analyzed. The analysis consisted of detailed visual and photographic inspection as well as gage system resistance measurements throughout the incremental disassembly process. Photographs of the installations before and after testing are presented in Appendix A, and the resistance measurement data are presented in Appendix B. During the inspection, all blades and jumps were analyzed, but the main concentration was on the gages that failed during the testing.

Initially, the entire assembly was inspected visually to verify that no visible damage occurred during shipping and also to verify that there were no changes in condition from that reported by NASA prior to shipping. The inspection included the concave surfaces of the third-stage blades which were visible with the fan module still in the shipping crate.

A resistance check was then taken at the point where the leads had been connected to the slip ring. The results were compared with the results obtained by NASA prior to shipping.

The fan module was then disassembled into individual stages. Each stage was examined for damage, with particular emphasis on the first and third stages. Photographs were taken of each of the stages.

Each blade on each stage, from the gage to the end of the lead on the disk, was visually inspected for any obvious failures, loose lead wires, cement erosion, or broken jumps. The blade-to-disk jumps were checked using a microscope.

A resistance measurement was then made to verify the leadwire continuity and insulation. The results of these measurements are presented in Appendix B.

A static check of the gages was then performed using a Budd strain indicator. Two types of test were performed. First, a force was applied to each blade to determine if the deflection was detected by the gage. If the deflection was detected, the force was removed and the gage checked for return to zero. Failure to return to zero or a nonlinear response of the indicator would be indicative of a problem.

The second test consisted of heating along the leadwire route and gage area with a small torch. The gage output was monitored for indications of any nonlinear response as well as a return to zero after heat removal. This technique was used in an attempt to isolate the problem areas.

The leads were cut just before the jump to the disks and the blades were then removed from the rotors. A visual inspection was performed of each blade. Of prime interest was the splice area. Resistance checks were then made, and, if the gage circuit was found to be open, additional checks were performed to identify the break location. Circuit resistance measurements were documented for further analysis of system failures.

Photographs were taken at this point for comparison with pictures taken prior to original assembly.

The blades were then analyzed under a microscope, primarily to determine the presence of erosion and delamination of the cement.

The last step in the analysis of the strain gage installations consisted of thickness measurements for those installations which did not have an erosion patch on the opposite side of the airfoil.

For Systems 1 through 5, thickness measurements were obtained using a measuring device similar to a dial indicator and with measurements after testing being taken at approximately the same location as before testing through the use of templates. It should be noted, however, that the technique used was sensitive to local blade thickness changes, and, as a result, the measurement repeatability is considered to be no better than $\pm$0.02 mm.

For Systems 6 and 7, intial thickness was documented by NASA using a single number as an average thickness over the entire gage and leadwire installation. Final measurememnts were taken at Pratt & Whitney Aircraft using a measurement tool supplied by NASA.

The results of these measurements were compared with measurements taken before testing and are presented in Appendix C.

Evaluation of the erosion patches consisted of a visual inspection to assess the overall condition of the patches, determine the most severe erosive environment, and make a qualitative judgement of the erosion resistance of the various materials. Thickness measurements were taken for a quantitative evaluation; however, localized erosion of the patches made comparison to the original average thickness numbers impossible. It now appears that thickness contour plots should have been produced prior to erosion patch installation to permit more accurate evaluation of the patch erosion.

5.3 RESULTS AND DISCUSSION

5.3.1 Overview

The overall reliability of the strain gage systems tested was good. However, a number of failures did occur during the engine test program. Overall, 32 percent of the gage systems failed during 62 hours of engine testing. The following sections will examine these failures in detail.

5.3.2 Engine Test Results

Table VI shows the chronological failure log for the strain gages during the engine test program. Failures were classified according to stage, installer, type of installation, and location. A failed gage was defined as a gage which was inoperative when the engine was rotating at windmilling speed or above. Many such gages showed normal continuity during static checks, but were inoperative when rotating. Resistance measurements were taken at various times during the program. The data are summarized in Appendix B.

The chronological failure log shows that three installations on the third stage, Blade S/Ns 22,

TABLE VI

CHRONOLOGICAL FAILURE LOG

Blade Serial Number	Stage	Installer	System Type	Side	Hours of Failure	Cause
28	1	P&WA	2	B	0-62	Jump
4	1	P&WA	4	B	0-62	Gage Splice
29	3	NASA	7	B	0-11	Slip Ring
22	3	NASA	6	B	1-11	Slip Ring
35	3	P&WA	5	A	1-11	Slip Ring
19	1	NASA	7	B	2-62	Jump
13	1	NASA	7	B	3-62	Jump
18	1	P&WA	4	A	3-62	Jump
2	3	P&WA	2	B	11-62	Jump
19	3	P&WA	2	A	11-62	Jump
33	3	P&WA	4	A	11-62	Jump
21	3	P&WA	4	A	11-62	Jump
31	3	P&WA	2	A	11-62	Jump
5	1	NASA	6	A	12-62	Jump
14	3	P&WA	2	B	12-62	Jump
23	3	NASA	7	A	15-62	Jump
5	3	NASA	6	A	17-29	Splice on Blade Root
31	1	NASA	6	A	40-62	Jump
40	3	NASA	7	A	47-62	Jump
25	3	P&WA	2	B	50-62	Jump
16	1	P&WA	2	A	30-34 47-62	Jump
32	3	P&WA	3	B	56-62	Splice on Blade Root

Totals at End of Test

Number of Failures By System Type

System 1	0 of 8	System 5	0 of 8
System 2	7of 8	System 6	3 of 10
System 3	1 of 8	System 7	4 of 10
System 4	4 of 8		

Number of Failures By Installation Location

Concave Surface	11
Convex Surface	8

System type numbers are defined in Table IV.
Location A = Above shroud, trailing edge, concave side
Location B = Above shroud, maximum thickness, convex side

29, and 35, appeared as failures until the new slipring was installed after eleven hours of testing. At that time, they were shown to be operating properly and remained so for the rest of the test. Therefore, these systems were not classified as failures in the analysis. The system on third-stage blade S/N 5 was open during the period from 17 hours to 29 hours, and then operated normally. During failure analysis, a wire separation was found at the splice on the blade root: therefore, this system will be counted as a failed system. Overall, a total of 19 gage systems out of 60 failed during the 62 hours of running, representing a failure rate of 32 percent.

Table VII documents the number of failures by system type. In evaluating the information in this table, it should be noted that the failures, in almost all cases, occurred in the jump region; therefore, valid conclusions cannot be drawn regarding the relative merits of the various types of strain gage systems.

Table VIII classifies the failures in the jump region. On the first stage, Systems 1, 3, 5, and 7 used the stranded nickel-plated copper wire jumps insulated with Kapton/-Teflon material. There were two jump failures in 12 systems, or 17 percent. Systems 2, 4, and 6 used Chromel/Alumel duplex wire insulated with Fiberglas/asbestos. There were five jump failures in eight systems, or 62 percent.

On the third stage, Systems 1,3,5, and 6 used the Chromel/Alumel

TABLE VII

FAILURES BY SYSTEM TYPE

Stage	System Type 1	2	3	4	5	6	7	Total
Total Gages Installed								
1	3	2	2	2	3	4	4	20
3	5	6	6	6	5	6	6	40
Number of Failures								
1	0	2	0	2	0	2	2	8
3	0	5	1	2	0	1	2	11
Percent Failed								
1	0	100	0	100	0	50	50	40
3	0	83	16	33	0	16	33	25

TABLE VIII

ANALYSIS OF BLADE-TO-DISK JUMP FAILURES

	First Stage		Third Stage	
	32 Gage Stranded Copper	28 Gage Chromel/ Alumel Duplex	28 Gage Chromel/ Alumel Duplex	36 Gage Chromel P
System Types Using Indicated Jumps	1,3,5,7	2,4,6	1,3,5,6	2,4,7
Total Gages Installed	12	8	22	18
Number of Failures	2	5	0	9
Percent Failed	17	62	0	50

duplex wire. No failures occurred in 22 systems of this type. Systems 2, 4, and 7 used 36 gage uninsulated Chromel P wire jumps. There were nine failures in 18 gages or 50 percent.

The failure rate of the stranded nickel-plated copper wire was less than that of the Chromel/Alumel duplex wire because the stranded construction resulted in less wire fatigue for a given blade movement. However, wicking of the GA-60 cement into the Fiberglas insulation reduced the free lead by 30 to 50 percent, resulting in a greater local straining of the wire.

The high failure rate of the 36-gage Chromel P wire on the third stage was attributed to two main factors: excessive leadwire yielding during strain relief loop formation and an inadvertent GA-60 epoxy cement coating of the jump loop.

The differences in the failure rate of the 28-gage Chromel/Alumel duplex wire between the first and third stages can be attributed to the difference in blade movement between the first and third stage. However, two failures occurred at the splice that were not attributable to blade movement.

5.3.3 Statistical Failure Rate

Figure 12 shows the strain gage system failure rate during engine testing together with the strain gage failure rate results for previous testing of this same engine type at NASA in flutter programs. As shown, a number of failures occurred during the first ten hours of testing, after which the failure rate was substantially slower. The initial higher failure rate is believed to be the result of poor jump formation. Unfortunately, most of these failures occurred during the time that the gages were not being monitored;

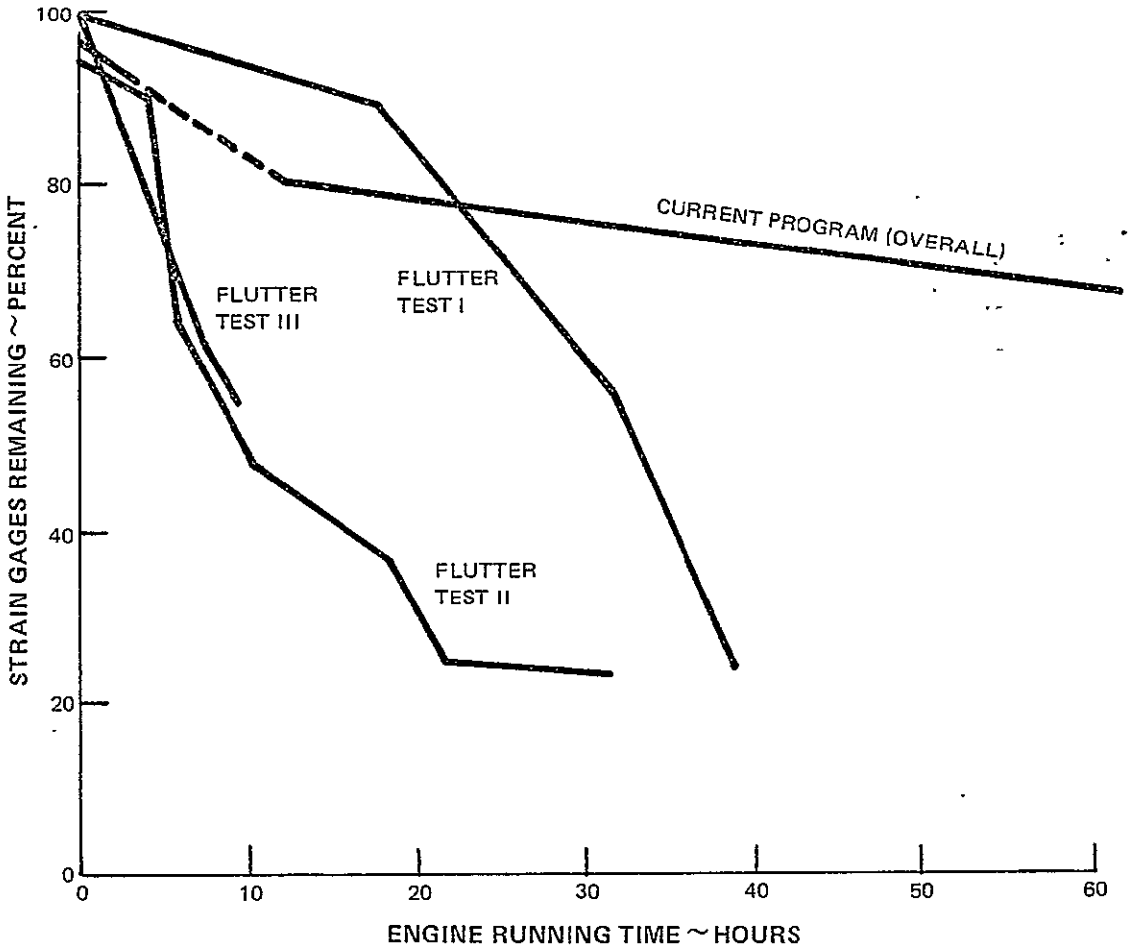

Figure 12 Strain Gage System Failure Rates for the Current Program and Previous Tests of the Same Engine Type

therefore, it is not known if the failures resulted from a single event or if they were spread throughout the first ten hours of engine running. However, no event is evident from the engine running logs that might be suspected of causing multiple gage system failures.

It is significant to note that the failure rate curve is relatively shallow for the latter portion of the test program, apparently because two strain gage system failure mechanisms that had been common in the previous NASA F-100 programs did not occur. One of these was erosion failures, which had occurred because some of the less erosion-resistant materials had been used. The other was gage grid overstressing that causes gage grid failures and could show up as open circuits or elevated resistance in the gage. The higher stress levels of the flutter test program caused failures of this type. In the current tests, stresses of this magnitude were not encountered.

5.3.4 Resistance Measurements

All 19 gage system failures occurred as breaks in the circuit, with 16 at jumps, two at root splices, and one at the gage grid.

Resistance measurements were used to locate circuit breaks that were fully open only during engine operation. When the engine was not rotating, some of these breaks would close but occasionally would still exhibit high contact resistance.

Faulty slip-ring connections were another source of difficulty, as documented in Appendix B. A total of 10 such faults were found, one of which was a fully open circuit with the remaining producing high contact resistance. In addition, open circuits occurred in six slip-ring channels in the first four hours of the test, resulting in removal and replacement with a new slip ring. Slip ring problems have also occurred in previous NASA test programs indicating that such problems are an inherent liability of slip ring systems with such a large number of minute connections. In the subject program, 360 such connections were required.

No resistance changes were found in the gage grids, although such changes had occurred in previous flutter tests (see Figure 12). The reason for this difference appears to be related to the lower stress levels in this test. The actual strain levels produced are estimated to be less than 300 microstrain, well below the gage grid endurance limit. Although strain level was measured, excessive circuit noise interfered with accurate data acquisition.

Resistance-to-ground measurements were made on each installation, and no reading below 10 megohms was found. Leakage to ground was a concern since it could result from thin or improperly cured cement, improper cementing of the leadwires, or moisture in the system.

5.3.5 System Installation Thickness Data

For Systems 1 through 5, the thickness measurement results show that the rate of erosion on the first stage was higher on the concave side than on the convex and that Plasmalloy powder had a higher rate of erosion than the Rokide rod. On the third stage, the rate of erosion was similar on both the convex and concave sides with the Plasmalloy powder having a slightly greater rate of erosion than the Rokide rod.

For Systems 6 and 7, measurements on the first stage showed that a maximum of 0.10 mm (25 percent) erosion occurred on the convex side but showed no erosion on the concave side. However, these readings are very misleading since severe delamination occurred on the leading edge of the installations on the concave surface. Because of the sharp increase in thickness of these installations, it is believed that the air flow was deflected upward at the leading edge, resulting in no erosion at the center of the installation strip where the measurement tool was designed to take the readings. On the third stage, a range of 0.02 mm to 0.08 mm (5 to 16 percent) erosion was indicated for both sides of the airfoils.

5.3.6 Erosion Patch Data

The patches installed by NASA on the first stage blades showed a considerable amount of erosion on the concave side while the convex side showed little erosion. The Plasmalloy powder systems showed the heaviest amounts of erosion in the area 1 cm to 2 cm below the shroud on the concave side. In a few cases, the entire patch was eroded away except for the Metco 450 precoat. The Rokide rod showed the least amount of erosion on the concave side. Measurement data proved to be inconclusive because in some areas the post-test thickness measurements were greater than the initial average thickness numbers.

Pratt & Whitney Aircraft installed patches on the concave side of the first and third stage. The final analysis consisted of establishing the high erosion area and then taking measurements by grit blasting through the patch surface at six locations across the span of the blade. These measurements were compared to the original measurements at 25 percent and 75 percent chord locations.

Several problems were encountered in making these comparisons and they rendered the results inconclusive. The greatest erosion occurred at locations other than at the 25 percent and 75 percent span locations. Since the final measurements were taken to document the highest erosion, no direct comparison could be made with initial measurements. An attempt was made to use average thickness numbers from the initial thicknesses but the final measurements showed wide variations with some of the final thickness numbers being greater than the averages. The results of this attempt to obtain quantitative data on erosion were also considered inconclusive.

A qualitative analysis was made of the six materials used as overcoats on erosion patches. The Rokide rod with a GA-60 overcoat showed the least erosion. Surface cracks were noted, however, on the patch just above the blade platform. Plasmalloy 331-M aluminum oxide powder with a GA-60 overcoat ranked second, showing little erosion. It should be noted that these two combinations of materials have the temperature limitation of the epoxy cement (260°C). The Rokide rod overcoat by itself ranked third, showing only a slight bit more erosion than the previous two materials. The composite installation of Rokide rod and Bean H, however, showed total erosion of the Rokide rod and Bean H overcoat with a minimum of precoat erosion.

The patches of GA-60, GA-60 with Fiberglas tape, and Plamalloy 331-M aluminum oxide powder were ranked closely together because of the near total erosion of these materials in the high erosion areas of the airfoil. All materials used for patches on the third stage looked good except for a slight amount of erosion along the leading edge. Therefore, no comparisons could be made as to which material was best on this stage.

5.3.7 Photographs

Appendix A contains photographs that were taken to document the strain gage installation systems.

Figures A-1 through A-4 show sections of the first and third fan stages with instrumented blades installed. Both before-test and after-test photographs are shown. Figure A-5 depicts a representative section of the leadwire routing. Before and after photographs of individual instrumented first-stage blades are shown in Figures A-6 through A-13. Similar views of first-stage erosion patches are presented in Figures A-14 through A-21. The analogous third stage instrumented blade photographs appear in Figures A-22 through A-31, and third stage erosion patch photographs are shown in Figures A-32 through A-35. Figures A-36 and A-37 are closeup views of blade-to-disk jumps, made with 36-gage Chromel P wire, which show a good and a broken jump.

In evaluating these photographs, it should be noted that the reproduction scales differ, but are indicated by rulers in each view. In addition, the order of the blades has been changed in some cases.

5.4 Inspection of Gage Systems

5.4.1 System Design 1

Number Installed - 8

First Stage
Convex: Blade Serial Number (S/N) 2 and 15
Concave: Blade S/N 27

Third Stage
Convex: Blade S/N 7 and 18
Concave: Blade S/N 1, 13, and 24

There were no failures of System Design 1 installations.

Visual inspection of the installations on the first stage showed little erosion of the overcoat on the convex side of Blade S/Ns 2 and 15. Erosion was greater on the concave side with Blade S/N 27 having exposed leadwire in the area between the root and shroud of the airfoil.

Where thickness measurements could be taken on the convex side, Blade S/N 2 showed that a maximum of 0.02 mm of the installation had eroded away while Blade S/N 15 had 0.05 mm to 0.10 mm of the installation gone in an area 17 cm to 20 cm above the blade platform. Measurements on the entire concave side showed that a range of 0.05 mm to 0.17 mm of the installation was gone due to erosion.

Inspection of the installations on the third stage showed a few spots of bare wire due to erosion on the convex side of Blade S/N 7 and 18. The concave side of Blade S/Ns 1, 13, and 24 showed a little erosion of the overcoat approximately 5 cm below the shroud of the blade.

Where measurements could be taken on the convex side, no more than 0.07 mm of the installation had eroded away on either blade. Measurements on the concave side showed that Blade S/N 1 had no measureable erosion while Blade S/N 13 and 24 had a range of 0.02 mm to 0.10 mm of overcoat erosion in an area between the root and shroud of the airfoil.

5.4.2 System Design 2

Number Installed - 8

First Stage
Convex: Blade S/N 28
Concave: Blade S/N 16

Third Stage
Convex: Blade S/N 2, 14, and 25
Concave: Blade S/N 8, 19, and 31

There were seven failures of System Design 2 installations with all failures traced to the leadwire jump area.

Visual inspection of the installations of the first stage showed little erosion on the convex side while the concave side showed heavy erosion along the leading edge, cracks in the Rokide H overcoat, and exposed leadwire in several areas.

Where thickness measurements could be taken on the convex side, a maximum of 0.07 mm of erosion had occurred with the highest erosion occurring directly over the gage. Measurements on the concave side showed that a range of 0.15 mm to 0.17 mm of erosion had occurred in an area 2 cm to 10 cm above the platform.

Both installations were listed as failures during testing. The system on Blade S/N 16 had normal resistance readings when the engine was stationary but would open circuit during engine rotation. This failure was traced to the jump area under the platform during blade deflection tests. The 28-gage Chromel Alumel wire became embrittled by the wicking of the GA-60 epoxy cement into the Fiberglas insulation resulting in an insufficient jump. The system on Blade S/N 28 was open circuited at the beginning of the test. This failure also occurred at the jump and for the same reason as the failure on Blade S/N 16.

Inspection of the installations on the third stage showed slight erosion on both the convex and concave sides of the airfoils. Blade S/N 8 had two spots below the shroud where the Rokide H overcoat had chipped off due to contamination of the precoat.

Where measurements could be taken on the convex side, a maximum of 0.07 mm of the overcoat had eroded away just below the shroud. Measurements on the concave side of Blade S/N 8 showed that a range of 0.03 mm to 0.07 mm erosion occurred in an area 5 cm to 10 cm above the blade platform with 0.12 mm erosion occurring above the shroud over the gage area. Blade S/N 19 and 31 had a range of 0.07 mm to 0.10 mm overcoat erosion in an area 10 cm to 12 cm above the blade platform.

Five of the six installations on the third stage were listed as failures. The installation on Blade S/N 8 was the only surviving system. All the failures were traced to broken 36-gage Chromel P wire at the jump area. Systems on Blades S/Ns 2, 14, and 25 had normal resistance readings but would open circuit during blade loading. The systems on Blades S/Ns 19 and 31 were found to have resistance increases of ten and twenty ohms, respectively, from pretest readings, and also would open circuit during blade loading. Close examination of the jumps revealed that the GA-60 epoxy cement used to overcoat the entire ceramic cement installation had inadvertently flowed onto the wire loops, significantly reducing the flexibility of the jumps. The epoxy coating was very thin on the loops for Blade S/N 8 and did not

reduce the flexibility significantly, thereby permitting this installation to survive. Severe yielding of the wire during jump loop fabrication could have occurred, contributing to the failure rate.

There were no secondary failures on the airfoils.

5.4.3 System Design 3

Number Installed - 8

First Stage
Convex: Blade S/N 30
Concave: Blade S/N 29

Third Stage
Convex: Blade S/N 9, 20, and 32
Concave: Blade S/N 3, 15, and 26

There was one failure of a System Design 3 installation.

Inspection of the installations of the first stage showed little erosion on the convex side, but severe erosion was found on the concave side along with partial leadwire exposure from the blade root to the shroud of the airfoil. Where thickness measurememnts could be taken on the convex side, a maximum of 0.12 mm of overcoat erosion had occurred over the gage. Measurements on the concave surface showed that a range of 0.15 mm to 0.18 mm erosion occurred in an area 2 cm to 7 cm above the platform. The erosion increased to the range of 0.28 mm to 0.33 mm in the area 12 cm to 15 cm above the platform.

Visual inspection of the installations on the third stage showed slight erosion on both sides of the airfoils. Partial leadwire exposure between the platform and shroud was observed on installations on the convex sides of Blades S/Ns 9 and 32 and on the installations on the concave sides of Blades S/Ns 3 and 15.

Thickness measurements were taken where possible. On the convex side, Blade S/N 9 had 0.05 mm of overcoat erosion while Blade S/N 20 had 0.17 mm erosion 10 cm above the platform decreasing to 0.07 mm at a distance 12 cm above the platform. Blade S/N 32 had 0.07 mm of overcoat erosion just below the shroud. Measurements on the concave side showed that Blade S/N 3 had 0.02 mm overcoat erosion 12 cm above the platform while both Blade S/N 15 and S/N 26 had a range of 0.15 mm to 0.21 mm overcoat erosion 10 cm above the blade platform.

The installation on Blade S/N 32 was the only listed failure of a System Design 3 installation. Erratic resistance readings were noted during exploratory tests including blade deflection tests, but no continuous open circuit could be produced. The failure was eventually traced to a broken side of the 28-gage Chromel/Alumel duplex wire in the splice area on the blade root. This failure could have occurred during fabrication of the splice since the splice overcoat showed no deterioration.

There were no secondary failures on the airfoil.

5.4.4 System Design 4

Number Installed - 8

First Stage
Convex: Blade S/N 4
Concave: Blade S/N 18

Third Stage
Convex: Blade S/N 4, 16, and 27
Concave: Blade S/N 10, 21, and 33

There were four failures of System Design 4 installations, three in the jump area, and one in the splice area.

Visual inspection of the installations on the first stage showed slight erosion on the convex side and a much higher degree of erosion on the concave side.

Thickness measurements on the convex side indicated that the greatest amount of erosion occurred over the gage where 0.13 mm of overcoat was gone. On the concave side, erosion ranged from 0.11 mm to 0.18 mm in the area 2 cm to 12 cm above the blade platform.

Both of the installations on the first stage failed. The installation on Blade S/N 4 was open circuited before the test began. This failure was traced to a broken wire in the splice area at the gage where the 36-gage Chromel P leadwire was attached to the gage extension wire. The cause of failure was a faulty splice.

The failure on Blade S/N 18 was traced to a broken 28-gage Chromel/Alumel wire at the jump that open circuited during engine rotation. As in the System Design 2 installation, the wire failure was caused by insufficient jump length resulting from embrittlement of the Fiberglas insulation by the GA-60 epoxy cement.

Inspection of the installations on the third stage showed slight erosion on both sides of the airfoil. Blade S/N 16 had a small amount of exposed leadwire above the shroud on the convex side while Blades S/Ns 10 and 21 had large amounts of exposed leadwire between the platform and the shroud on the concave side.

Thickness measurements made on the convex side of Blade S/N 16 showed 0.07 mm of erosion below the shroud and 0.10 mm of erosion over the gage. Measurements on Blade S/N 27 were very erratic with as much as 0.13 mm of erosion indicated below the shroud.

Measurements on the concave side of Blade S/N 10 showed 0.18 mm of erosion 10 cm above the platform, while measurements on the concave side of Blade S/N 21 indicated 0.08 mm of erosion 2 cm above the platform. Erosion on the concave side of Blade S/N 23 was measured as 0.15 mm 10 cm above the platform.

The two system failures on the third stage occurred on Blades S/Ns 21 and 23. Both systems became open circuited during engine rotation, but provided continuity when the engine was stationary, although the resistance was 30 to 40 ohms higher than the values measured prior to testing. The failures were traced to broken 36-gage Chromel wires at the jumps. The cause of the failures was the same as for the System Design 2 installations: inadvertent coating of the loops with epoxy cement and possible wire yielding during loop fabrication.

There were no secondary failures on the airfoils.

5.4.5 System Design 5

Number Installed - 8

First Stage
Convex: Blade S/N 17
Concave: Blade S/N 1 and 3

Third Stage
Convex: Blade S/N 30, 36, and 38
Concave: Blade S/N 35 and 37

There were no failures of System Design 5 installations.

Visual inspection of the installations on the first stage revealed only slight erosion of the installations on the convex side, while significant erosion, extensive leadwire exposure, and a few small spots of delamination of the Rokide HT rod and Bean H cement were found on the concave side.

No erosion was found where thickness measurements could be made on the convex side. Thickness measurements on the concave side of Blade S/N 1 revealed 0.25 mm of erosion in an area 12 cm to 15 cm above the platform. On the concave side of Blade S/N 3, thickness measurements indicated that 0.18 mm of material had eroded in an area 7 cm to 10 cm above the platform.

Inspection of the installations on the third stage showed slight erosion on both surfaces except for Blade S/N 35 which had a portion of the leadwire exposed below the shroud on the concave side due to erosion.

Thickness measurements on the convex side of Blade S/N 30 indicated 0.05 mm of erosion while measurements on the convex side of Blade S/N 38 indicated 0.03 mm of erosion. Measurements on the concave side of Blade S/N 35 indicated erosion of the overcoat ranging from 0.06 mm to 0.10 mm in the area extending from 2 to 7 cm above the platform. Similar measurements on the concave side of Blade S/N 37 indicated a maximum erosion of the overcoat of 0.15 mm in the region 10 cm above the platform.

5.4.6 System Design 6

Number Installed - 10

First Stage
Convex: No gages installed
Concave: Blade S/N 5, 14, 20, and 31

Third Stage
Convex: Blade S/N 11, 22, and 39
Concave: Blade S/N 5, 17, and 28

There were three failures of System Design 6 installations.

Two of the failures occurred on installations on the first stage blades. Both of these systems showed open circuits during engine rotation, but circuit continuity when the engine was stationary. Post-test resistance readings on the gage system installed on Blade S/N 31 agreed with the pretest measurements, but post-test resistance measurements for the Blade S/N 5 installation indicated a ten-ohm increase. The failure on Blade S/N 31 was traced to a broken 28-gage Chromel/Alumel duplex wire at the jump. As for the System Design 2 failures, the cause was an insufficient jump. The failure of the system on Blade S/N 5 was traced to a broken trunk lead between the slip ring and the first-stage disk.

Visual inspection of the installations on the concave side of the

first-stage blades indicated that all four systems had erosion and delamination along the leading edge of the overcoat with surface cracks near the root of the blades. Blades S/Ns 2 and 5 had extensive leadwire exposure as a result of erosion and also exhibited delamination between the platform and the shroud. Blades S/Ns 14 and 31 had exposed leadwire, but only at the platform fillet. Thickness measurements indicated that very little erosion (0.02 to 0.03 mm) occurred in the region behind the leading edge away from the delaminated area.

The one failure that occurred in a third-stage blade installation was on Blade S/N 5. This installation indicated normal resistance with a stationary engine and open circuited conditions during engine rotation. The failure was traced to a broken 28-gage Chromel/Alumel wire at the splice to the 36-gage Chromel P wire on the root of the blade. As with the System Design 3 failures, the failure probably occurred during splice fabrication.

Inspection of the installations on the third stage revealed delamination of the overcoat on the convex side of Blade S/N 11 above the shroud near the trailing edge. This delamination resulted in some leadwire exposure. No delamination was found on the other third-stage blades, however. The installation on the concave side of Blade S/N 5 exhibited a few surface cracks in the Rokide H overcoat.

Thickness measurements on the convex side of Blade S/N 11 indicated erosion loss of 0.07 mm of overcoat, while measurements on the concave side of Blade S/N 5 revealed 0.05 mm of overcoat erosion.

There were no secondary failures on the airfoils.

5.4.7 System Design 7

Number Installed - 10

First Stage
Convex: Blade S/N 6, 13, 19, and 32
Concave: No gages installed

Third Stage
Convex: Blade S/N 6, 29, and 34
Concave: Blade S/N 12, 23, and 40

There were four failures of System Design 7 installations with all failures occurring in the jumps.

Visual inspection of the installations on the convex side of the first stage showed only slight erosion, but actual measurements showed erosion levels ranging from 0 on Blade S/N 13 to 0.1 mm on Blade S/N 19.

Two failures occurred on the first stage installations. Both were revealed by open circuits during the test. The failures were traced to broken jumps which were made with 32-gage nickel-plated copper wire with Kapton/Teflon insulation. Failure was attributed to the use of too short a jump as a result of cementing the wire too close to the edge of the blade platform. The short jump length resulted in excessive strain during flexing which ultimately fatigued the jump to failure.

Inspection of the installations on the third stage showed a slight delamination of the overcoat on

the convex side of Blade S/N 34 while surface cracks but no delamination were found on the installations on the concave side of Blade S/N 12. Some delamination of the overcoat was found in the gage area of the installation on Blade S/N 40.

Thickness measurements taken on the convex and concave sides showed erosion levels ranging from 0.07 mm to 0.08 mm on Blades S/Ns 6, 34, and 40.

Both failures on the third stage occurred in the jump area and were traced to broken 36-gage Chromel P wire, as in System Design 2. The yielding of the jump loop significantly reduced the flexibility of the wire, causing it to break at the center of the loop.

SECTION 6.0

CONCLUSIONS AND RECOMMENDATIONS

6.1 OVERVIEW

A program was conducted to determine the reliability of various strain gage systems when applied to rotating fan blades in an aircraft gas turbine engine. Sixty strain gage systems of seven different designs were installed on the first and third stages of an F-100 engine fan and were tested in conjunction with an afterburner rumble experiment. There were 19 failed gages in 62 hours of engine operation, for a survival rate of 68 percent. Blade-to-disk jumps were the main failure mode.

The Strain Gage Systems Evaluation Program was successful in analyzing the effects of some of the factors involved in the current state of the art of strain gage installation. However, the tests were not capable of duplicating all of the operating conditions associated with gage failures encountered in previous experience.

The severe erosive environment on the concave surface of the first stage blades provided a good test condition for determining the effects of erosion. Most of the commonly used high temperature materials and some epoxies were subjected to this environment through the use of strain gage and erosion patch installations. The length of the test was sufficient for evaluation purposes.

Temperature levels did not reach the goal of 315°C. The third stage gages reached 250°C for about 4 hours, but during the rest of the program, the temperature did not exceed 115°C. The results of the high temperature run do not show any unusual failure effects, so this test did not reveal any temperature-related problems. For the materials tested, 315°C is considered to be a conservative temperature.

Noise on the strain gage channels impeded the stress level measurements on the blades. However, it is inferred from some noise-free data that strain levels were in the 0 to ±300 microstrain range, a value well within the endurance limit of these gage installations. No stress-related failures were observed. Previous flutter testing (see Figure 12) which imposed high stress levels had resulted in failures in the strain gage grid and root leadwires. However, this test did not create such conditions.

G-loading reached about 40 kG for approximately 60 percent of the tests, slightly short of the program goals. No failures related to G-loading were observed.

The evaluation of the different jump techniques used in the test was complicated by the faulty application of epoxy cement in the vicinity of the jump loops. The 28-gage Chromel/Alumel duplex wire jumps were embrittled by the cement wicking action and the 36-gage Chromel P wire was stiffened, reducing the jump flexibility. This resulted in the majority of failures on both stages.

6.2 EVALUATION OF SYSTEM COMPONENTS

6.2.1 Precoats, Attachment Coats, and Overcoats

As a precoat, Rokide HT and H rod performed well on all installations. On the first stage where the most erosion occurred, there was some delamination over the Bean H cement, but the precoat remained intact.

Rokide H or HT rod also provided the best results as an overcoat when applied to a Rokide HT or H precoat. On the concave side, erosion was minor and did not cause any failures. On the convex side, there was very little evidence of erosion. There was no delamination of the Rokide on Rokide installations.

The performance of the flame sprayed Plasmalloy powder as a precoat was comparable to that of the flame sprayed Rokide rod with respect to delamination. Erosion characteristics would be expected to be the same as the Plasmalloy powder overcoat.

The flame sprayed Plasmalloy powder overcoat did not perform as well in the erosive environment of the concave surface of the first stage in comparison with the Rokide HT or H rod overcoat. However, no delamination was observed.

The composite installations using Bean H cement to secure the gages and leadwires between a precoat and overcoat of Rokide HT or H rod did not perform as well with respect to erosion and delamination when compared with pure Rokide installations. Erosion resulted in the loss of the Rokide overcoat at the leading edge of the installations exposing the Bean H cement. At this point, delamination of the Bean H cement with the Rokide may have occurred or the poor erosion resistance of the Bean H cement may have resulted in an increased rate of erosion, undermining the Rokide overcoat and resulting in delamination. This condition was most severe on the concave surface of the first-stage blades.

Based on visual examination of the erosion patches in the highly erosive environment of the concave surface of the first-stage blades, the Rokide rod and flamesprayed powder with a GA-60 epoxy cement overcoat were the most durable materials. Rokide rod provided the next best erosion resistance. Flamesprayed powder and GA-60 cement by themselves provided poor erosion resistance. Materials used on the third stage could not be evaluated because of the very low levels of erosion on this stage.

6.2.2 Gage Type, Wire, and Size

The strain gages for five systems used Nichrome V wire gages wound by Pratt & Whitney Aircraft while two systems used commercial BLH platinum-8 percent tungsten wire gages. Both gage types performed well with only one gage-related problem occurring throughout the entire program.

6.2.3 Leadwire

Five systems used Chromel P 36-gage uninsulated wire while one system each used 40 and 36 gage platinum-nickel wire. No problems or failures were attributed to these leadwires. There were no

secondary failures on the airfoils.

6.2.4 Blade-to-Disk Jumps

The stranded nickel-plated copper alloy wire with the Kapton/Teflon insulation was the most durable jump material. However, the insulation imposes a temperature limitation, restricting its use to the first stage. Only two installations out of twelve (17 percent) using this wire failed, and both failures were caused by insufficient slack in the jump, resulting from the inadvertent cementing of the wire close to the edge of the blade platform.

The 28-gage Chromel/Alumel duplex wire jumps on the third stage survived the test with no failures among the 22 gages using this jump. This success was attributed to the minimal blade-to-disk motion of this stage. The first-stage jumps were not as successful because the jump flexibility was reduced by wicking of the epoxy cement into the Fiberglas insulation. Five of eight jumps failed (62 percent). The total for both stages was five failures in 30 jumps (17 percent).

The Chromel P 36-gage uninsulated wire provided the poorest performance. These jumps were made only in the third stage, and included a 0.08 cm radius loop to provide for relative movement between the blade and disk. This motion, however, was minimized by shimming the blade and by the application of GA-60 epoxy cement between the blade and disk during final assembly. However, in applying a GA-60 epoxy overcoat to strengthen the SP-1 cement attachment coat, the jump wires were inadvertently coated. The result of the epoxy coating was to reduce the flexibility of the loop and concentrate what little movement there was at the center of the loop or at a crack in the epoxy coating. The fatigue strength of the wire in the loop may also have been reduced as the result of over-straining during the fabrication process. It would appear that the jumps might have survived in the absence of the cement coating. Nine of eighteen jumps of this type failed (50 percent). The failures were clearly a result of fatigue and not pure acceleration loading since acceleration loading would have distorted the jump wire loops, and no distortion was observed.

6.3 RECOMMENDATIONS

On the basis of the results of the program, the following recommendations can be made:

1. High erosion areas, particularly the concave surface between the shroud and the platform, should be avoided on the first stage. When gages are installed on the concave surface, the leadwires should be routed around the trailing edge and down the convex surface.

2. When using Bean H composite installations, the flame sprayed Rokide HT or H rod overcoat should be extended further on the flame sprayed Rokide precoat. In addition, the thickness of the overcoat should be increased by 0.05 mm.

3. Flame sprayed Rokide HT or H rod overcoats on leadwork should be at least 0.08 mm thick to avoid rapid erosion and leadwire exposure.

4 Caution should be exercised when using cements around blade-to-disk jumps. In the case of bare wire jumps, all cements should be cleaned from the jump wire loop. In the case of jump wire covered with insulation, the insulation can act as a wick to the cement, which reduces the flexibility of the jump. A sufficient amount of flexible loop should be maintained for the jump.

5. Caution should be exercised when forming bare wire jump loops to avoid any damage to the wire.

6. Thickness measurement techniques should be improved, particularly for large areas such as the erosion patches used by Pratt & Whitney Aircraft in this test.

8. The use of GA-60 cement overcoat on Rokide rod and flamesprayed powder should be investigated further where temperature levels permit its use, because of its erosion resistant characteristics.

APPENDIX A

PHOTOGRAPHS SHOWING VISUAL INSPECTION RESULTS OF GAGE SYSTEMS AND EROSION PATCHES

Note: In reviewing the following photographs, it should be noted that the reproduction scale varies but in all cases is indicated by a ruler included in the photograph. In addition, the order of the blades varies between the before- and after-test photographs.

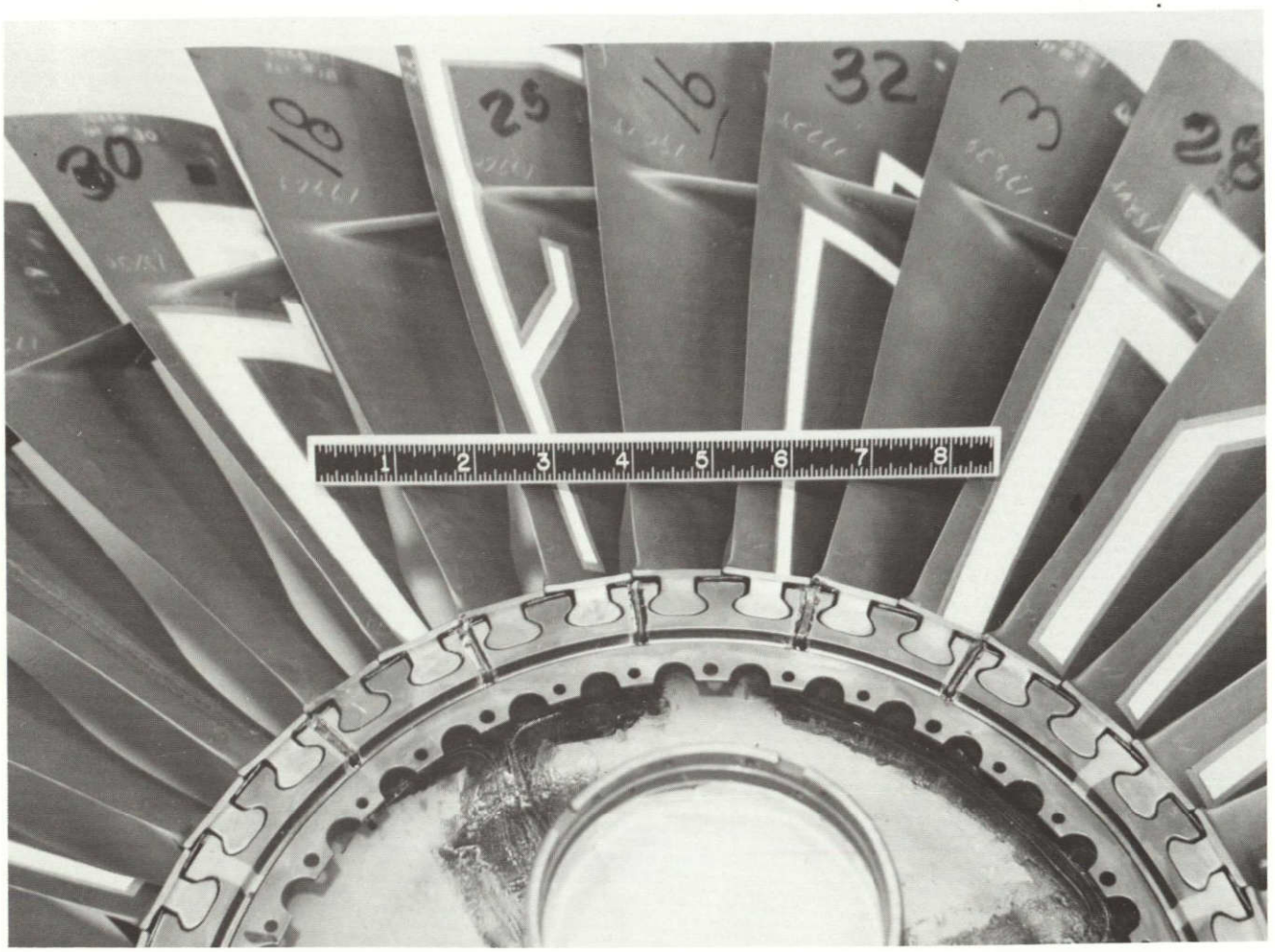

Figure A-1 Section of First Stage Instrumented Blade Assembly Before Testing - Concave Side

(77-444-0020-H)

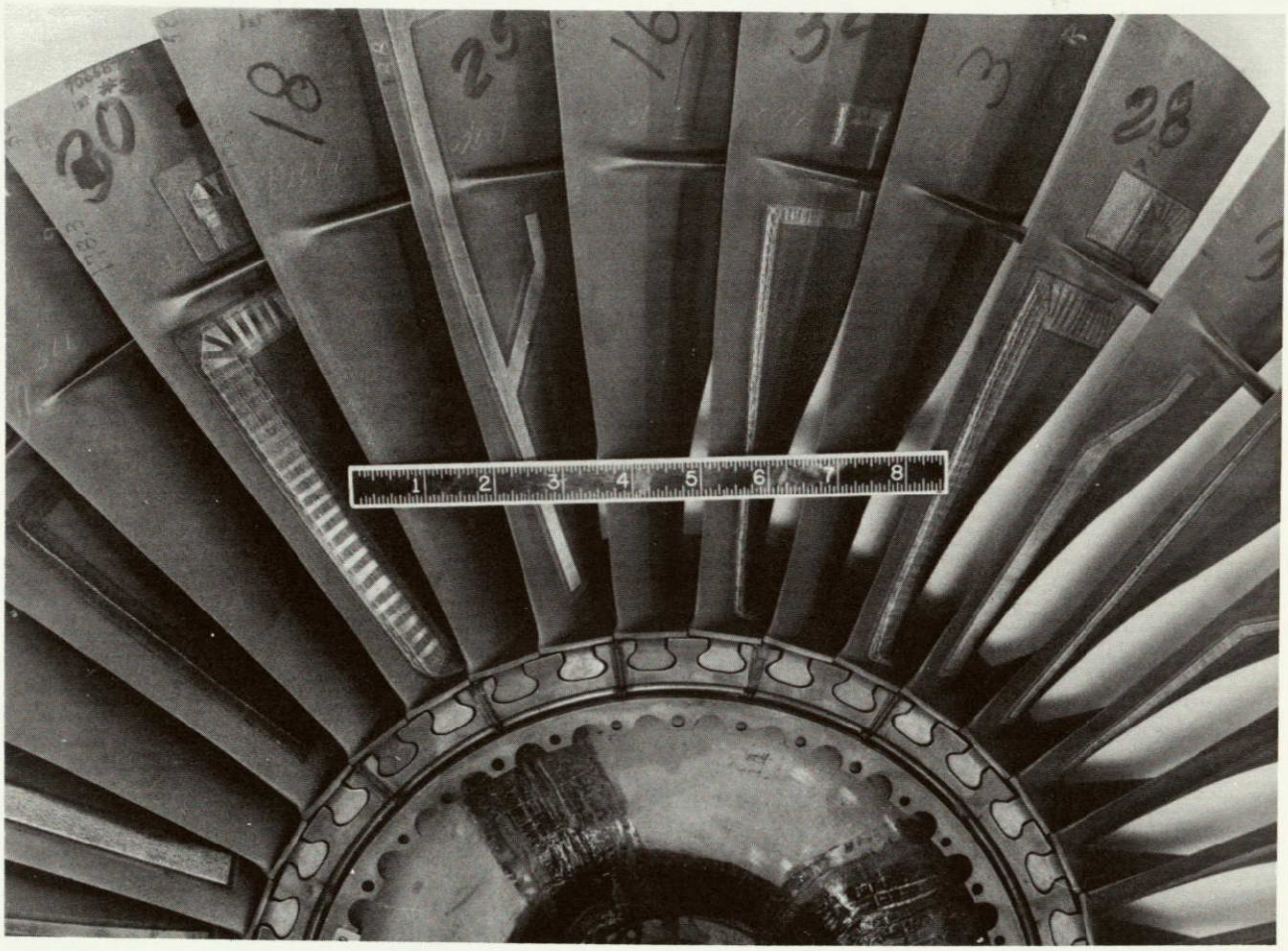

Figure A-2 Section of First Stage Instrumented Blade Assembly After Testing - Convex Side

(77-444-0337-I)

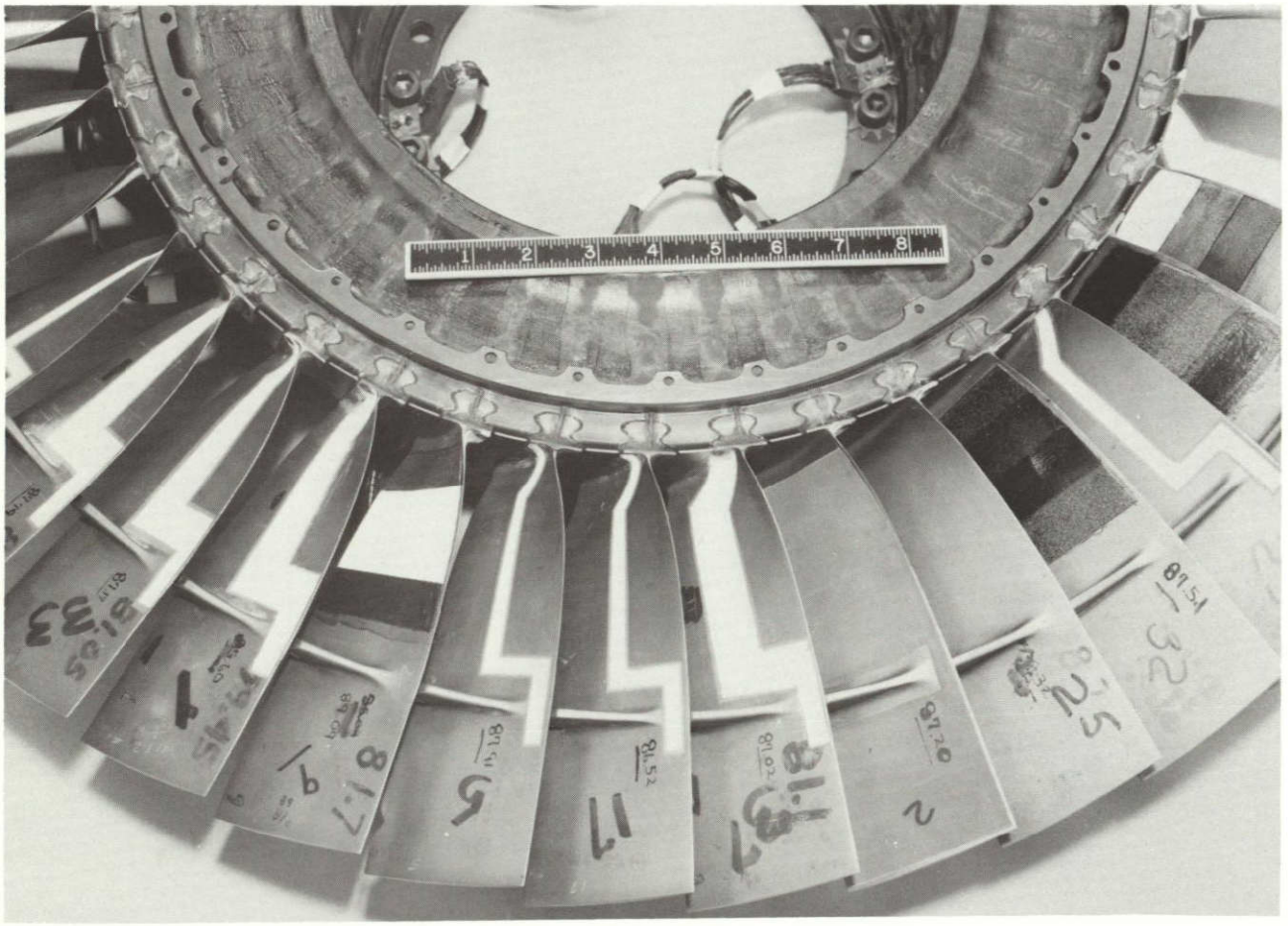

Figure A-3 Section of Third Stage Instrumented Blade Assembly Before Testing - Concave Side

(77-444-0020-D)

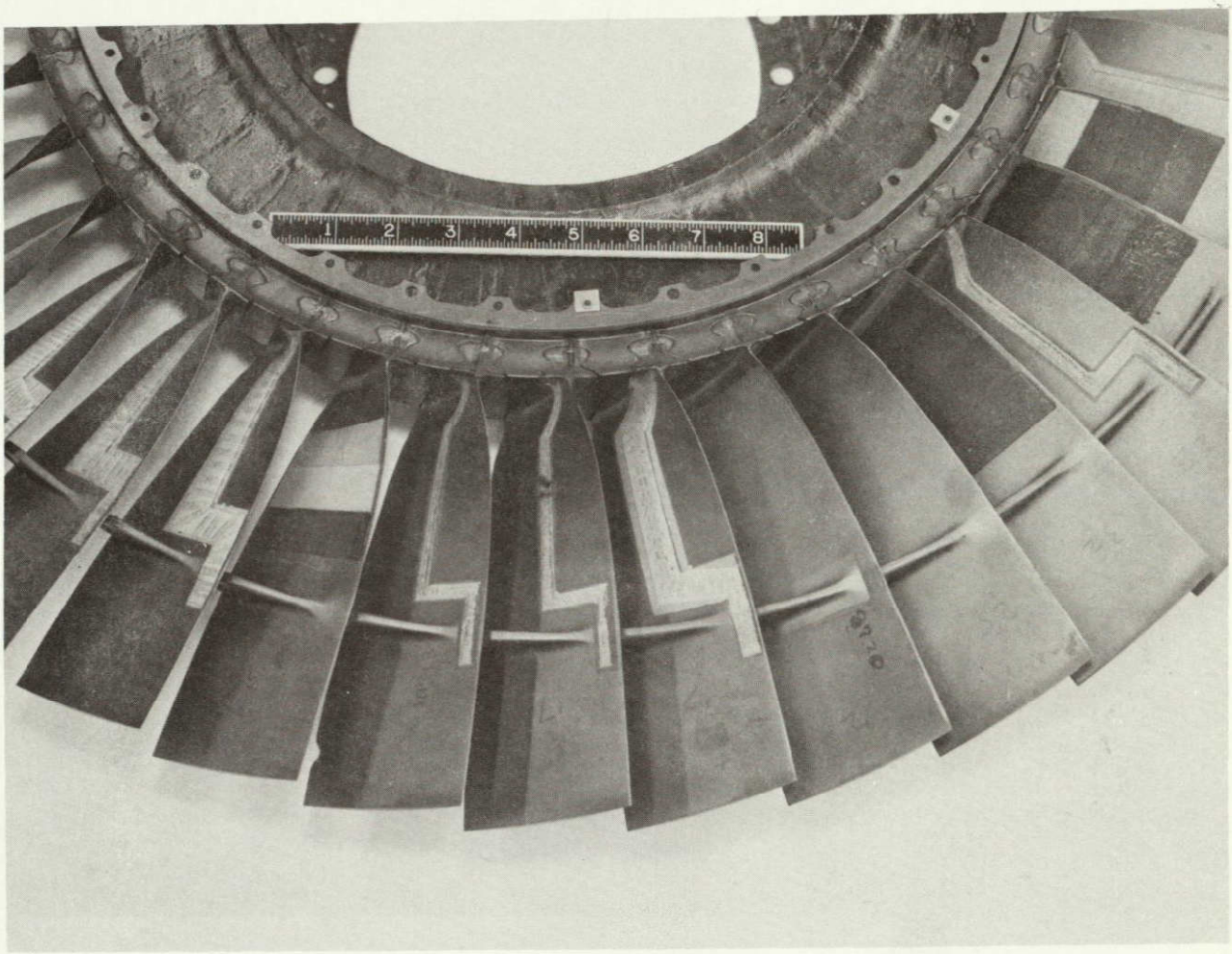

Figure A-4 Section of Third Stage Disk Lead Wire Routing
(77-444-0020-F)

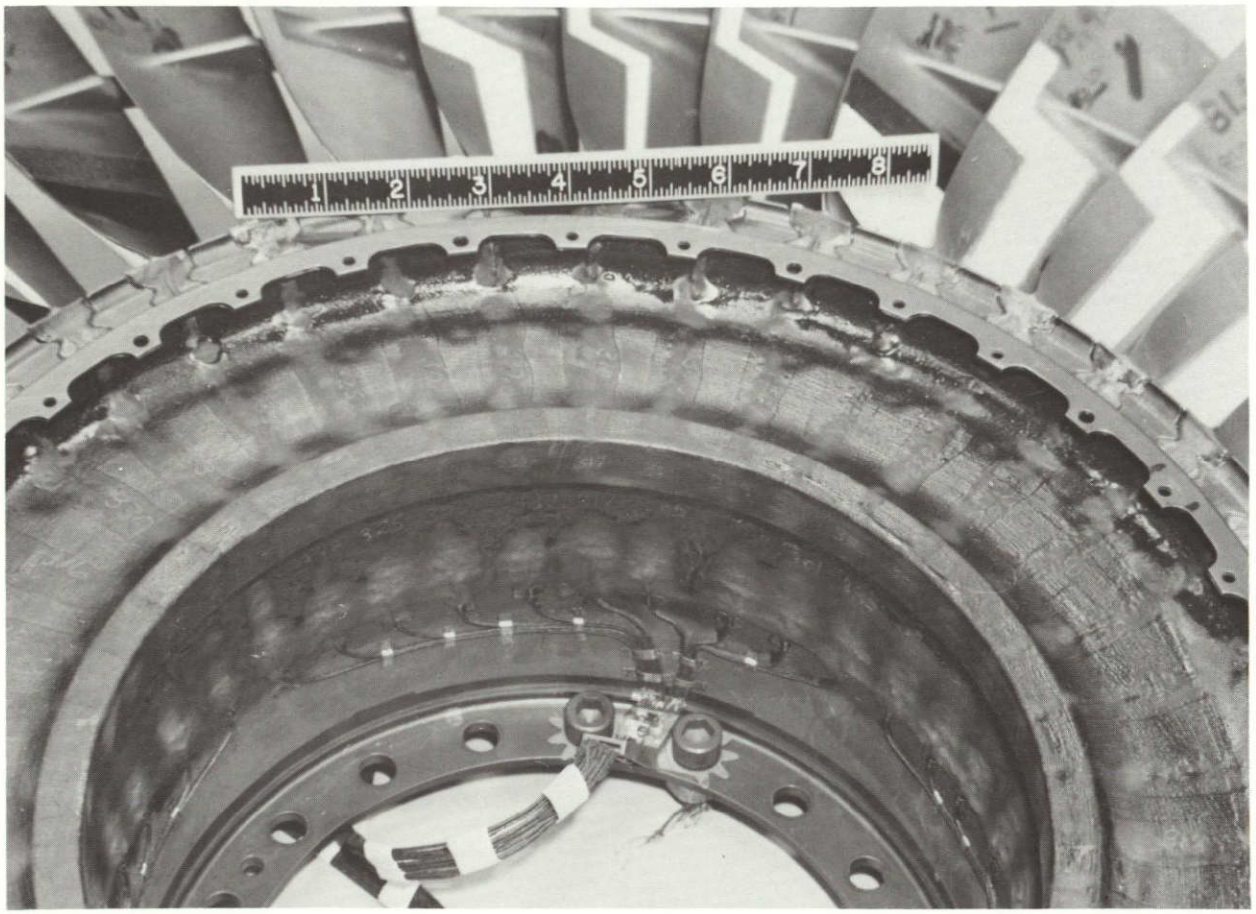

Figure A-5 Section of Third Stage Instrumented Blade Assembly After Testing - Concave Side

(78-444-0337-C)

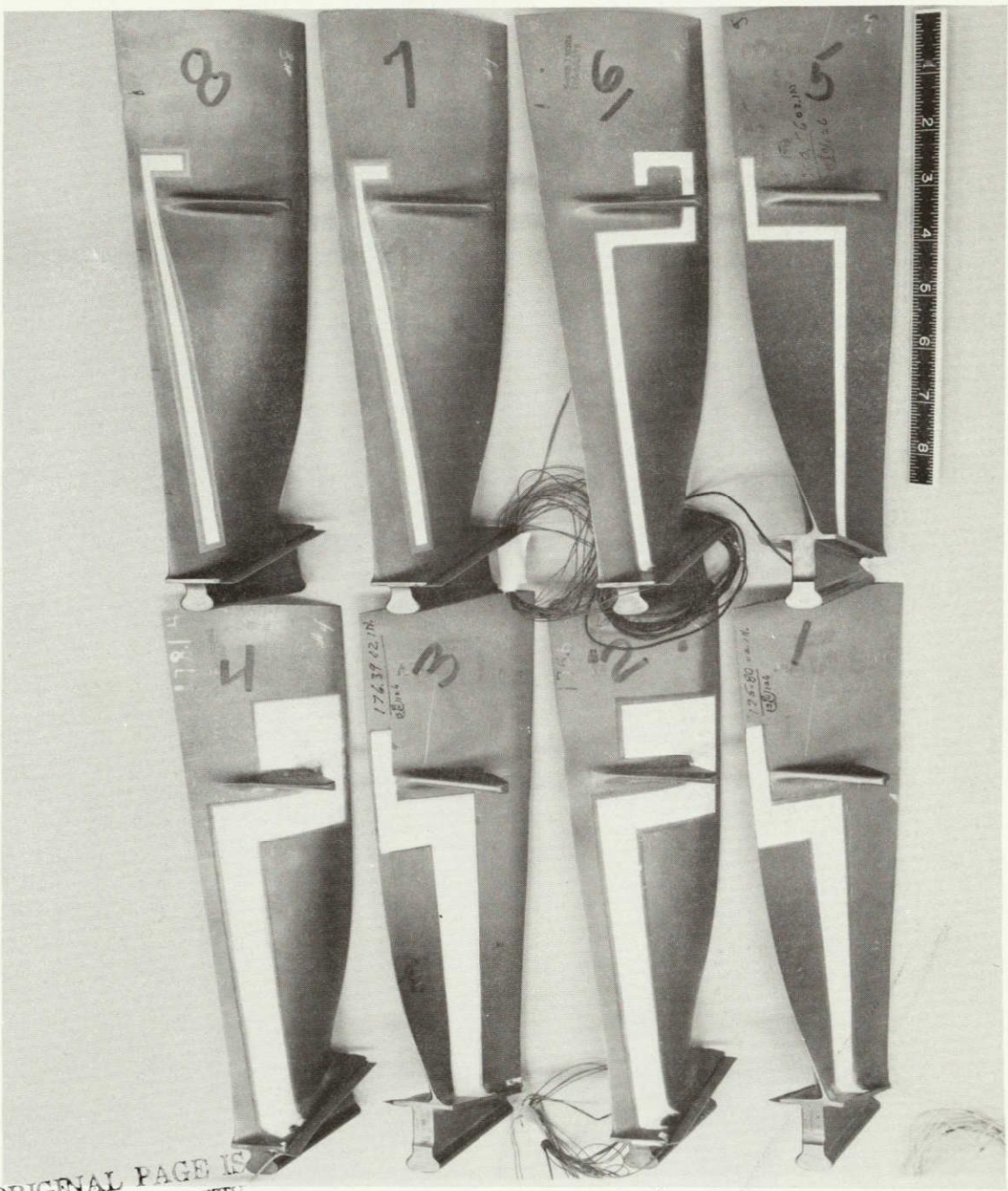

Figure A-6 Instrumented First Stage Blades S/N 1 Through 8 Before Testing (77-444-4001-F)

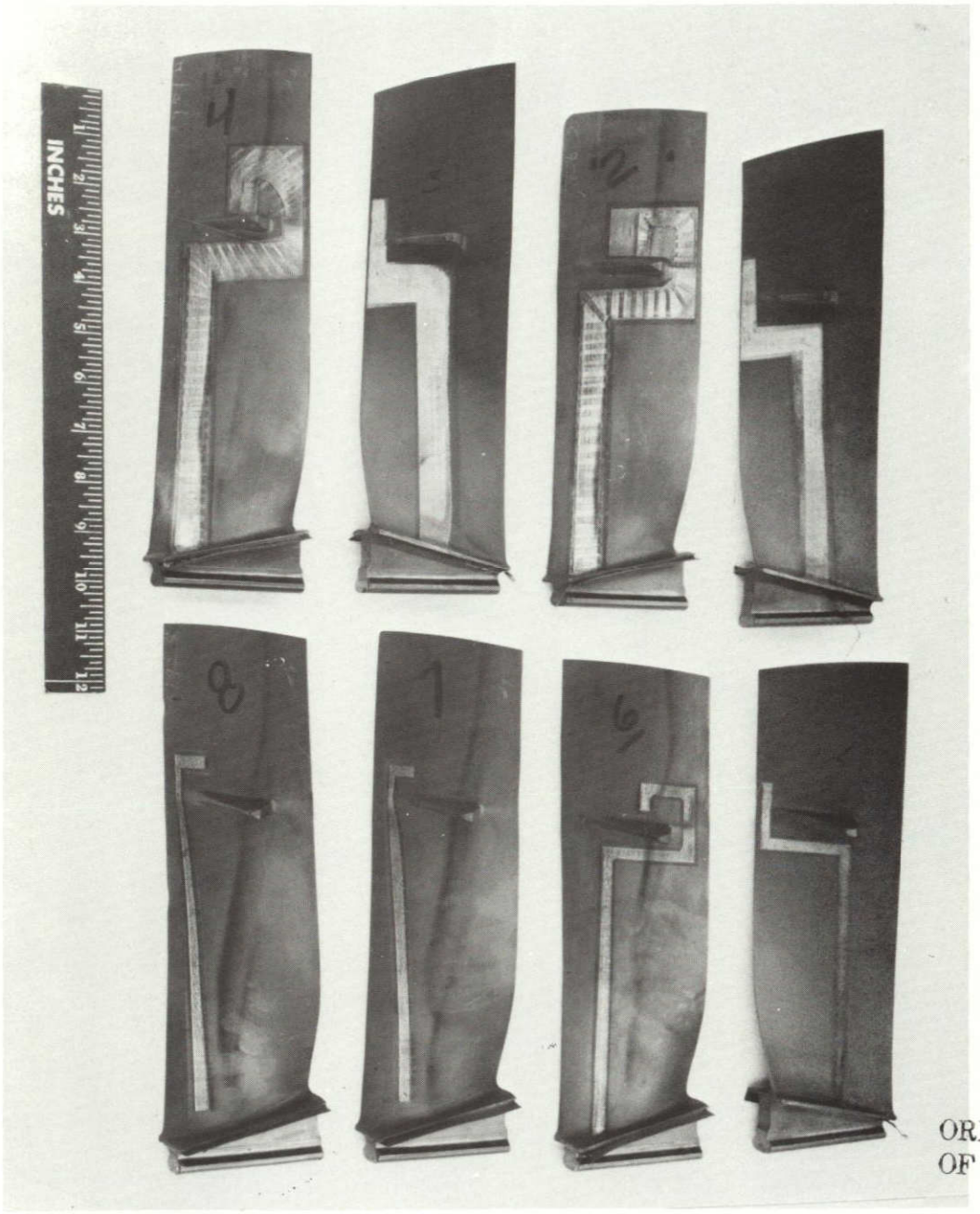

Figure A-7 Instrumented First Stage Blades S/N 1 Through 8 After Testing (78-444-4233-A)

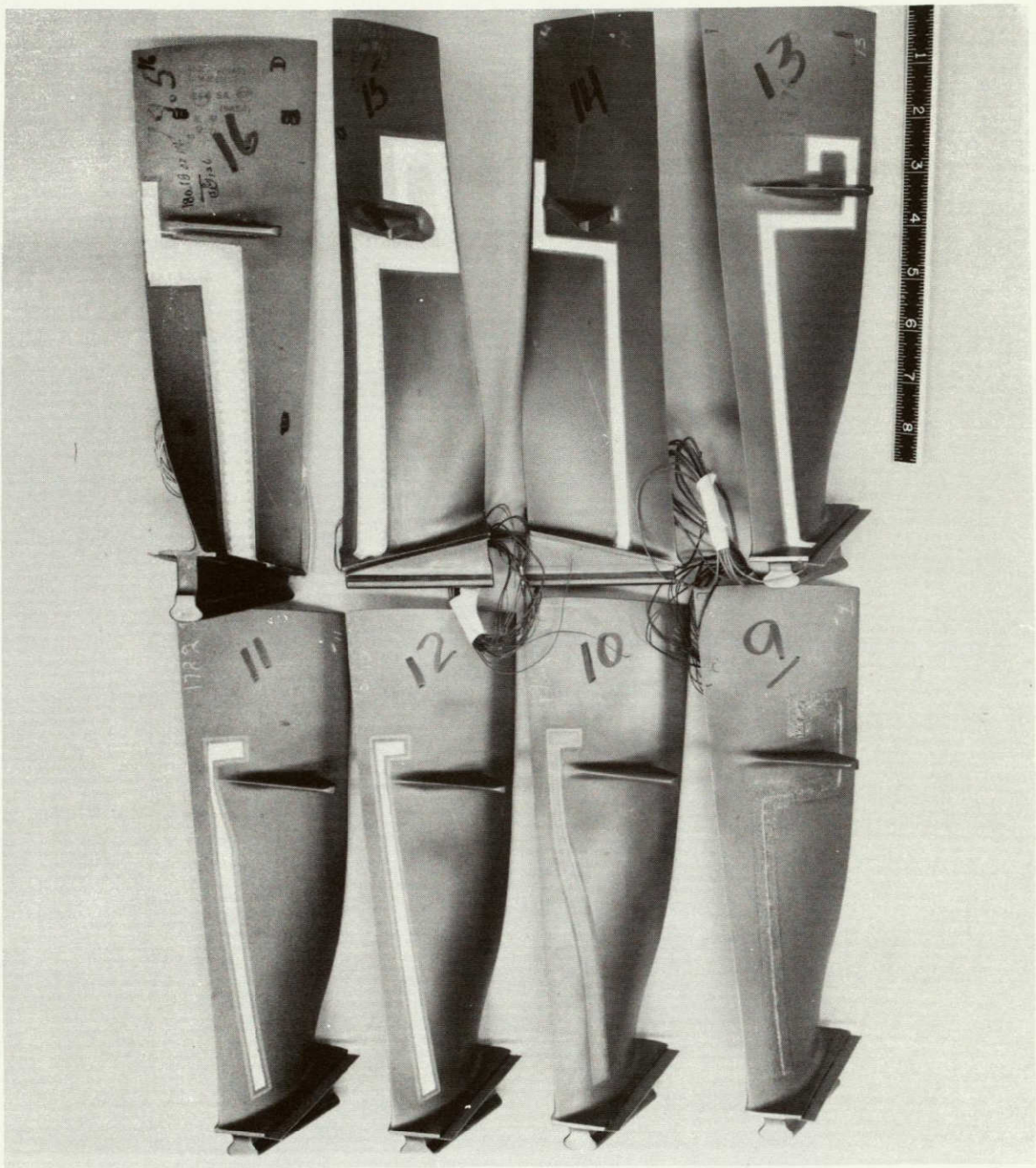

Figure A-8 Instrumented First Stage Blades S/N 9 Through 16 Before Testing (77-444-4001-G)

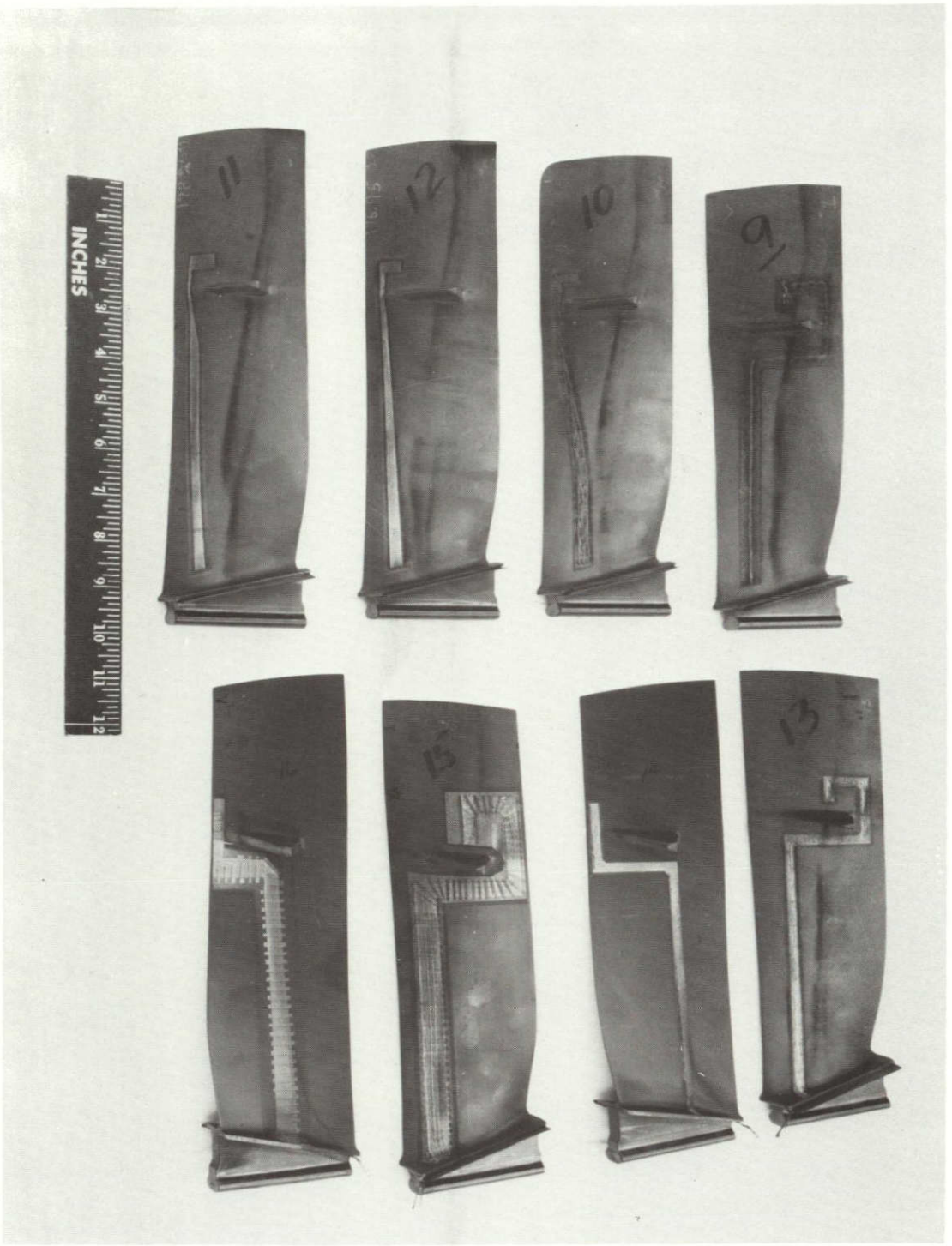

Figure A-9 Instrumented First Stage Blades S/N 9 Through 16 After Testing (78-444-4233-B)

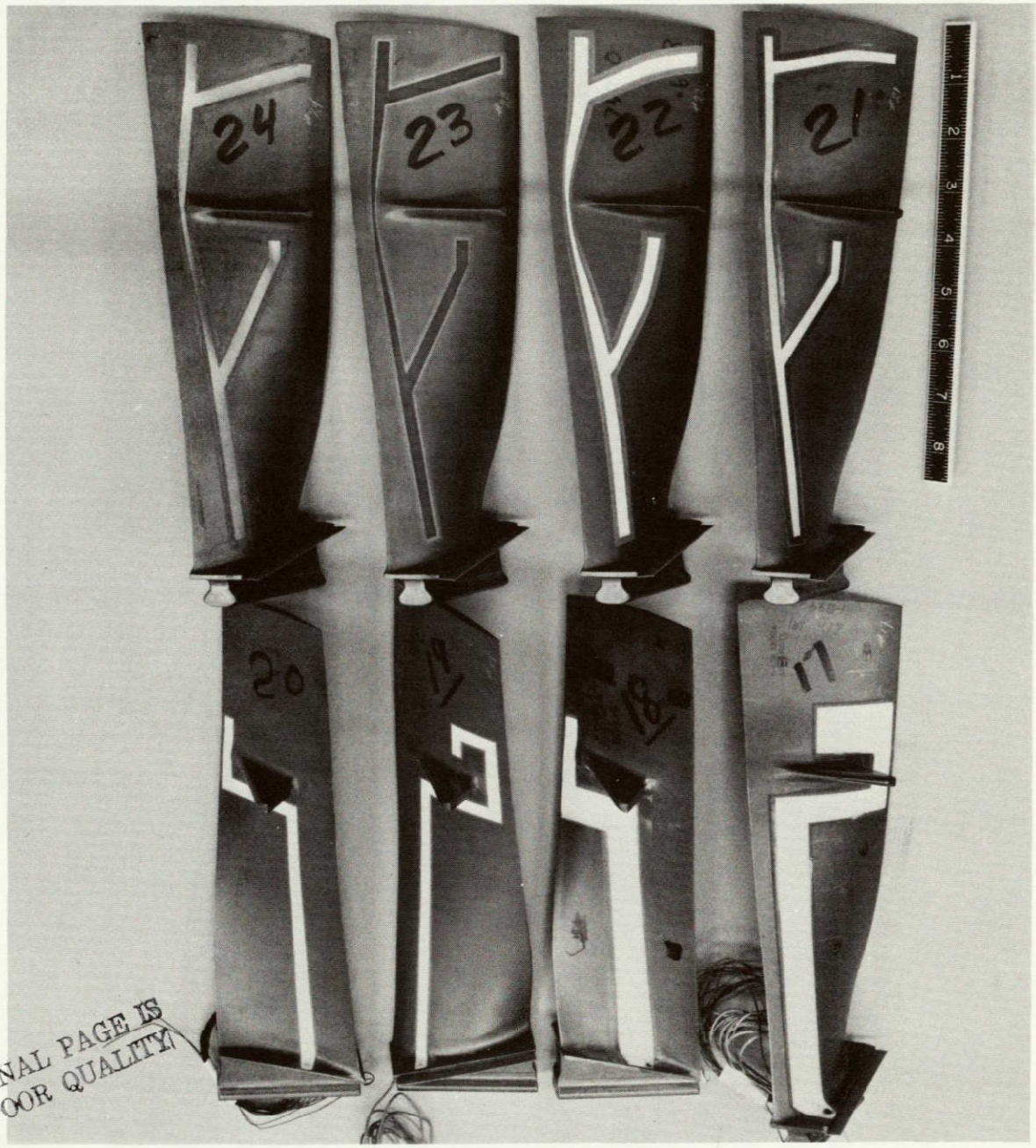

Figure A-10 Instrumented First Stage Blades S/N 17 Through 24 Before Testing (77-444-4001-H)

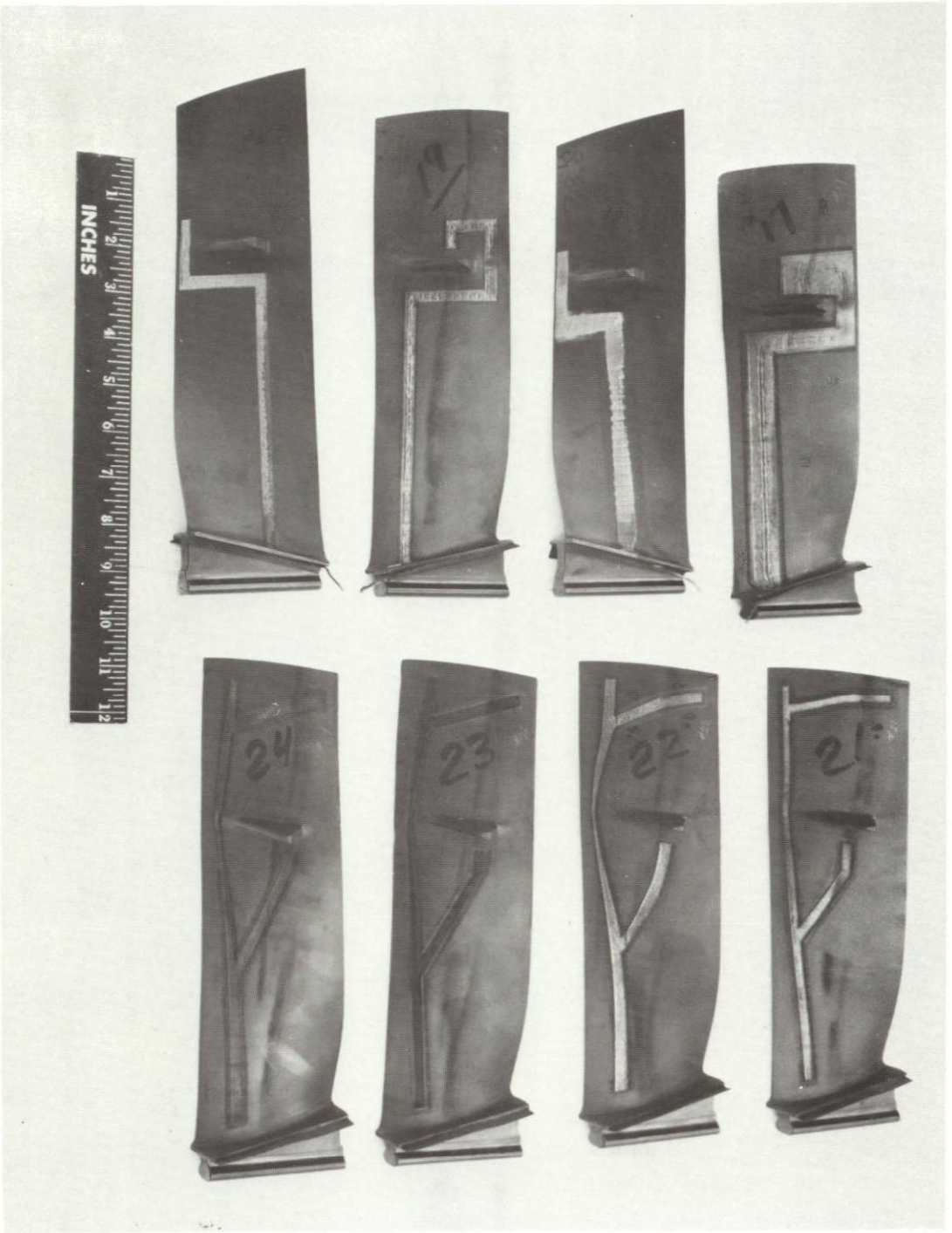

Figure A-11 Instrumented First Stage Blades S/N 17 Through 24 After Testing (78-444-4233-C)

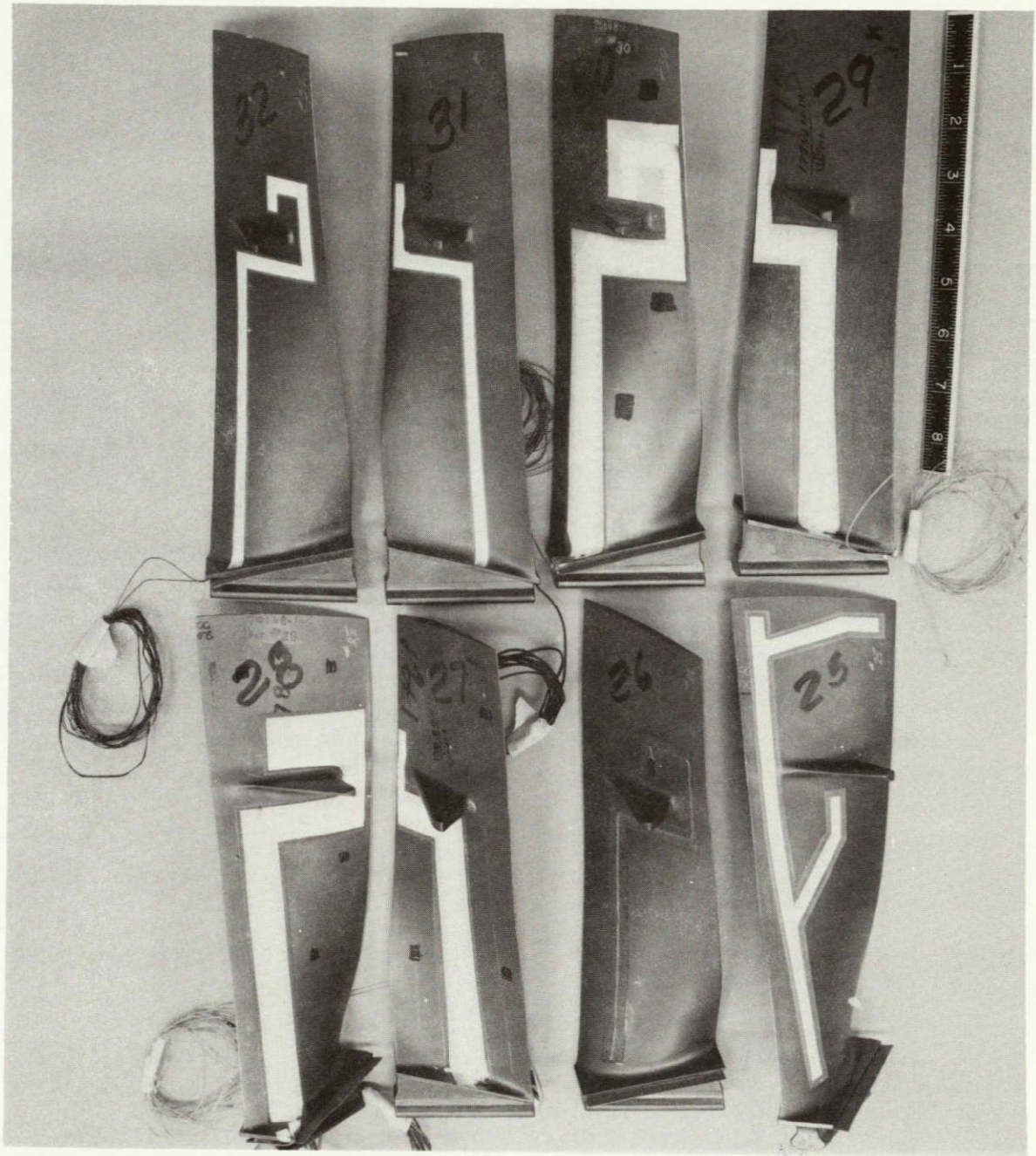

Figure A-12 Instrumented First Stage Blades S/N 25 Through 32 Before Testing (77-444-4001-I)

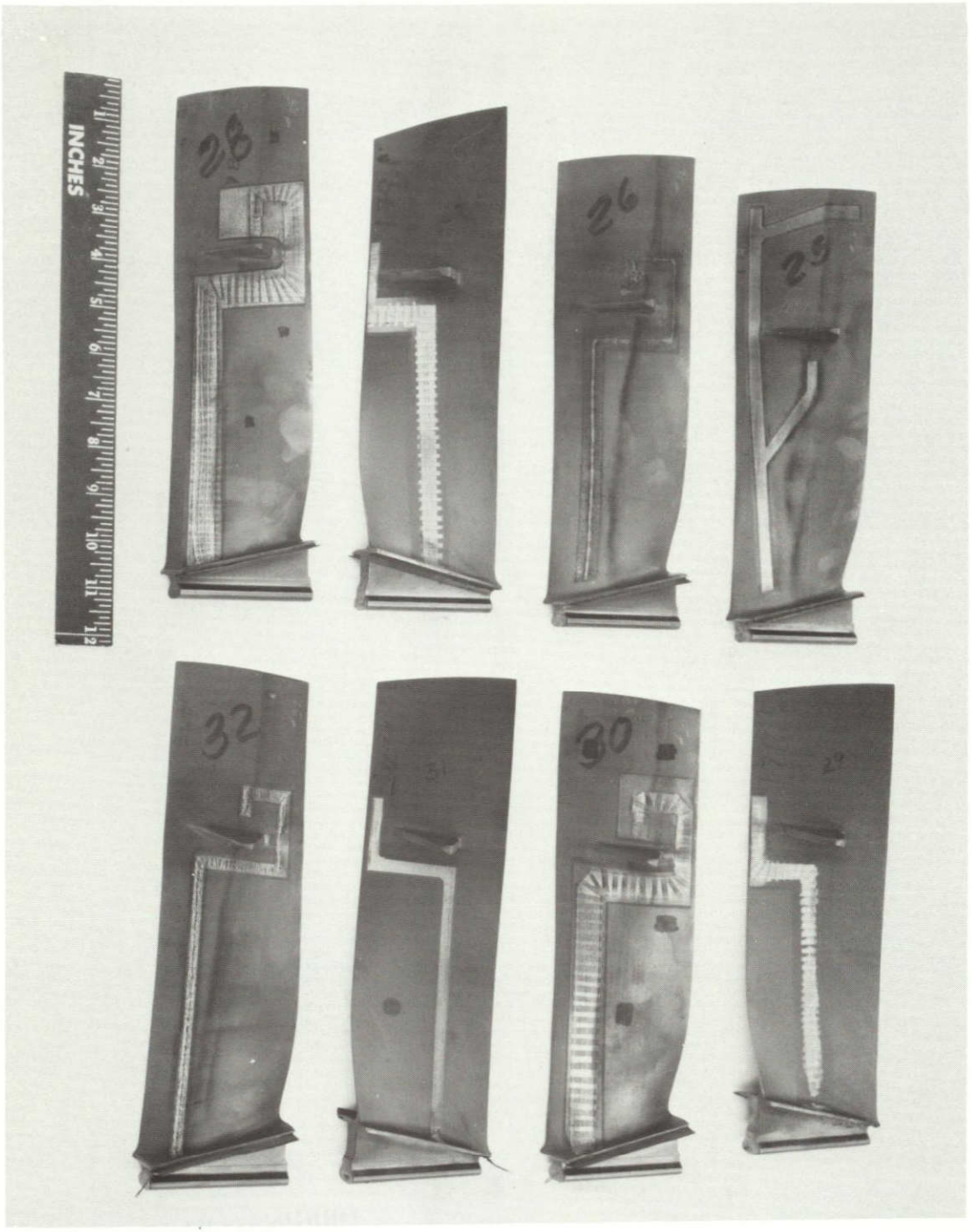

Figure A-13 Instrumented First Stage Blades S/N 25 Through 32 After Testing (78-444-4233-D)

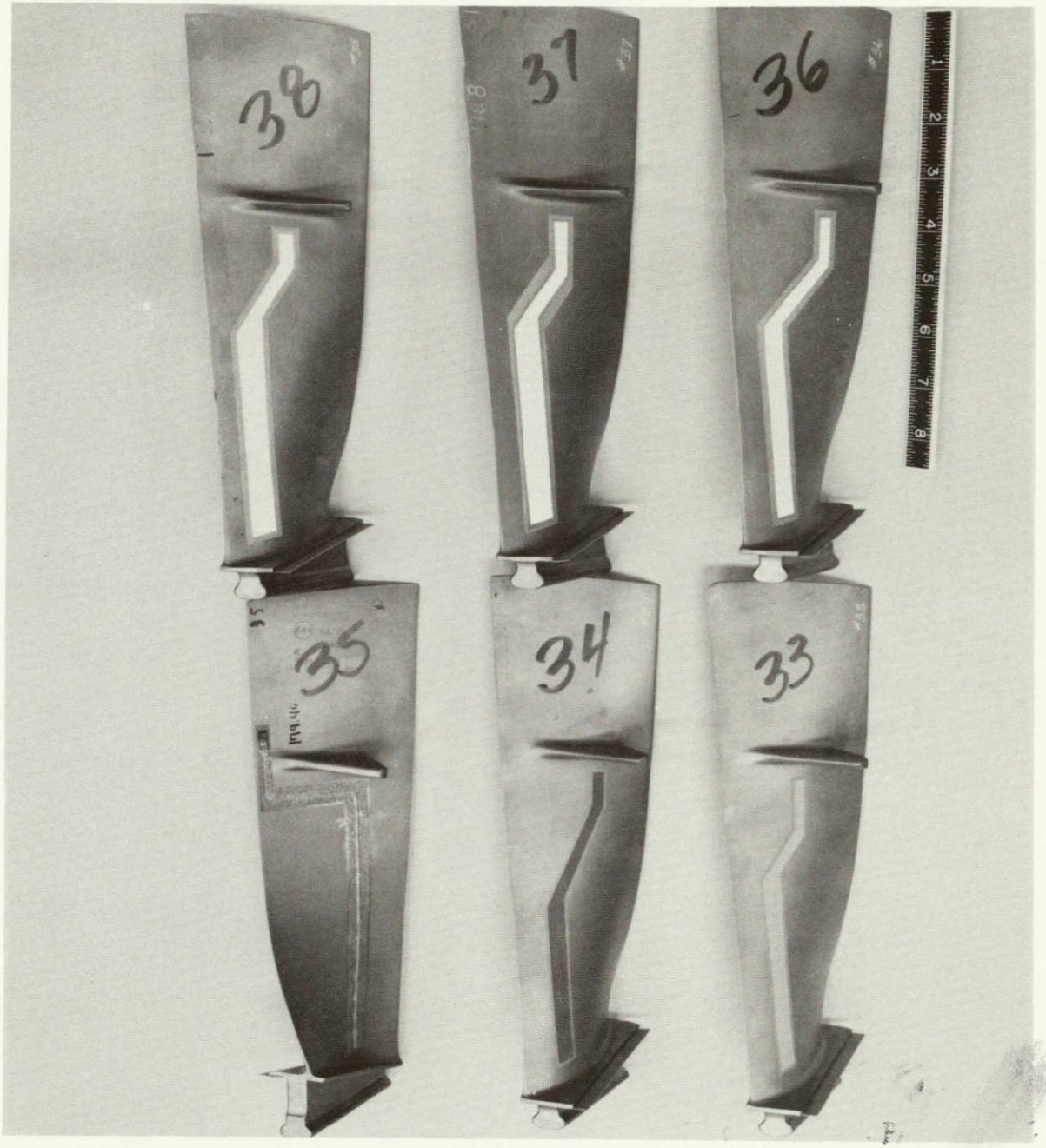

Figure A-14 Erosion Patch First Stage Blades S/N 33 Through 38 Before Testing (77-444-4001-J)

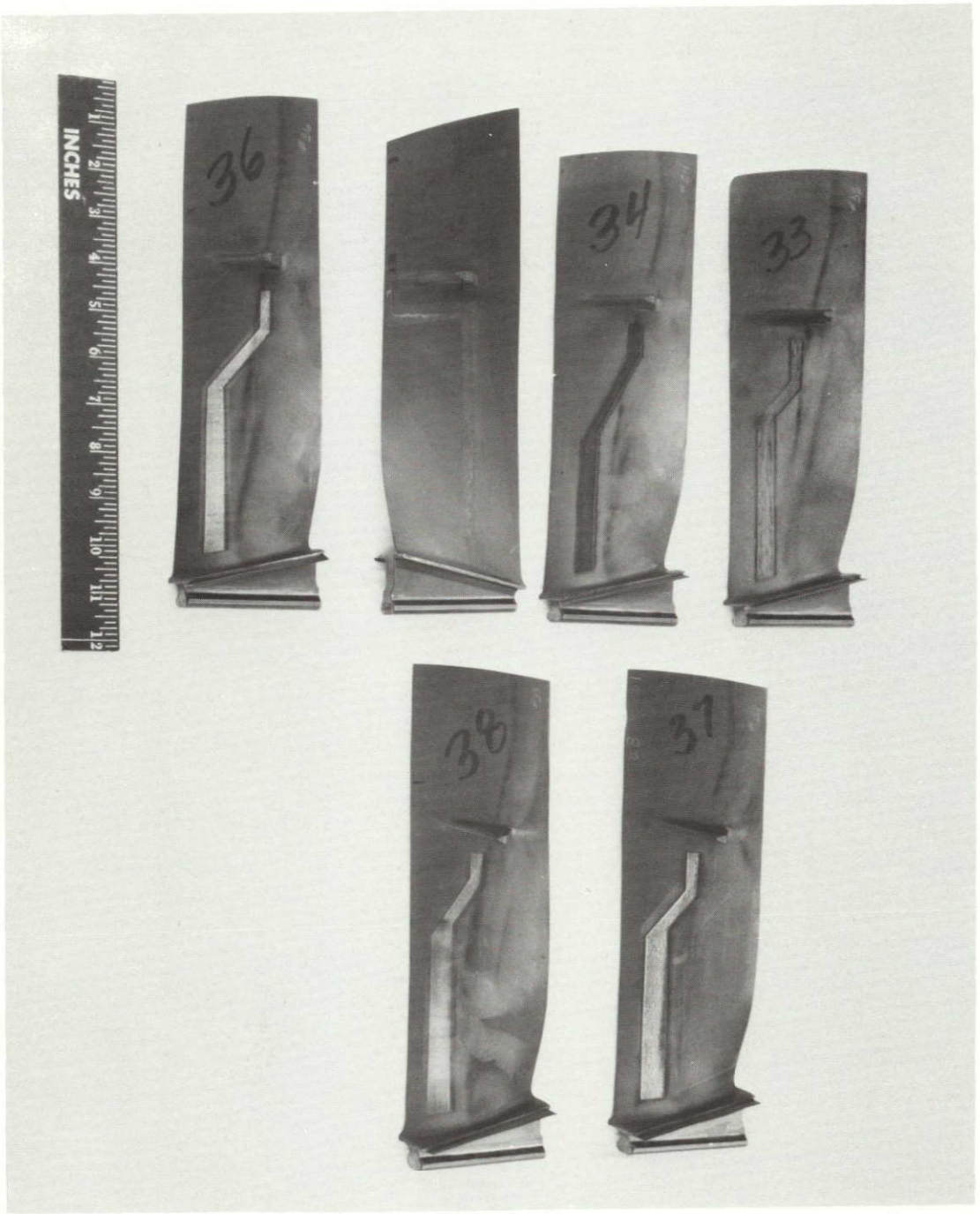

Figure A-15 Erosion Patch First Stage Blades S/N 33 Through 38 After Testing (78-444-4233-E)

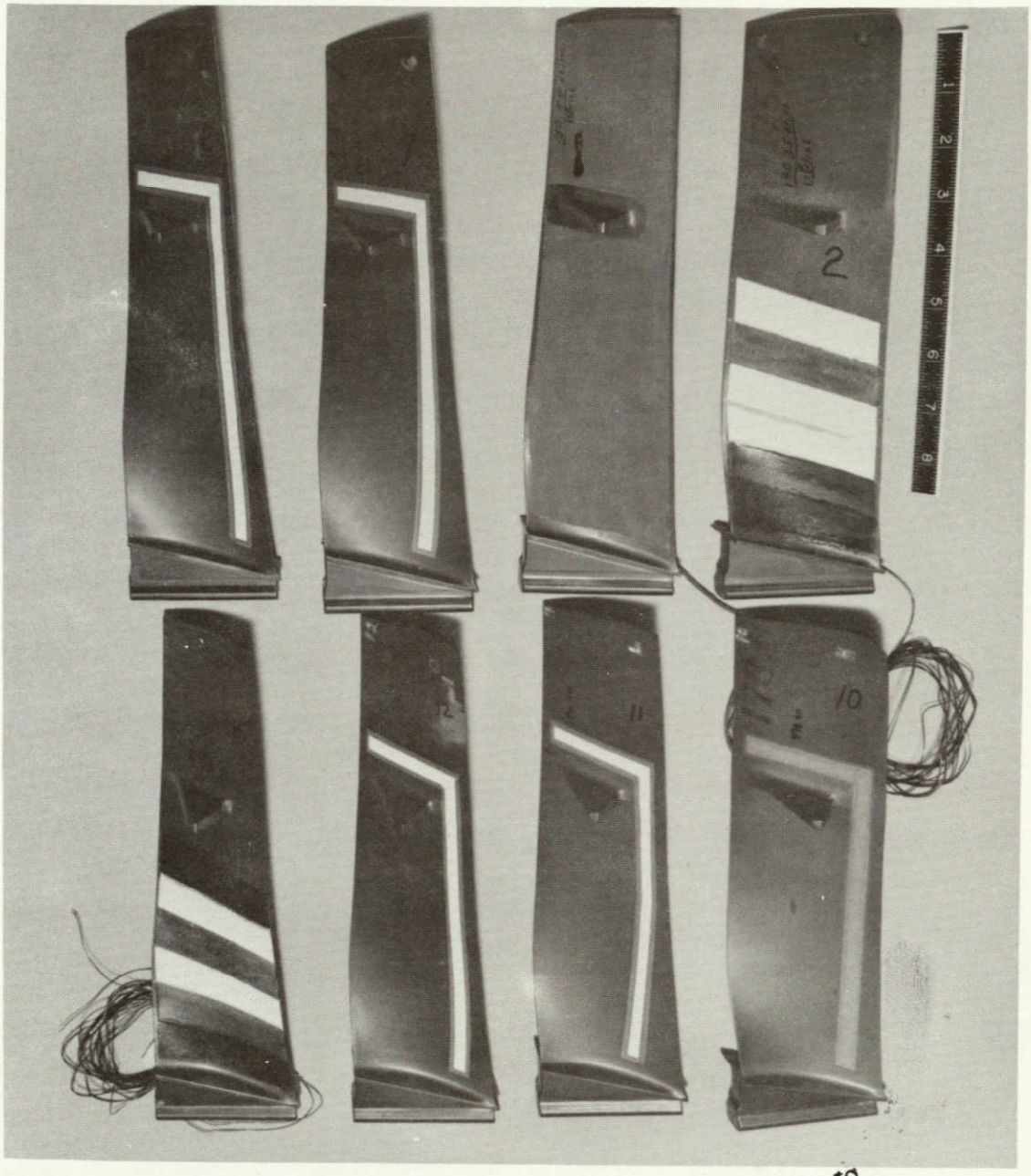

Figure A-16 Erosion Patch First Stage Blades S/N 2, 4, 7, 8, 10, 11, 12, 15 Before Testing (77-444-0004-A)

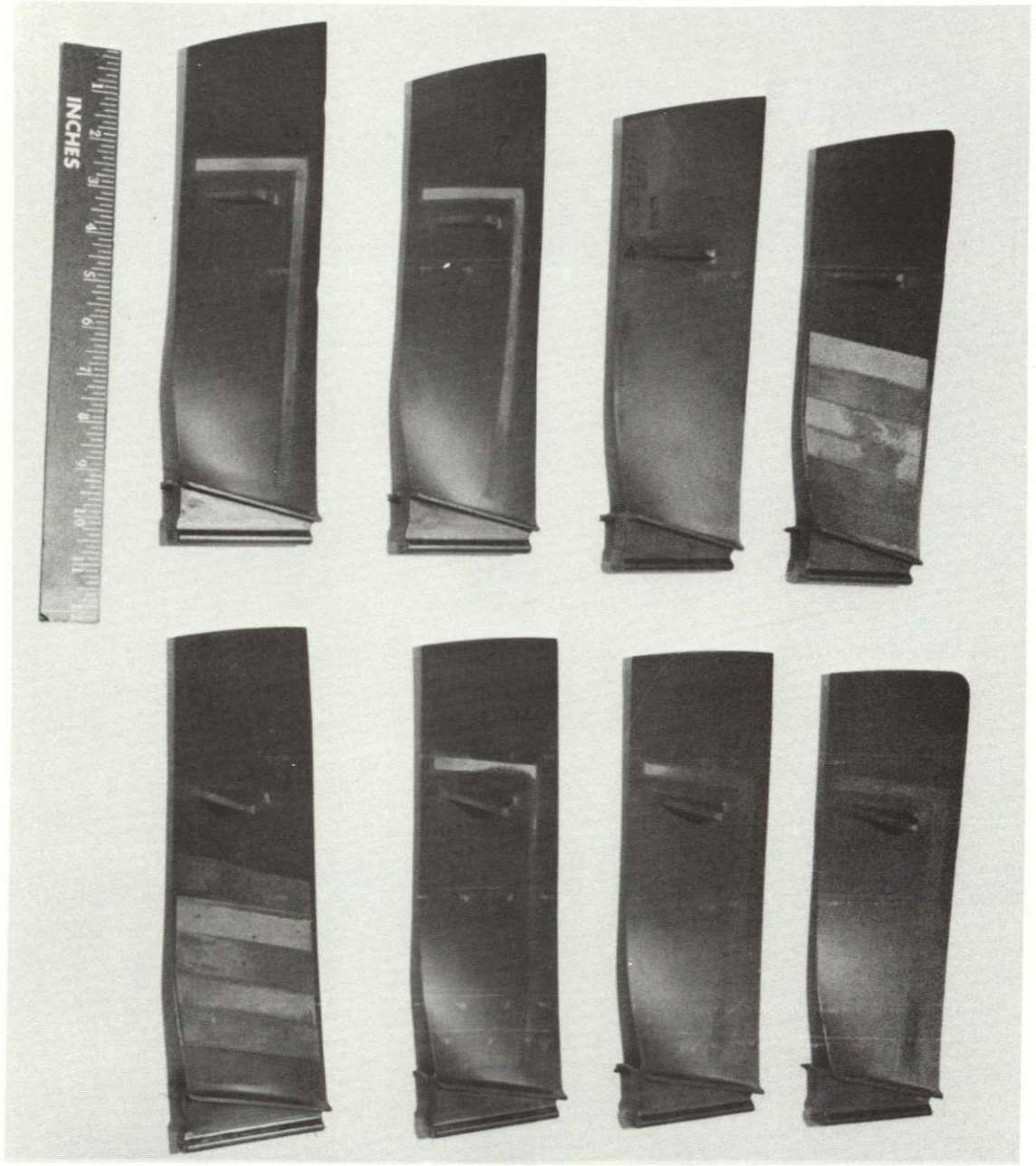

Figure A-17 Erosion Patch First Stage Blades S/N 2, 4, 7, 8, 10, 11, 12, 15 After Testing (78-444-0374-A)

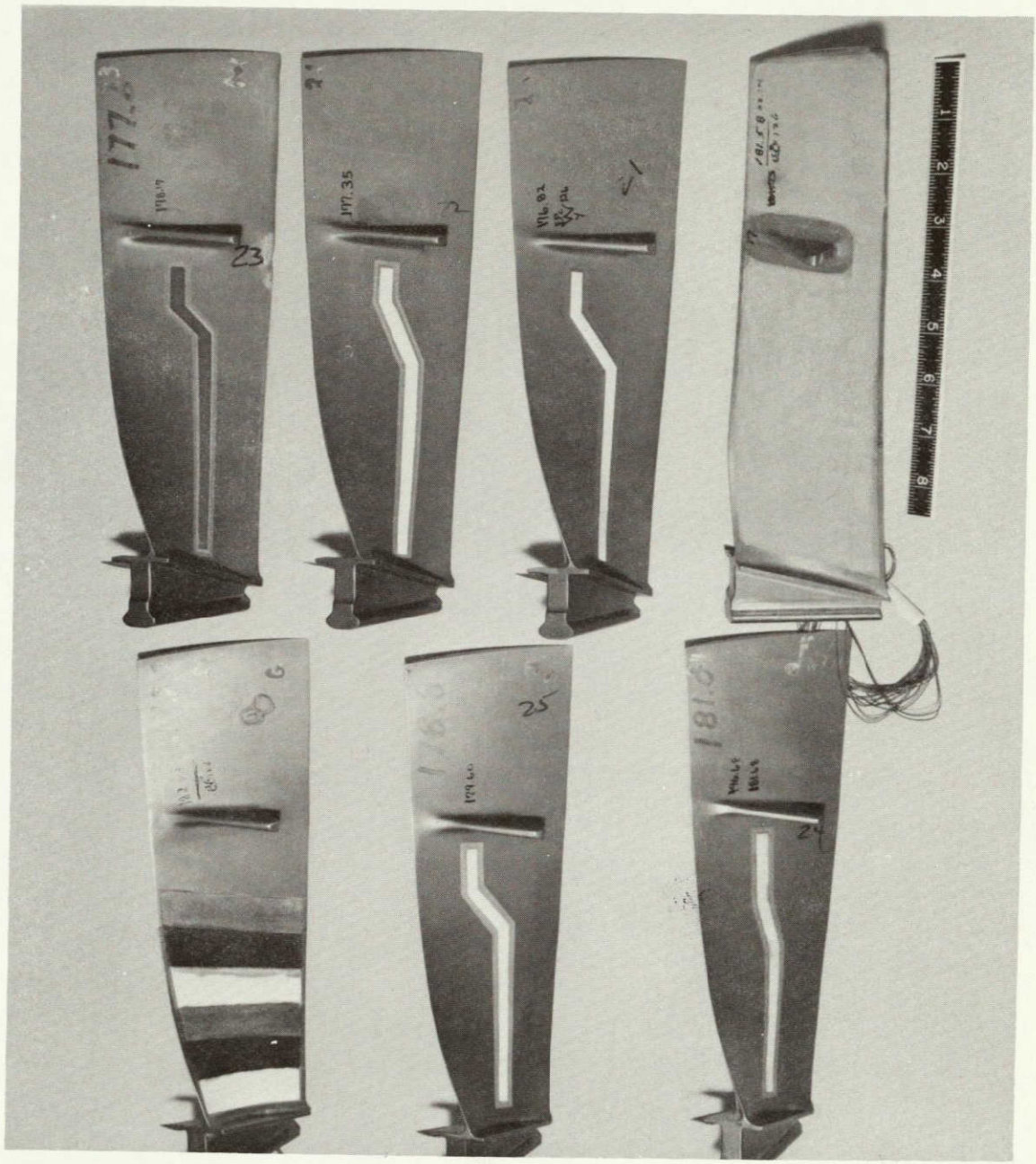

Figure A-18 Erosion Patch First Stage Blades S/N 17, 21, 22, 23, 24, 25, 28 Before Testing (77-444-0004-B)

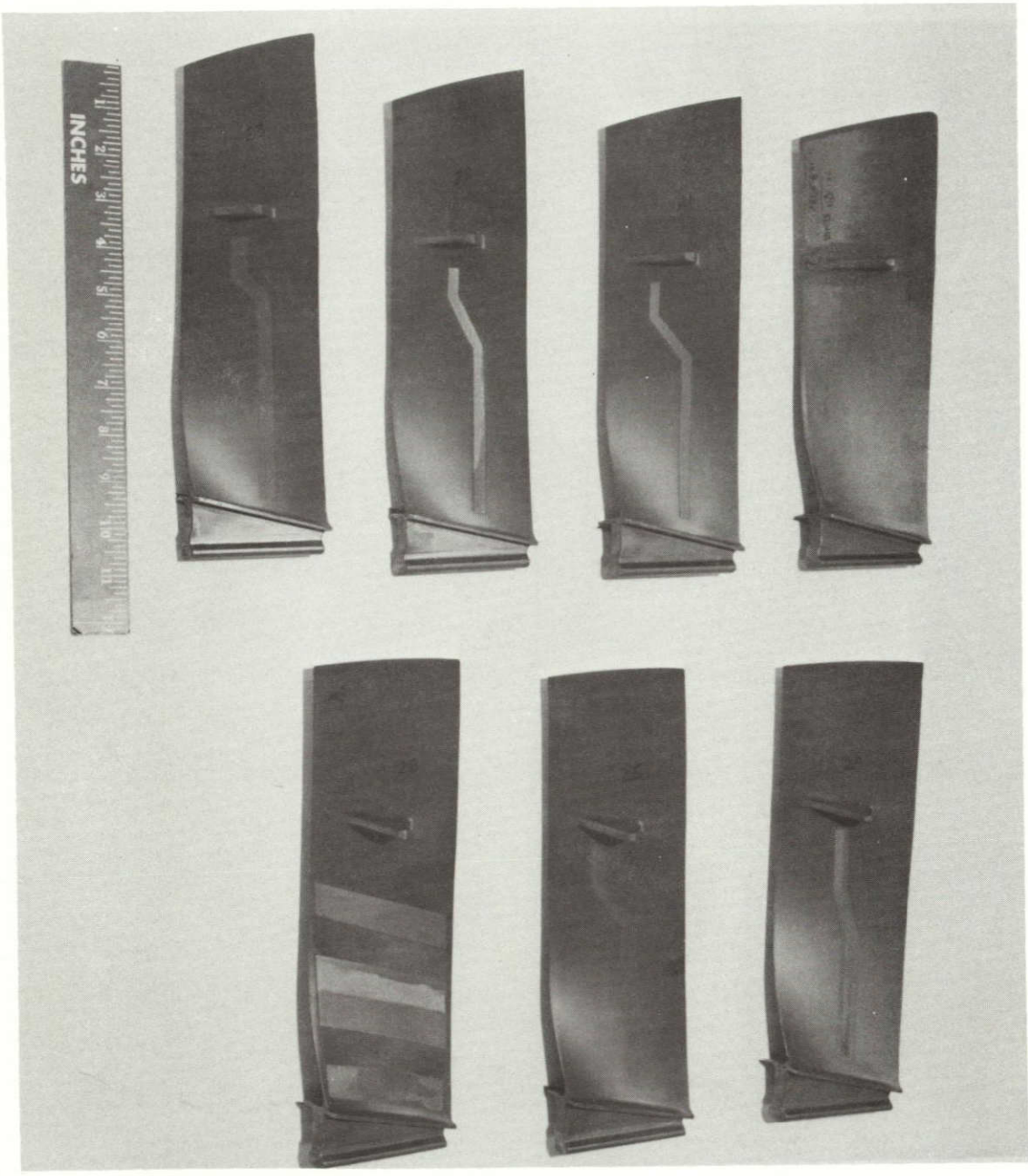

Figure A-19 Erosion Patch First Stage Blades S/N 17, 21, 22, 23, 24, 25, 28 After Testing (78-444-0374-B)

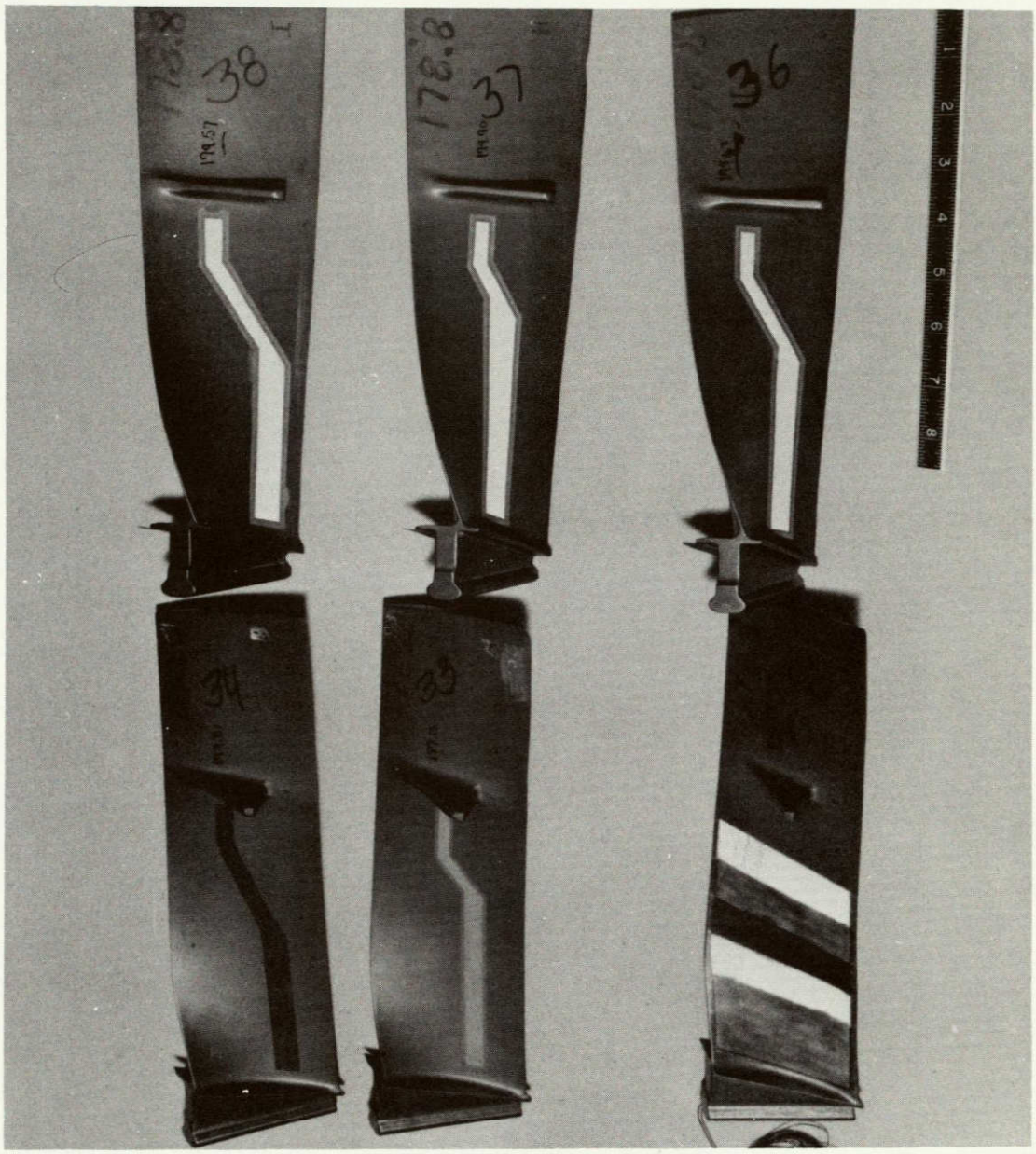

Figure A-20 Erosion Patch First Stage Blades S/N 30, 33, 34, 36, 37, 38 Before Testing (77-444-0004-C)

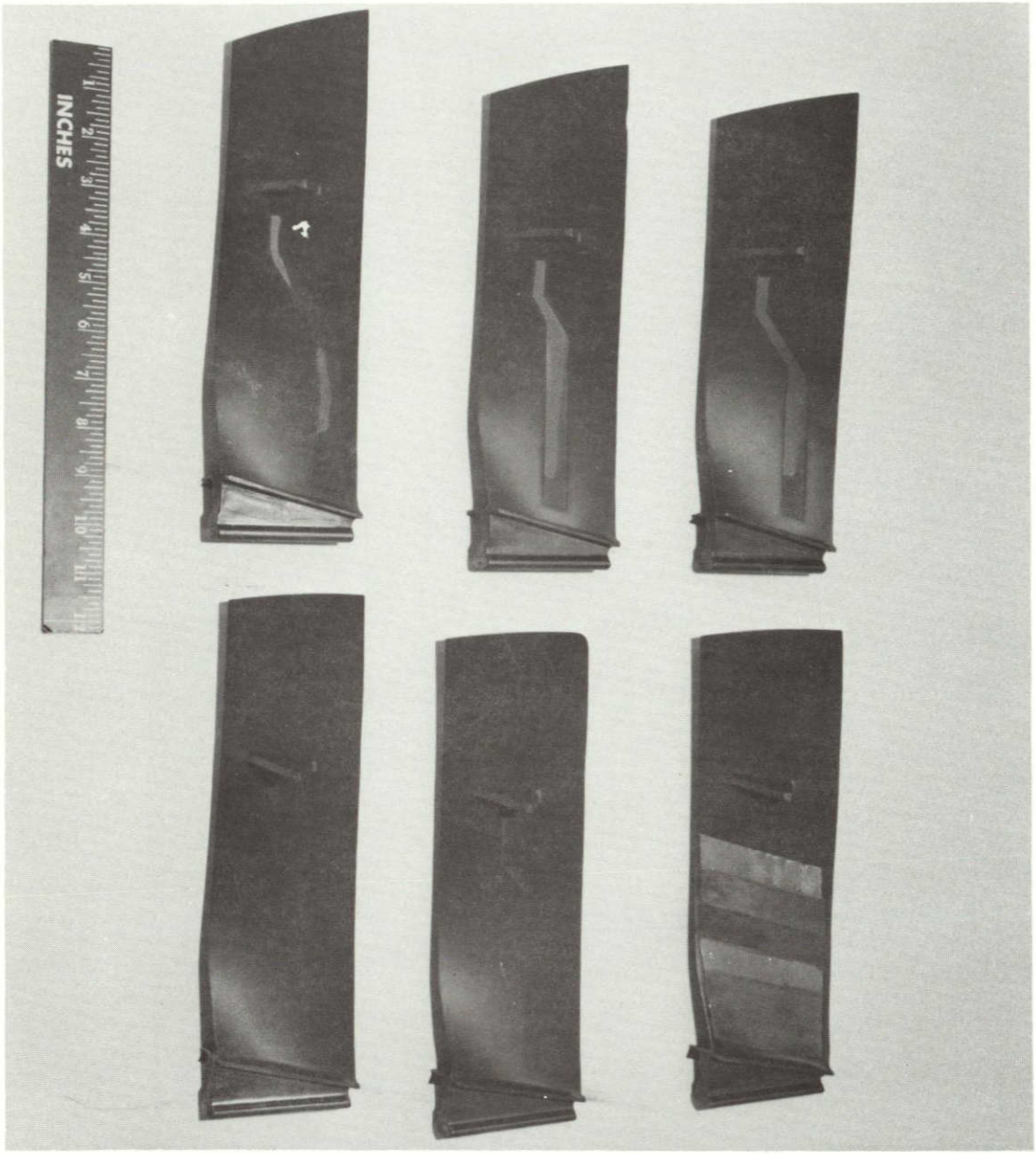

Figure A-21 Erosion Patch First Stage Blades S/N 30, 33, 34, 36, 37, 38 After Testing (78-444-0374-C)

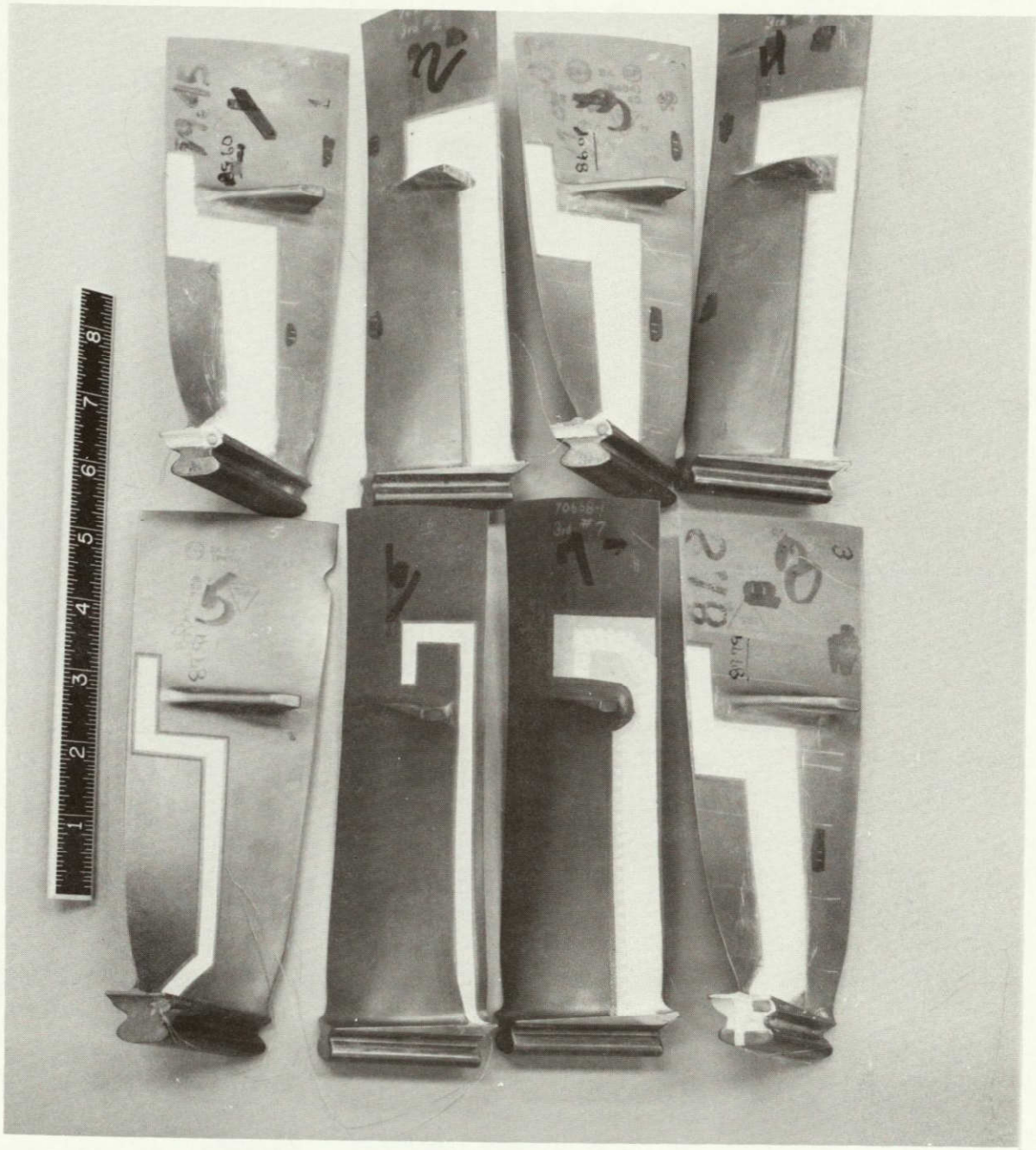

Figure A-22 Instrumented Third Stage Blades S/N 1 Through 8 Before Testing (77-444-4001-A)

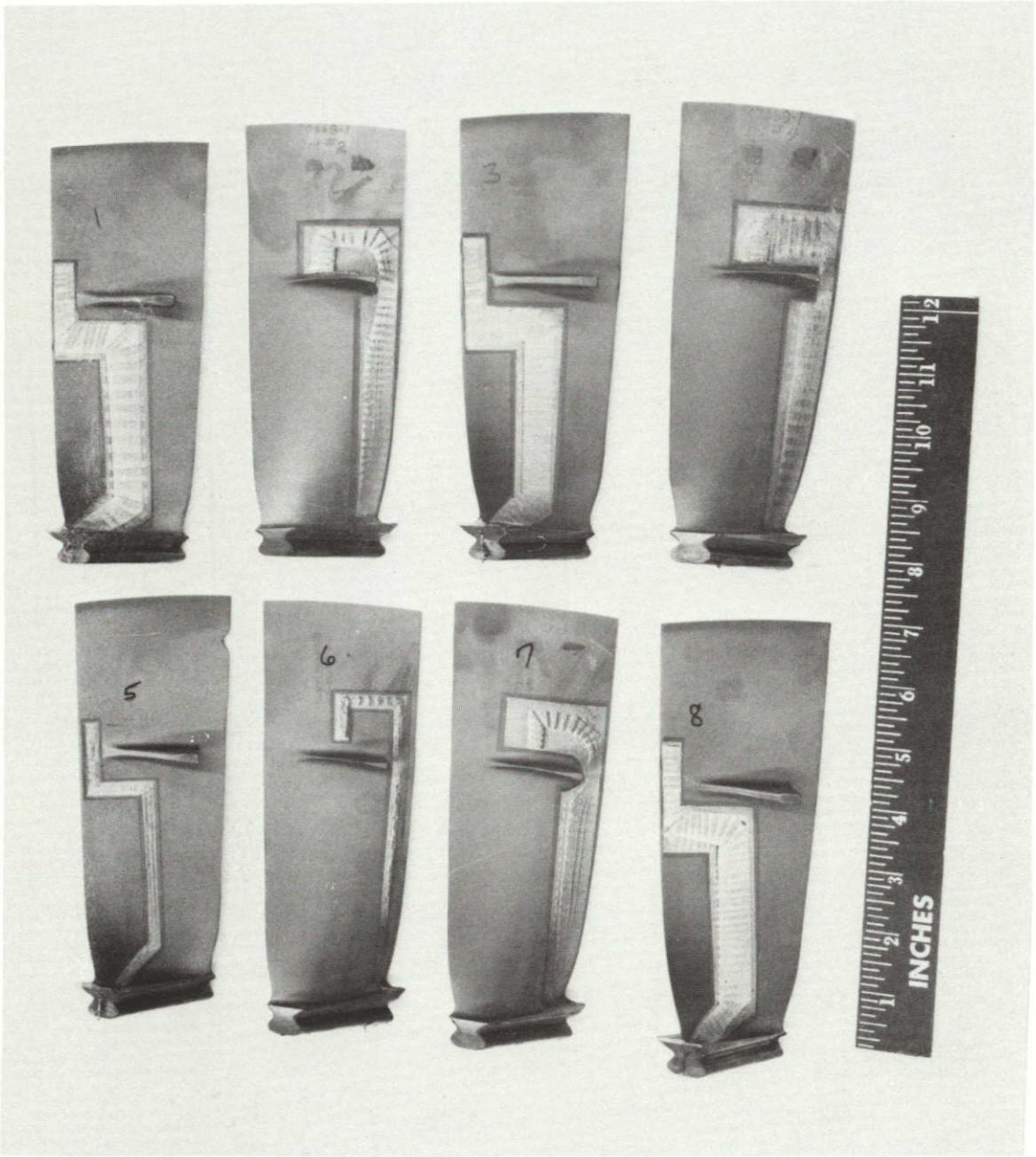

Figure A-23 Instrumented Third Stage Blades S/N 1 Through 8 After Testing (78-444-4233-F)

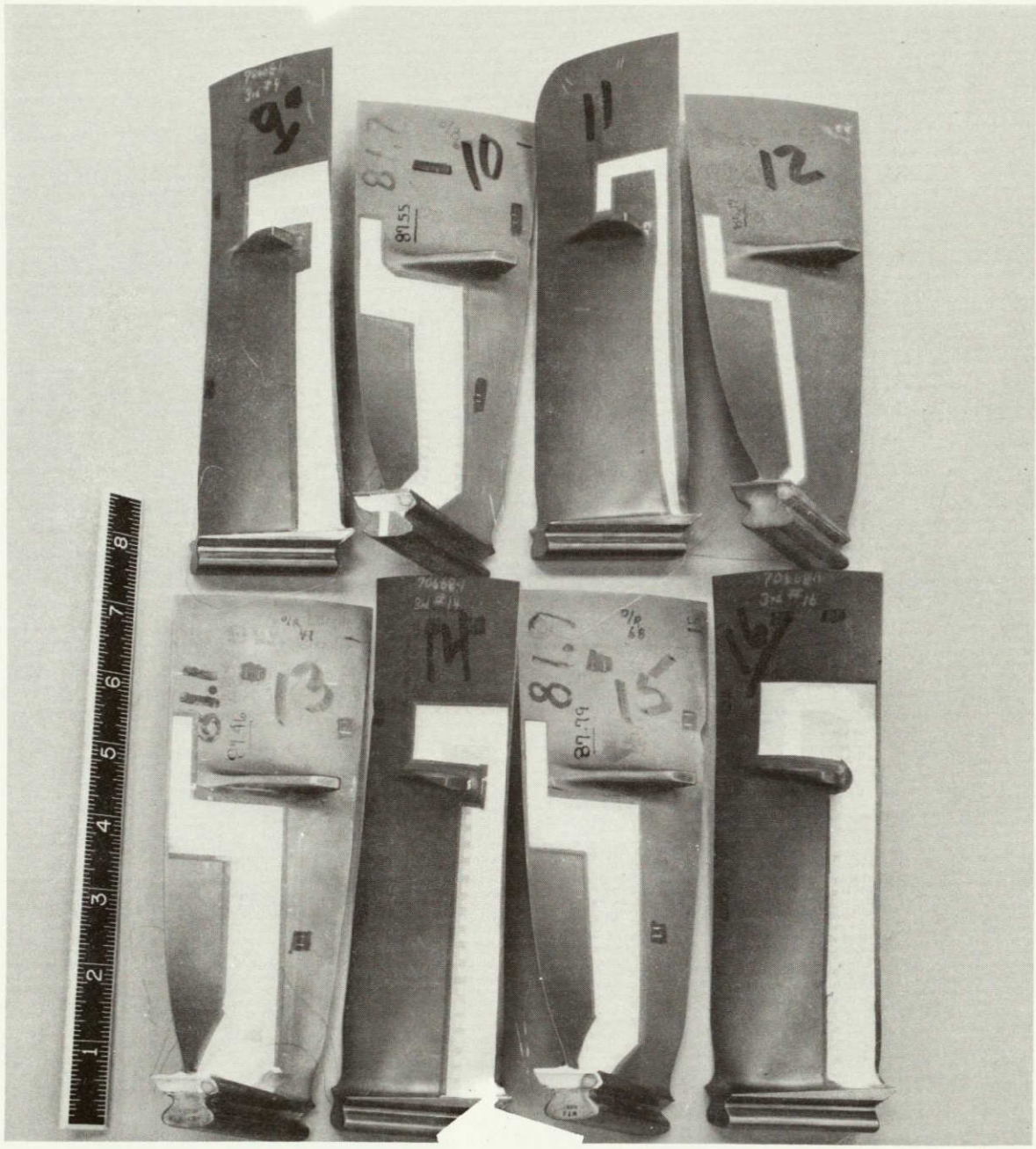

Figure A-24 Instrumented Third Stage Blades S/N 9 Through 16 Before Testing (77-444-4001-B)

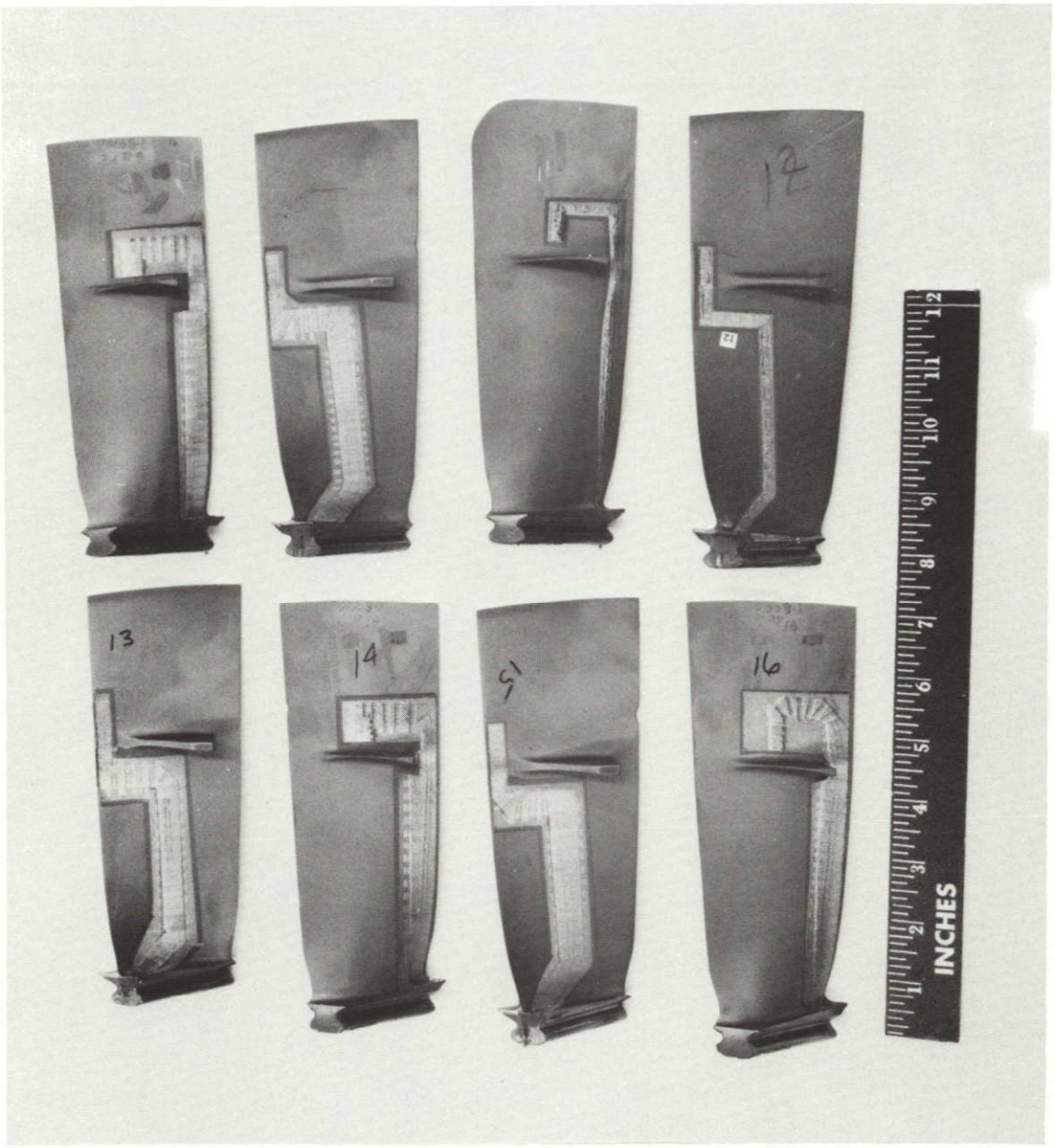

Figure A-25 Instrumented Third Stage Blades S/N 9 Through 16 After Testing (78-444-4233-G)

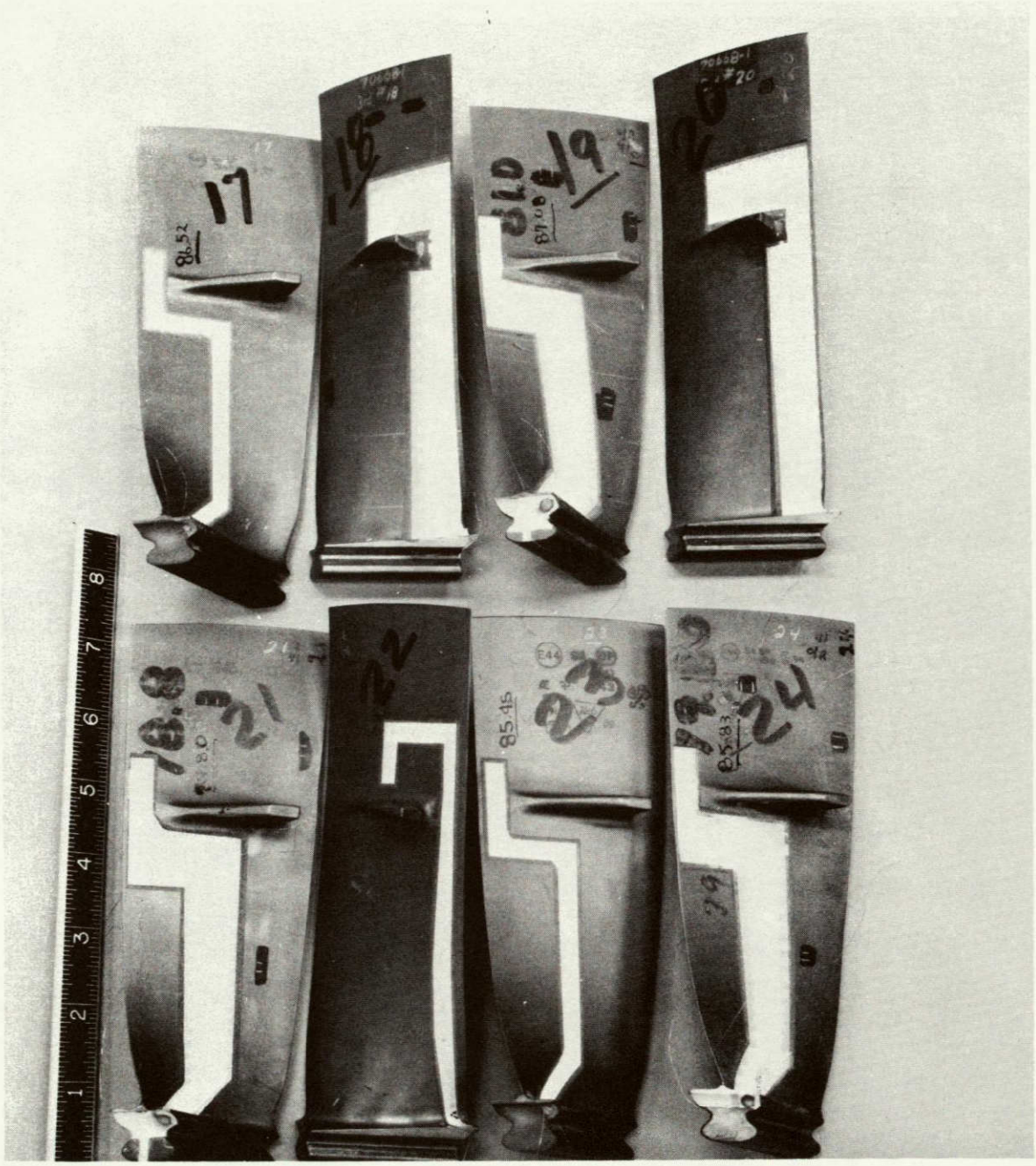

Figure A-26 Instrumented Third Stage Blades S/N 17 Through 24 Before Testing (77-444-4001-C)

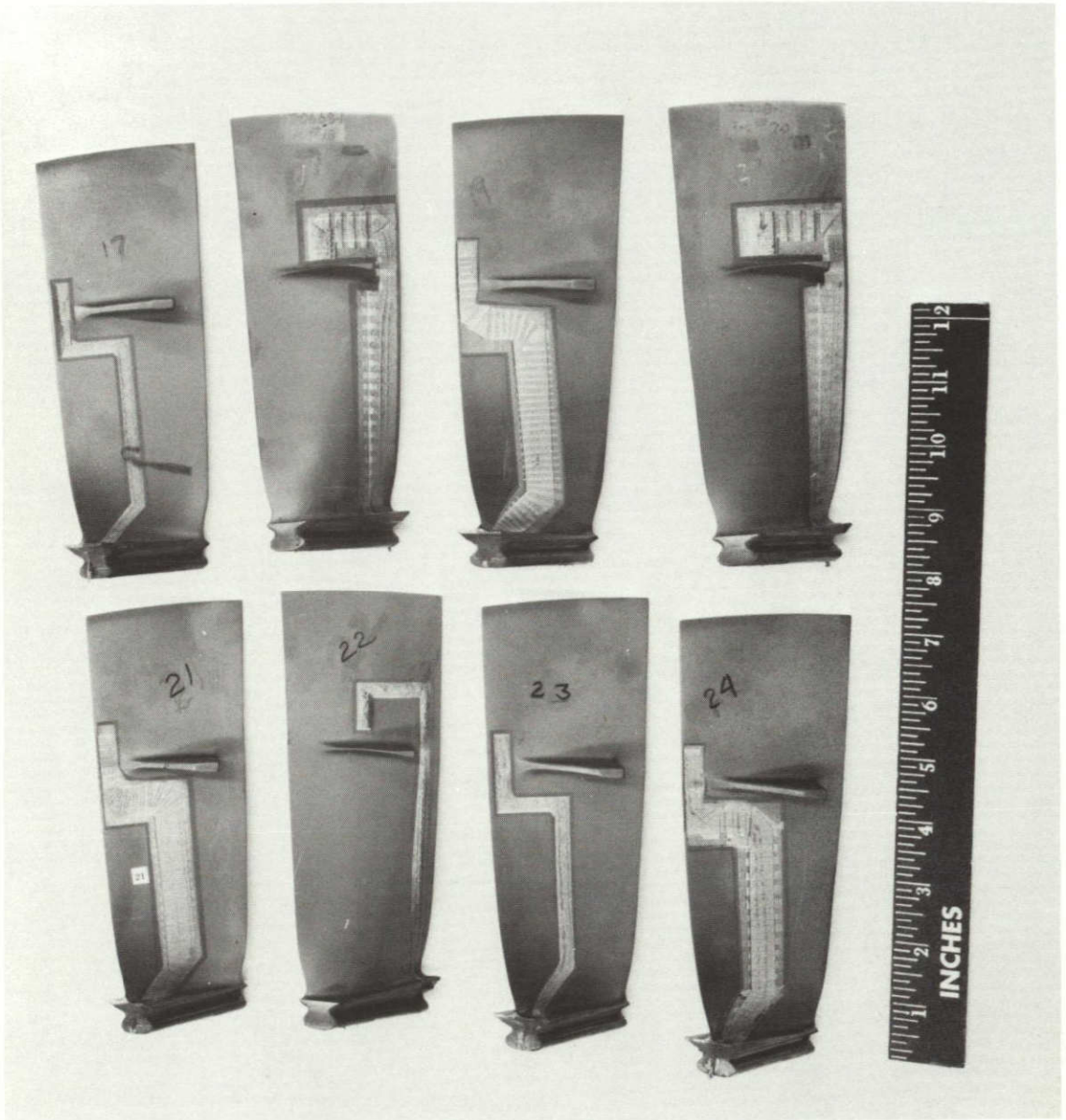

Figure A-27 Instrumented Third Stage Blades S/N 17 Through 24 After Testing (78-444-4233-H)

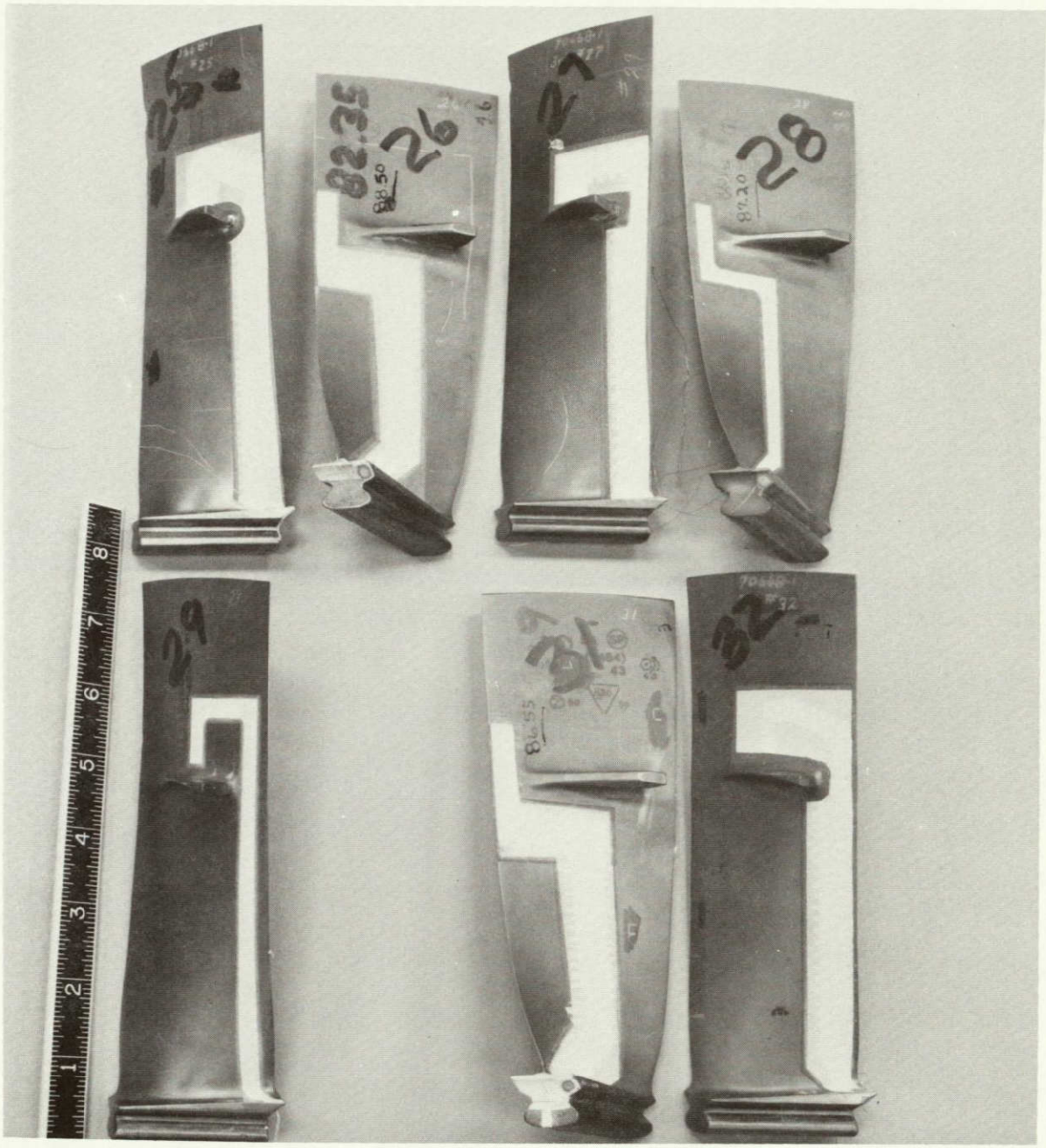

Figure A-28 Instrumented Third Stage Blades S/N 25 Through 29 and 31 Through 32 Before Testing (Blade S/N 30 was not available at time photograph was taken) (77-444-4001-D)

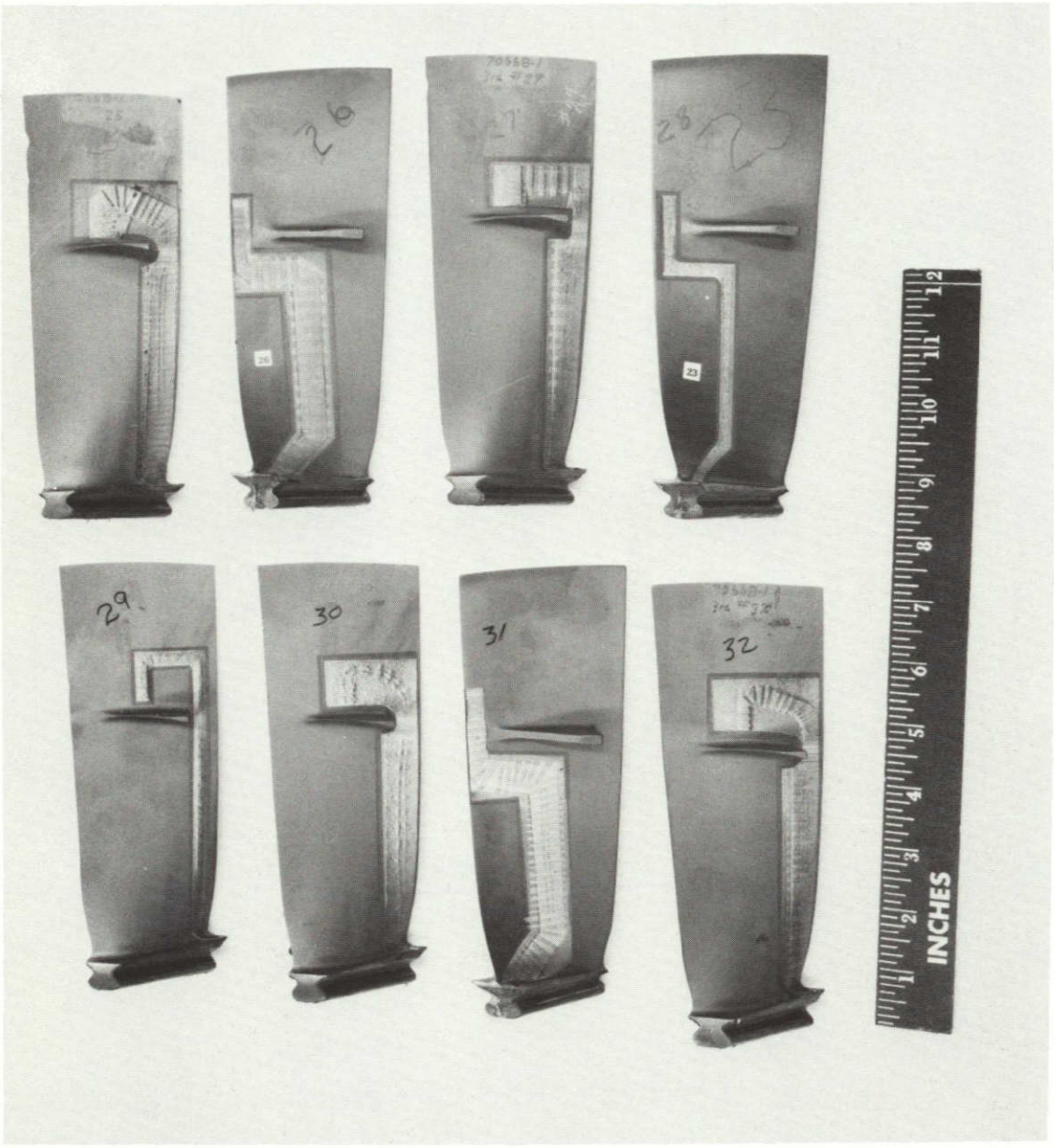

Figure A-29 Instrumented Third Stage Blades S/N 25 Through 32 After Testing (78-444-4233-I)

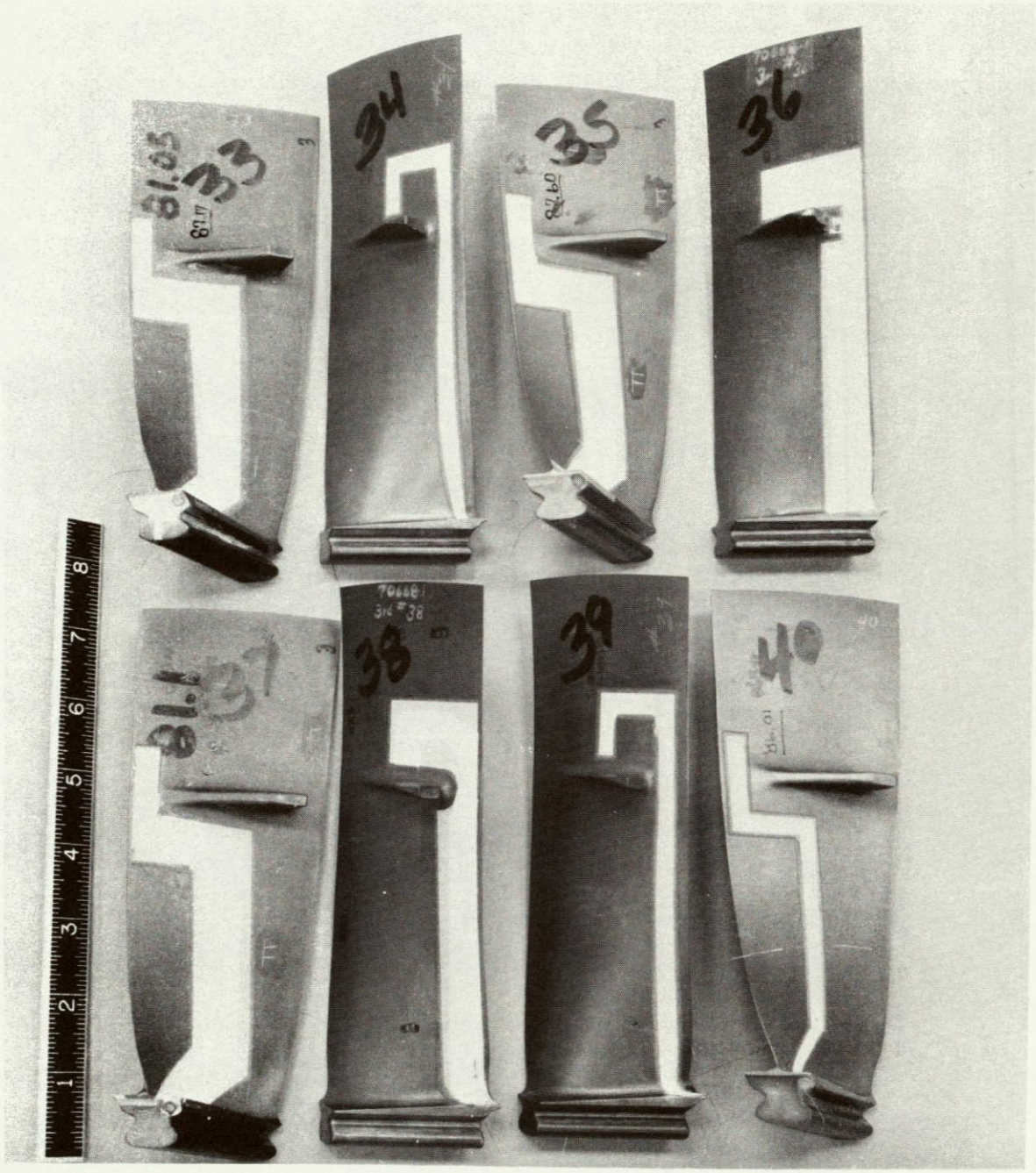

Figure A-30 Instrumented Third Stage Blades S/N 33 Through 40 Before Testing (77-444-4001-E)

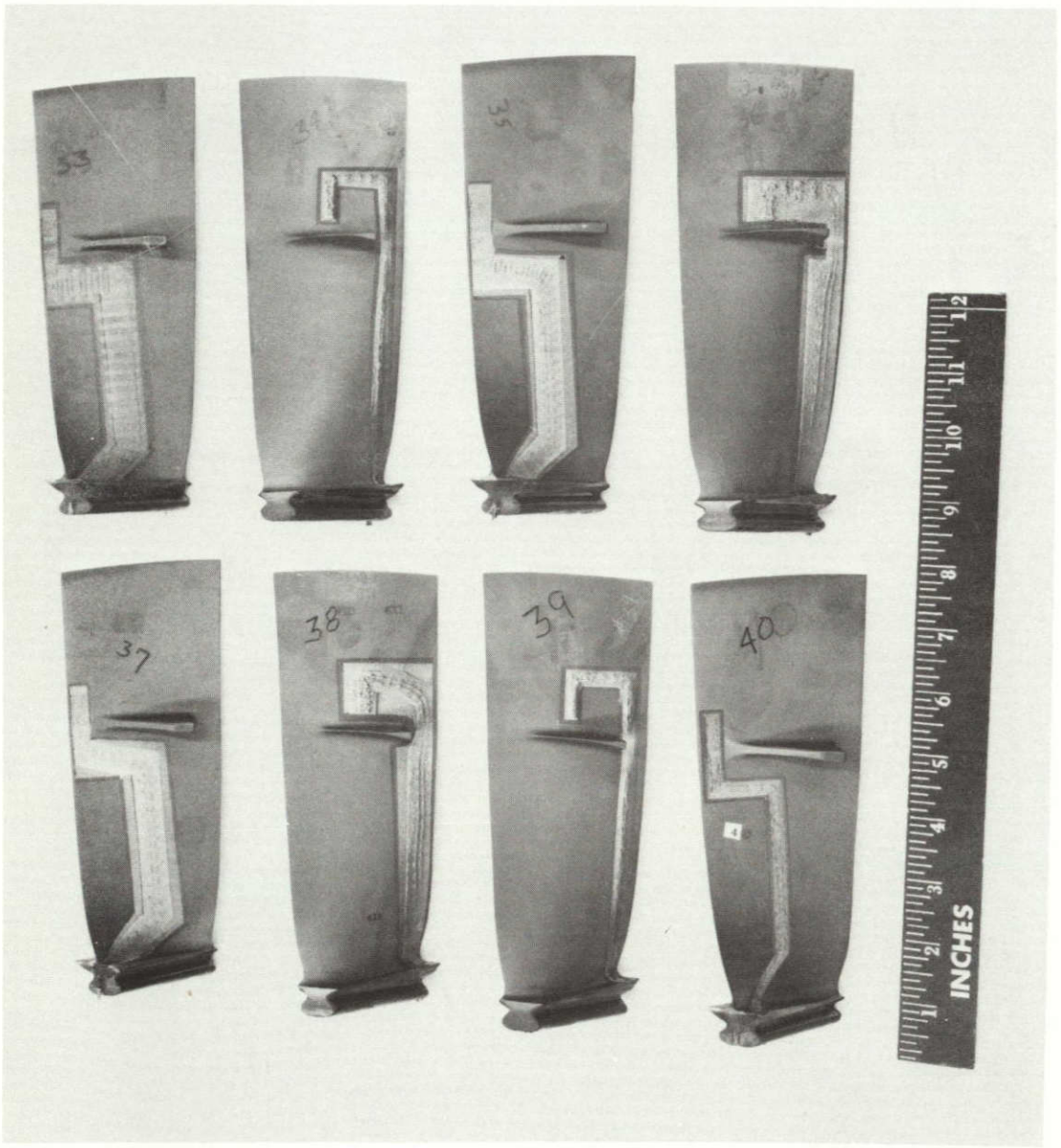

Figure A-31 Instrumented Third Stage Blades S/N 33 Through 40 After Testing (78-444-4233-J)

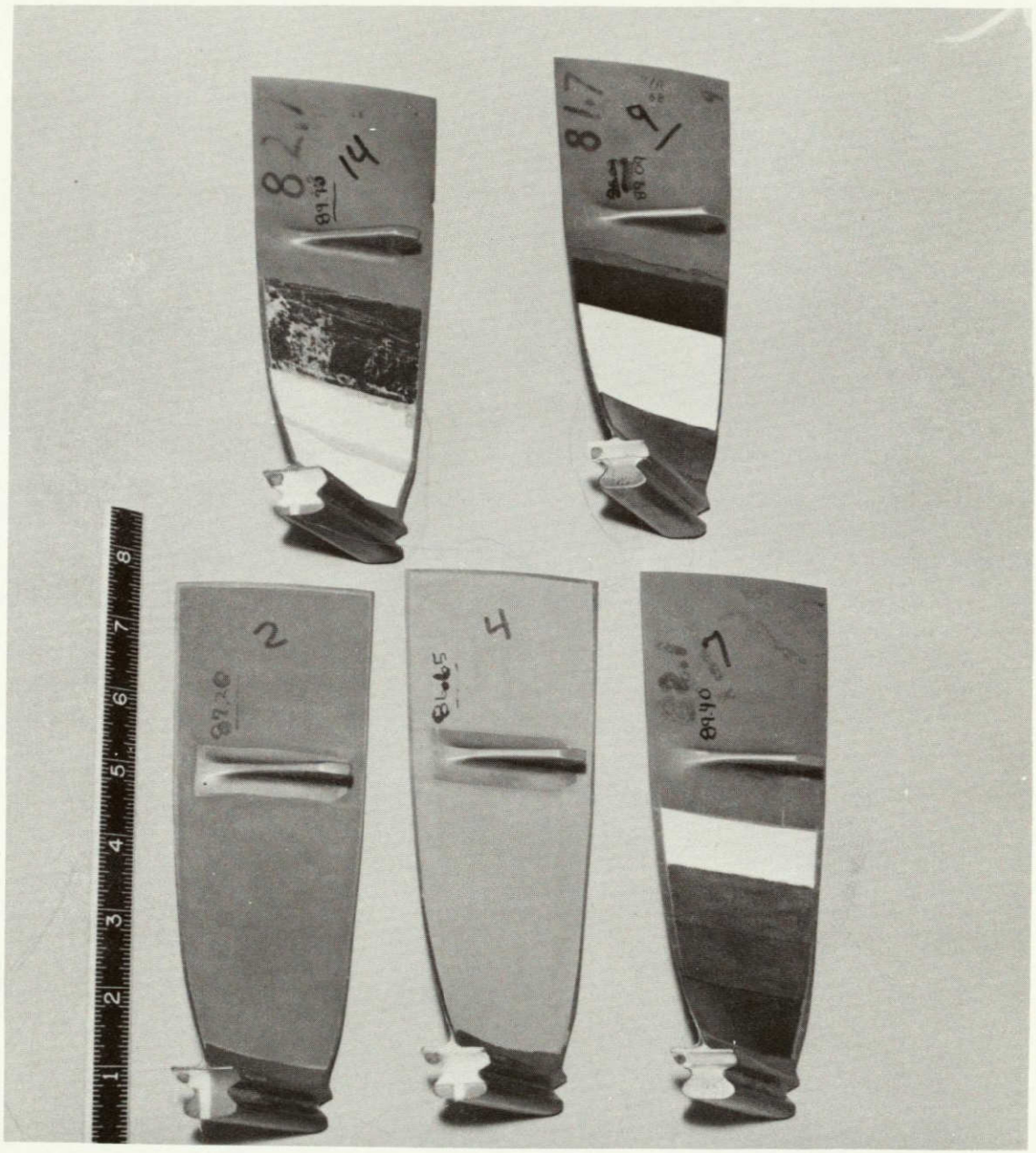

Figure A-32 Erosion Patch Third Stage Blades S/N 2, 4, 7, 9, 14 Before Testing (77-444-0004-D)

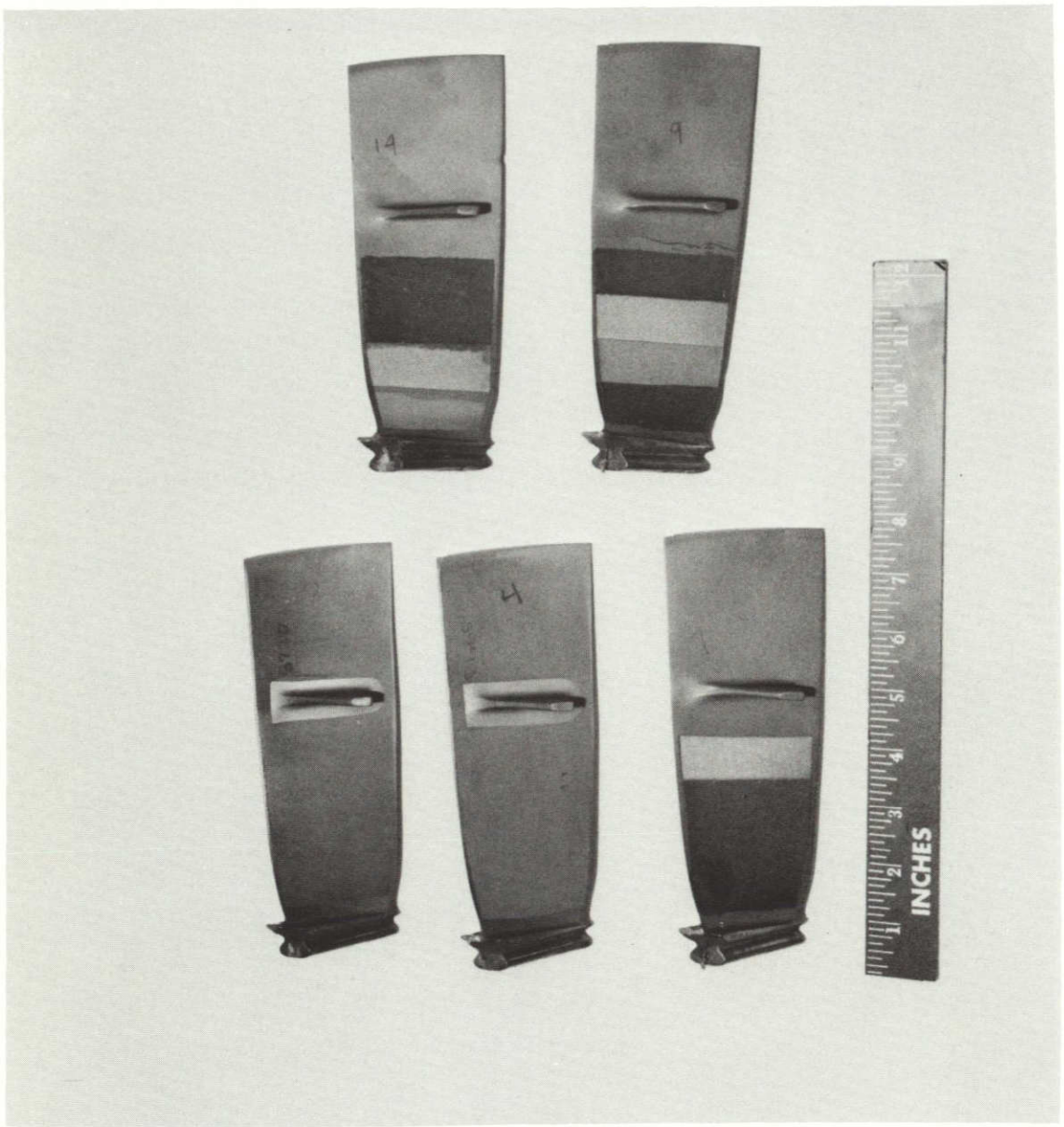

Figure A-33 Erosion Patch Third Stage Blades S/N 2, 4, 7, 9, 14 After Testing (78-444-0374-E)

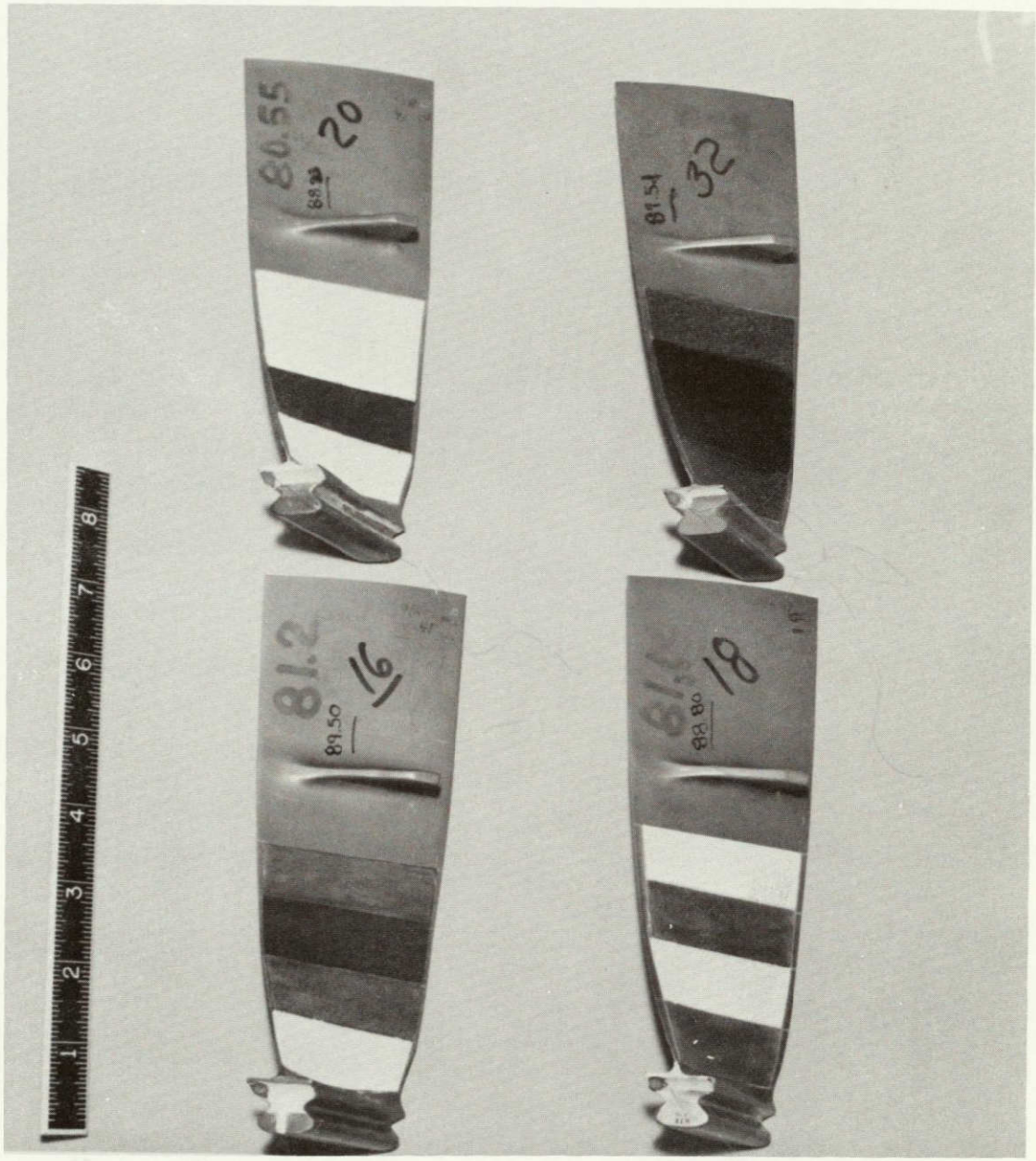

Figure A-34 Erosion Patch Third Stage Blades S/N 16, 18, 20, 32 Before Testing (77-444-0004-E)

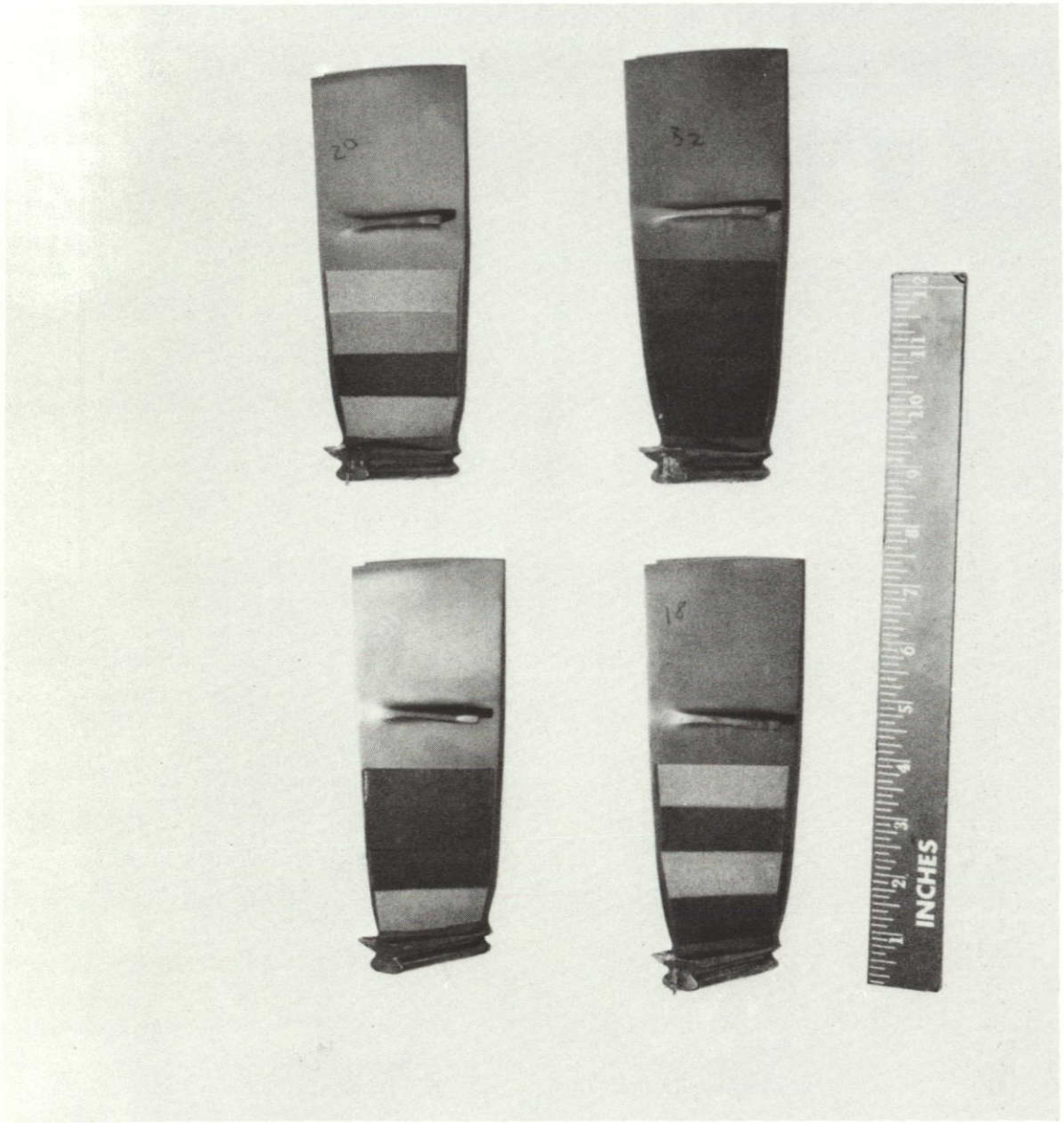

Figure A-35 Erosion Patch Third Stage Blades S/N 16, 18, 20, 32 After Testing (78-444-0374-D)

Figure A-36 Third Stage Blade to Disk Jump With Good 36 Gage Chromel P Wires (78-444-0340-D)

C-2

Figure A-37 Third Stage Blade to Disk Jump With Broken 36 Gage Chromel P Wires (78-444-0340-A)

APPENDIX B

RESISTANCE MEASUREMENT DATA

TABLE B-1

RESISTANCE MEASUREMENT DATA (OHMS)

Blade Serial Number	Stationary Engine Data						Rotating Engine Data			
	Prior to Installation	After Installation	Prior to Test	After Test	Before Jump	On Blade	Measured at Slip Ring	Measured at Connector	Measured at Engine Leadwires	Measured at Front of Engine
FIRST STAGE										
1	303.1	335	341	341	331	331	332	332	332	332.9
2	304.5	341	348	350	337	337	338	338	338	338.8
3	304.5	337	344	344	333	333	335	335	335	335.7
4*	304.9	369	-	-	-	-	-	-	-	-
15	304.8	342	348	348	337	337	339	339	339	339.6
16*	306.1	359	345	345	-	331	336	336	336	337.3
17	307.2	341	348	348	338	338	339	339	339	340.0
18*	307.4	362	345	345	-	332	-	-	346	-
27	306.8	335	341	341	331	331	333	332	333	333.4
28*	304.8	367	-	-	-	337	-	-	-	-
29	305.1	334	340	342	-	331	333	333	332	333.5
30	305.2	345	350	351	-	341	342	342	342	342.9
5*		158	149	159	133	133	138	-	137	-
6		164	172	172	-	160	160	160	160	161.6
13*		185	176	-	-	159	-	165	163	164.7
14		135	145	145	132	132	133	132	132	133.5
19*		188	178	-	-	161	-	-	-	167.7
20		135	144	144	132	132	132	132	132	133.7
31*		159	149	149	-	131	137	-	-	-
32		165	175	176	162	162	163	162	162	-

* Failed During Testing

- Open Circuit

TABLE B-1 (Continued)

Blade Serial Number	Stationary Engine Data					Rotating Engine Data			
	Prior to Installation	After Installation	Prior to Test	After Test	Before Jump	On Blade	Measured at Slip Ring	Measured at Connector	Measured at Engine Leadwires	Measured at Front of Engine
THIRD STAGE (Continued)										
35	305.7	379	361	363	330	328	353	353	353	353.8
36	306.2	380	362	364	330	327	353	353	353	353.6
37	306.4	380	361	362	331	330	353	353	353	353.9
38	304.2	372	355	355	324	323	346	346	346	346.7
5*		176	161	161	128	127	149	149	149	149.5
6		180	166	166	131	130	154	154	153	155.5
11		175	162	162	128	126	150	148	148	149.4
12		179	165	165	130	128	153	152	152	153.7
17		177	164	163	129	127	149	148	149	149.8
22		178	163	163	129	127	151	150	150	151.6
23*		181	165	166	130	129	154	153	154	155.3
28		177	163	163	129	127	151	150	151	151.9
29		180	165	165	130	129	153	152	152	153.8
34		181	165	166	131	130	153	153	154	154.5
39		177	163	163	130	127	151	150	150	151.7
40*		179	165	166	131	130	154	153	153	154.4

* Failed During Testing

TABLE B-1 (Continued)

Blade Serial Number	Stationary Engine Data						Rotating Engine Data			
	Prior to Installation	After Installation	Prior to Test	After Test	Before Jump	On Blade	Measured at Slip Ring	Measured at Connector	Measured at Engine Leadwires	Measured at Front of Engine
THIRD STAGE										
1	306.2	374	355	355	325	323	347	347	347	347.6
2*	306.4	378	359	-	328	326	393	386	362	366.7
3	306.2	373	356	361	327	325	348	347	348	348.2
4	307.0	379	359	360	328	326	351	351	351	360.0
7	304.8	370	352	354	323	321	345	344	344	345.1
8	305.4	377	359	359	327	325	351	350	350	351.5
9	306.2	374	357	358	327	325	349	348	349	349.5
10	304.4	374	356	357	325	323	349	348	348	349.2
13	307.0	374	357	357	326	324	348	347	347	348.2
14*	304.7	379	361	388	329	327	369	366	359	359.7
15	305.0	373	356	356	325	323	347	347	348	348.1
16	304.4	379	360	360	327	325	351	351	351	352.1
18	305.0	373	354	354	325	323	346	346	346	346.5
19*	305.5	374	356	363	324	322	354	354	355	355.9
20	306.9	375	362	363	327	326	354	349	349	350.2
21*	303.9	375	357	392	324	323	371	372	361	361.8
24	305.1	372	353	354	323	320	345	345	345	345.6
25*	304.7	377	360	364	326	325	351	351	351	351.9
26	307.5	378	360	361	329	327	353	352	352	353.2
27	306.1	380	360	361	329	327	353	352	352	353.2
30	306.9	377	363	363	327	324	351	350	350	351.2
31*	306.1	377	360	381	328	326	364	364	357	357.7
32*	310.0	379	360	362	326	323	354	354	359	359.1
33*	305.3	376	358	382	325	324	372	367	357	357.9

* Failed During Testing

- Open Circuit

APPENDIX C

THICKNESS MEASUREMENT DATA

TABLE C-I

NASA THICKNESS MEASUREMENT DATA

Blade Serial Number	Gage Type	Leadwire Diameter (mm)	Gage Location	Initial Thickness (mm)	Final Thickness (mm)
FIRST STAGE					
6	1212-2A	0.076	Convex	0.38	0.36
13	1212-2A	0.076	Convex	0.38	0.38
14	1212-5B	0.127	Concave	0.41	0.41
31	1212-5B	0.127	Concave	0.41	0.41
19	1212-2A	0.076	Convex	0.46	0.36
32	1212-2A	0.076	Convex	0.38	0.33
5	1212-5B	0.127	Concave	0.46	0.46
20	1212-5B	0.127	Concave	0.36	0.36
THIRD STAGE					
29	1212-5B	0.127	Convex	0.36	0.33
39	1212-5B	0.127	Convex	0.43	0.38
5	1212-5B	0.127	Concave	0.48	0.43
40	1212-5B	0.127	Concave	0.38	0.30
12	1212-5B	0.127	Concave	0.51	0.46
11	1212-5B	0.127	Convex	0.48	0.41
6	1212-5B	0.127	Convex	0.43	0.36
34	1212-5B	0.127	Convex	0.46	0.38
22	1212-5B	0.127	Convex	0.46	0.43
23	1212-5B	0.127	Concave	0.30	0.28
28	1212-5B	0.127	Concave	0.27	0.25
17	1212-5B	0.127	Concave	0.38	0.36

TABLE C-II

PRATT & WHITNEY AIRCRAFT FIRST STAGE THICKNESS MEASUREMENT DATA

Blade Serial Number	Measured Thickness (mm) Height Above Platform (cm) 2.54	5.08	7.62	10.16	12.7	15.24	17.78	17.78	20.32	Over Gage
1 (CC-5)										
Initial	0.482	0.279	0.178	0.305	0.330	0.457	0.254	0.432		0.406
Final	0.305	0.254	0.152	0.127	0.076	0.229	0.203	0.254		0.381
2 (CX-1)										
Initial	0.381	0.457	0.356	0.482	0.432	0.457	0.457		0.482	0.508
Final	*	*	*	*	*	0.432	0.457		0.457	0.508
3 (CC-5)										
Initial	0.406	0.482	0.432	0.381	0.482	0.508	0.356	0.457		0.533
Final	0.178	0.406	0.254	0.178	0.406	0.381	0.229	0.254		0.482
4 (CX-4)										
Initial	0.584	0.559	0.686	0.584	0.660	0.660	0.579		0.508	0.356
Final	*	*	*	*	*	0.533	0.529		0.457	0.228
15 (CX-1)										
Initial	0.356	0.330	0.356	0.406	0.406	0.381	0.432		0.457	0.356
Final	*	*	*	*	*	0.356	0.330		0.406	0.330
16 (CC-2)										
Initial	0.482	0.457	0.406	0.381	0.381	0.457	0.457	0.330		0.432
Final	0.304	0.305	0.254	0.203	0.305	0.406	0.304	0.254		0.381
17 (CX-5)										
Initial	0.482	0.254	0.305	0.432	0.457	0.457	0.406		0.279	0.254
Final	*	*	*	*	0.457	0.457	0.381		0.279	0.254
18 (CC-4)										
Initial	0.305	0.482	0.381	0.432	0.381	0.432	0.432	0.406		0.482
Final	0.127	0.356	0.279	0.229	0.203	0.330	0.304	0.304		0.381
27 (CC-1)										
Initial	0.406	0.457	0.381	0.457	0.381	0.482	0.457	0.432		0.406
Final	0.279	0.330	0.279	0.279	0.279	0.432	0.406	0.254		0.381
28 (CX-2)										
Initial	0.457	0.406	0.457	0.432	0.406	0.457	0.482		0.381	0.432
Final	*	*	*	*	*	0.457	0.457		0.330	0.356
29 (CC-3)										
Initial	0.356	0.406	0.432	0.203	0.432	0.482	0.457	0.432		0.457
Final	0.203	0.229	0.203	0.178	0.102	0.203	0.304	0.330		0.355
30 (CX-3)										
Initial	0.381	0.432	0.457	0.432	0.356	0.406	0.432		0.432	0.279
Final	*	*	*	*	*	0.330	0.304		0.355	0.152

Symbols in parentheses indicate side of airfoil (CC - concave; CX - convex) and system type (1-5)

*Measurement not taken because of erosion patch on opposite side of blade

TABLE C-III

PRATT & WHITNEY AIRCRAFT THIRD STAGE THICKNESS MEASUREMENT DATA

Blade Serial Number	Measured Thickness (mm) Height Above Platform (cm) 2.54	5.08	7.62	10.16	10.16	12.7	Over Gage
1 (CC-1)							
Initial	0.457	0.457	0.482	0.254	0.305		0.457
Final	0.457	0.457	0.457	0.254	0.305		0.457
2 (CX-2)							
Initial	0.457	0.381	0.381	0.482		0.381	0.356
Final	*	*	*	*		*	*
3 (CC-3)							
Initial	0.381	0.482	0.432	0.432	0.432		0.482
Final	0.381	0.381	0.432	0.432	0.406		0.482
4 (CX-4)							
Initial	0.432	0.457	0.482	0.482		0.457	0.482
Final	*	*	*	*		*	*
7 (CX-1)							
Initial	0.381	0.305	0.330	0.279		0.254	0.330
Final	*	*	*	0.203		0.254	0.305
8 (CC-2)							
Initial	0.356	0.381	0.457	0.482	0.356		0.356
Final	0.356	0.356	0.381	0.457	0.356		0.229
9 (CX-3)							
Initial	0.508	0.381	0.482	0.457		0.305	0.482
Final	*	*	*	0.406		0.254	0.432
10 (CC-4)							
Initial	0.381	0.381	0.381	0.381	0.406		0.381
Final	0.356	0.356	0.279	0.203	0.381		0.381
13 (CC-1)							
Initial	0.432	0.482	0.457	0.457	0.482		0.431
Final	0.432	0.482	0.406	0.432	0.406		0.431
14 (CX-2)							
Initial	0.381	0.482	0.356	0.254		0.254	0.457
Final	*	*	*	0.254		0.203	0.432

Symbol in parentheses indicate side of airfoil (CC - concave; CX - convex) and system type (1-5)

*Measurement not taken because of erosion patch on opposite side of blade

TABLE C-III (Continued)

PRATT & WHITNEY AIRCRAFT THIRD STAGE THICKNESS MEASUREMENT DATA

Blade Serial Number	Measured Thickness (mm) Height Above Platform (cm) 2.54	5.08	7.62	10.16	10.16	12.7	Over Gage
15 (CC-3)							
Initial	0.584	0.482	0.457	0.482	0.432		0.356
Final	0.533	0.432	0.432	0.279	0.432		0.356
16 (CX-4)							
Initial	0.457	0.432	0.482	0.432		0.457	0.457
Final	*	*	*	0.330		0.381	0.356
18 (CX-1)							
Initial	0.457	0.432	0.406	0.381		0.457	0.381
Final	*	*	*	0.381		0.406	0.356
19 (CC-2)							
Initial	0.432	0.508	0.432	0.457	0.406		0.457
Final	0.381	0.457	0.406	0.381	0.330		0.432
20 (CX-3)							
Initial	0.457	0.356	0.406	0.305		0.406	0.432
Final	*	*	*	0.127		0.330	0.432
21 (CC-4)							
Initial	0.432	0.432	0.457	0.457	0.457		0.432
Final	0.356	0.381	0.432	0.406	0.381		0.381
24 (CC-1)							
Initial	0.432	0.432	0.457	0.559	0.482		0.305
Final	0.356	0.406	0.406	0.457	0.482		0.279
25 (CX-2)							
Initial	0.533	0.279	0.381	0.432		0.457	0.330
Final	*	*	*	0.432		0.381	0.305
26 (CC-3)							
Initial	0.482	0.533	0.381	0.482	0.457		0.457
Final	0.457	0.533	0.381	0.330	0.457		0.457
27 (CX-4)							
Initial	0.482	0.482	0.406	0.508		0.381	0.457
Final	0.457	0.356	0.330	0.381		0.254	0.381

Symbol in parentheses indicate side of airfoil (CC - concave; CX - convex) and system type (1-5)

*Measurement not taken because of erosion patch on opposite side of blade

TABLE C-III (Continued)

PRATT & WHITNEY AIRCRAFT THIRD STAGE THICKNESS MEASUREMENT DATA

Blade Serial Number	Measured Thickness (mm) Height Above Platform (cm) 2.54	5.08	7.62	10.16	10.16	12.7	Over Gage
30 (CX-5)							
Initial	0.457	0.406	0.432	0.432		0.432	0.432
Final	*	*	*	0.432		0.381	0.432
31 (CC-2)							
Initial	0.457	0.305	0.356	0.432	0.457		0.406
Final	0.457	0.305	0.356	0.330	0.381		0.406
32 (CX-3)							
Initial	0.432	0.381	0.432	0.457		0.457	0.432
Final	*	*	*	0.457		0.381	0.356
33 (CC-4)							
Initial	0.508	0.482	0.482	0.482	0.457		0.457
Final	0.457	0.457	0.706	0.330	0.381		0.432
35 (CC-5)							
Initial	0.432	0.330	0.457	0.457	0.254		0.356
Final	0.356	0.279	0.356	0.457	0.254		0.356
36 (CX-5)							
Initial	0.381	0.356	0.356	0.381		0.432	0.406
Final	0.254	--	--	--		--	0.355
37 (CX-5)							
Initial	0.457	0.406	0.356	0.457		0.457	0.381
Final	0.457—	0.330	0.330	0.305		0.457	0.356
38 (CC-5)							
Initial	0.330	0.305	0.356	0.305	0.356		0.381
Final	0.305	0.305	0.330	0.305	0.305		0.381

Symbol in parentheses indicate side of airfoil (CC - concave; CX - convex) and system type (1-5)

*Measurement not taken because of erosion patch on opposite side of blade

-- Error in initial measurements (final numbers greater than original)

APPENDIX D

STRAIN GAGE SYSTEM INSRUMENTATION DESCRIPTION

APPENDIX D

STRAIN GAGE SYSTEM INSTRUMENTATION DESCRIPTION

A. Overview

The overall strain gage measurement system is shown in Figure D-1. The system has the capability of recording AC and DC strain gage signals, and has provisions for analyzing intermittent circuit effects.

The strain gages are powered one at a time, and a complete scan can be completed in less than 15 minutes. The strain gages can also be monitored individually by the operator to analyze any unusual signals.

Because of the limitation of slip ring connectors, two gages had to share a common terminal in most cases. A gage-to-blade resistance measurement capability was included in the monitoring system.

B. Scanner

1. Random Access Mode - Scanner switches to and stays on channel selected by thumbwheel switch.

2. Continuous Scan Mode, Internal Clock - The scanner sequences through a consecutive group of channels with starting and ending points determined by thumbwheel switches. The stepping rate is determined by a range pushbutton switch and continuous vernier potentiometer.

3. Strain gages are connected to Channels 1 through 60. Channel 61 is a 350 ohm resistor for reference purposes. Channels 62 through 70 were unused.

C. Amplifiers

1. Amplifier I is an AC-coupled amplifier with a gain of 100. Its function is to provide noise and dynamic data information for scope monitoring and tape recording.

2. Amplifier II is a DC-coupled amplifier with a gain of 1. Its function is to isolate the DC voltage measurement of strain gage excitation from a digital panel meter and the analog tape recorder.

3. Amplifier III is an amplifier with a gain of 1. Its function is to measure the isolation resistance of each switched strain gage to engine ground. A 3-volt battery provides the isolation voltage source. The isolation resistance forms a voltage divider with a 50,000 ohm resistor.

D. Miscellaneous Electronics

1. Constant current source - a 10-ma nominal current source excites the strain gages one at a time as they are selected by the scanner. Channel 61 provides a current magnitude check.

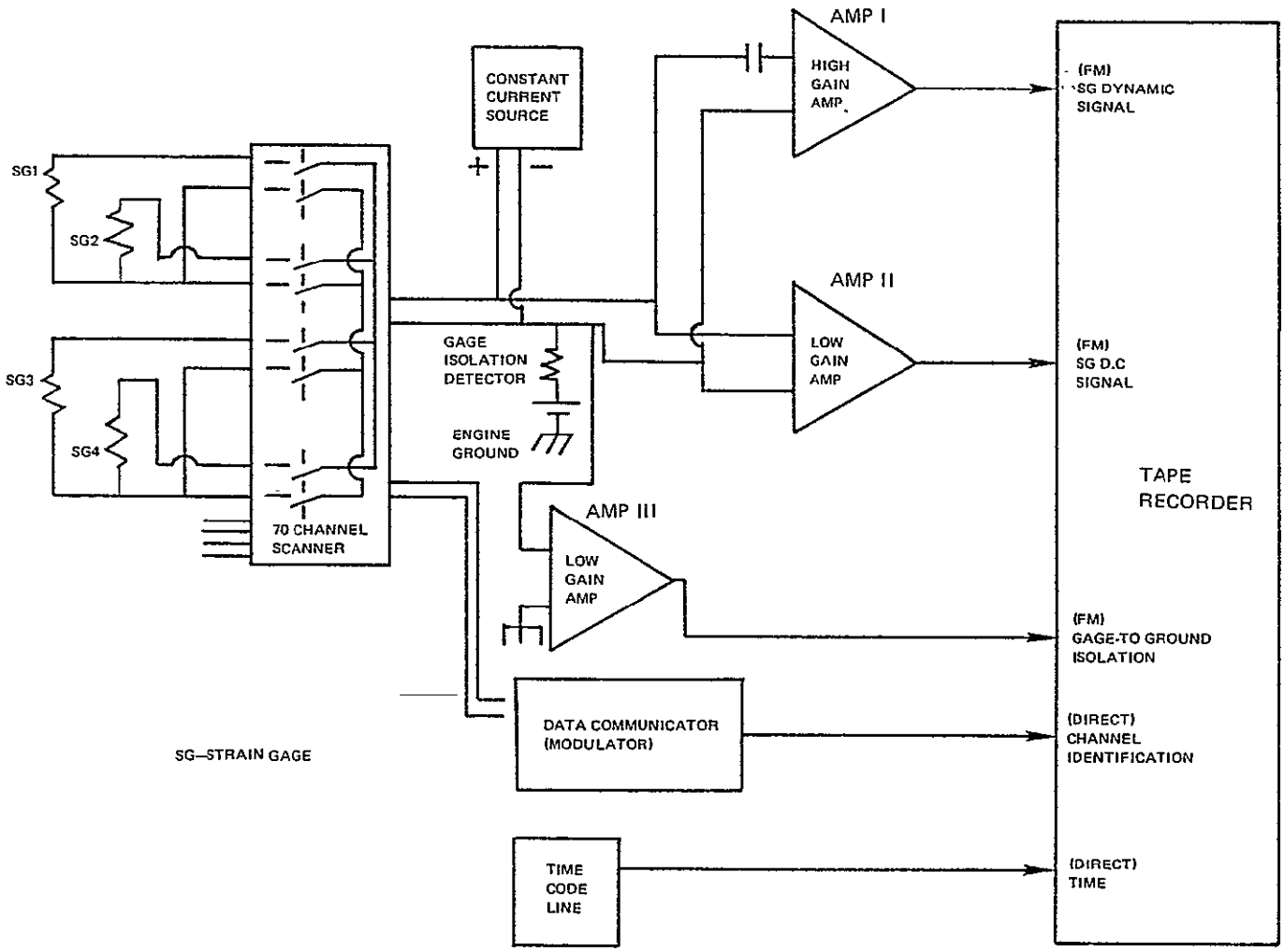

Figure D-1 Strain Gage Data Acquisition System - The system provides automatic sequential strain gage system data acquisition.

2. Data Communicator - Channel Number Serial Interface Transmitter/Receiver System - This system records on one tape channel the scanner channel code to identify on the tape recording which strain gage is being scanned. Upon replaying the tape, with the "RECORD/-PLAYBACK" switch in playback position, the tape recorder will drive the scanner (and its display) to show recorded scanner channel.

E. Tape Recorder

Provides a mixture of FM and direct channels for recording:

1. Gage data and noise (FM)

2. Gage DC voltage (FM)

3. Gage RMS-DC converter (FM) - not used ____

4. Gage isolation (FM)

5. IRIG B time code (Direct)

6. Channel ID (Direct)

All FM channels are run in the high range (1.5 - 10V)

All direct channels are run in the low range (0.20 - 1.5V)

F. Procedures

1. Tape recorder is generally operated at 3 3/4 ips to provide about 8 hours of recording time. This tape speed provides a bandwidth of about 1kHz. If higher bandwidth is desired at intermittent intervals to provide dynamic data recording, a tape speed of 15 ips can be used to provide a bandwidth of 5kHz; a tape speed of 30 ips provides a bandwidth of 10 kHz. A log of tape speed versus tape footage is kept for playback interpretation.

2. The FM channels require DC calibration. Prior to each run and at the end of each run, a segment of amplifier zero output and a segment of Channel 61 reference resistor output is run on the tape. The reference resistor provides a reference level for both the gage DC voltage and for the isolation measurement.

3. Nominal DC voltage on 120-ohm gages is 1.5 $\pm$ 0.2V.

   Nominal DC voltage on 350-ohm gages is 3.5 $\pm$ 0.2 V.

   Nominal DC isolation measurement voltage is + 3V.

APPENDIX E

EROSION PATCH CONDITION DATA

TABLE E-I

NASA FIRST-STAGE EROSION PATCH INSTALLATION AND EVALUATION SUMMARY

Blade Serial Number	Type of Erosion Patch	Condition After Test
10	0.17 mm Bean H Cement	Heavy erosion on concave (cc) side Slight erosion on convex (cx) side
22	0.37 mm Rokide H Rod	Slight erosion on concave (cc) side Slight erosion on convex (cx) side
24	0.17 mm Metco Aluminum Oxide Powder Plus Barrier H Overcoat	Heavy erosion on concave (cc) side Slight erosion on convex (cx) side
34	0.17 mm PBX Ceramic Cement	Total erosion on concave (cc) side Slight erosion on convex (cx) side
7	0.17 mm Rokide H Rod	Heavy erosion on concave (cc) side Slight erosion on convex (cx) side
23	0.17 mm PBX Ceramic Cement	Heavy erosion on concave (cc) side Slight erosion on convex (cx) side
33	0.17 mm Bean H Ceramic Cement	Total erosion on concave (cc) side Slight erosion on convex (cx) side
26	M-Bond 610 Epoxy Cement	Slight erosion on concave (cc) side
36	0.17 mm Rokide H Rod	Slight erosion on concave (cc) side Slight erosion on convex (cx) side
8	0.25 mm Rokide H Rod	Slight erosion on concave (cc) side Slight erosion on convex (cx) side
38	0.25 mm Metco 105 Aluminum Oxide Powder	Heavy erosion on concave (cc) side Slight erosion on convex (cx) side
25	0.25 mm Metco 105 Aluminum Oxide Powder	Total erosion on concave (cc) side Slight erosion on convex (cx) side
9	M-Bond 610 Epoxy Cement	Slight erosion on concave (cc) side
35	M-Bond 610 Epoxy Cement	Total erosion on concave (cc) side
37	0.37 mm Rokide H Rod	Slight erosion on concave (cc) side Slight erosion on convex (cx) side
11	0.17 mm Metco 105 Aluminum Oxide Powder	Total erosion on concave (cc) side Slight erosion on convex (cx) side
21	0.17 mm Rokide H Rod Plus Barrier H Overcoat	Slight erosion on concave (cc) side Slight erosion on convex (cx) side
12	0.37 mm Metco 105 Aluminum Oxide Powder	Heavy erosion on concave (cc) side Slight erosion on convex (cx) side

TABLE E-II

PRATT & WHITNEY AIRCRAFT EROSION PATCH INSTALLATION
AND EVALUATION SUMMARY

Blade Serial Number	Patch* Location	Patch* Type	Measured Thickness (mm) 25% From Trailing Edge Before Test	25% From Trailing Edge After Test	75% From Trailing Edge Before Test	75% From Trailing Edge After Test	Post Test Condition and Comments
FIRST STAGE							
2	1	1	0.38	0.33	0.38	0.31	Good
2	2	2	0.33	0.28	0.46	0.41	Good
2	3	3	0.46	0.41	0.38	0.28	Erosion toward leading edge
2	4	4	0.25	0.15	0.33	0.23	Heavy erosion from the center to the leading edge, bare metal
2	5	6	0.05	0.03	0.08	0.05	Good
2	6	7	0.20	0.18	0.33	0.28	Good
15	1	7	0.25	0.20	0.20	0.13	Good
15	2	1	0.51	0.46	0.51	0.43	Good
15	3	2	0.51	0.46	0.46	0.38	Good
15	4	5	0.41	0.34	0.46	0.41	Good
15	5	4	0.56	0.51	0.56	0.48	Good
15	6	6	0.08	0.03	0.08	0.05	Good
28	1	5	0.34	0.31	0.38	0.31	Good
28	2	7	0.20	0.15	0.23	0.18	Good
28	3	1	0.23	0.20	0.20	0.15	Good
28	4	2	0.23	0.15	0.23	0.20	Good
28	5	6	0.18	0.13	0.20	0.10	Erosion near leading edge
28	6	4	0.20	0.15	0.20	0.10	Erosion to bare metal from center of patch to leading edge
30	1	4	0.41	0.33	0.38	0.25	Edge of spray eroded away at leading edge and outboard edge
30	2	5	0.46	0.43	0.46	0.41	Good
30	3	7	0.08	0.05	0.08	0.03	Heavy erosion from leading edge to center
30	4	1	0.38	0.28	0.38	0.28	Good
30	5	2	0.38	0.31	0.41	0.31	Good
30	6	2	0.43	0.31	0.43	0.31	Good

* Patch locations shown in Figures 4 and 5

Patch Type:
1 Rokide HT Rod
2 Rokide HT Rod Plus GA-60 Cement
3 Rokide HT Rod Plus Bean H Cement Plus Rokide HT Rod
4 Plasmalloy 331-M Powder
5 Plasmalloy 331-M Powder Plus GA-60 Cement
6 GA-60 Cement (2 Coats)
7 GA-60 Cement (2 Coats) Plus Fiberglas (2 Coats)
8 PLD Cement**
9 Plasmalloy 331-M Powder Plus PLD Cement
10 PLD Cement Plus Fiberglas
11 Rokide HT Rod Plus PLD Cement

**PLD cement is a single-component polyimide adhesive.

TABLE E-II (Continued)

Blade Serial Number	Patch* Location	Patch* Type	Measured Thickness (mm) 25% From Trailing Edge Before Test	25% From Trailing Edge After Test	75% From Trailing Edge Before Test	75% From Trailing Edge After Test	Post Test Condition and Comments
THIRD STAGE							
7	1	1	0.33	0.31	0.15	0.10	Good
7	2	2	0.31	0.28	0.23	0.20	Good
7	5	5	0.34	0.34	0.33	0.31	Good
7	6	6	0.10	0.10	0.20	0.18	Good
9	1	7	0.41	0.38	0.46	0.43	Good
9	2	1	0.41	0.41	0.51	0.48	Good
9	5	4	0.56	0.56	0.71	0.66	Good
9	6	5	0.84	0.76	0.71	0.66	Good
14	1	6	0.18	0.15	0.15	0.13	Good
14	2	7	0.25	0.25	0.38	0.38	Good
14	5	3	0.38	0.34	0.38	0.33	Good
14	6	4	0.38	0.34	0.46	0.46	Good
16	1	5	0.66	0.58	0.66	0.64	Good
16	2	6	0.13	0.13	0.13	0.08	Good
16	5	2	0.66	0.66	0.56	0.48	Good
16	6	3	0.74	0.71	0.38	0.31	Good
18	1	4	0.20	0.20	0.20	0.18	Good
18	2	5	0.38	0.38	0.38	0.28	Good
18	5	1	0.20	0.18	0.38	0.33	Good
18	6	2	0.46	0.46	0.46	0.34	Good
20	1	3	0.56	0.53	0.38	0.41	Good
20	2	4	0.64	0.58	0.64	0.56	Good
20	5	7	0.20	0.18	0.20	0.15	Good
20	6	1	0.41	0.31	0.41	0.33	Good
30	1	7	0.28	0.28	0.18	0.15	Good
30	2	8	0.34	0.34	0.31	0.25	Good
30	5	9	0.31	0.28	0.34	0.33	Good
30	6	10	0.08	0.05	0.10	0.08	Good
32	1	9	0.51	0.48	0.41	0.41	Good
32	2	10	0.08	0.05	0.08	0.05	Good
32	5	11	0.13	0.08	0.18	0.15	Good
32	6	8	0.56	0.53	0.51	0.46	Good

* Patch locations shown in Figures 4 and 5

Patch Type:
1 Rokide HT Rod
2 Rokide HT Rod Plus GA-60 Cement
3 Rokide HT Rod Plus Bean H Cement Plus Rokide HT Rod
4 Plasmalloy 331-M Powder
5 Plasmalloy 331-M Powder Plus GA-60 Cement
6 GA-60 Cement (2 Coats)
7 GA-60 Cement (2 Coats) Plus Fiberglas (2 Coats)
8 PLD Cement**
9 Plasmalloy 331-M Powder Plus PLD Cement
10 PLD Cement Plus Fiberglas
11 Rokide HT Rod Plus PLD Cement

**PLD cement is a single-component polyimide adhesive.

APPENDIX F

STRAIN GAGE INSTRUMENTATION INSTALLATION SUMMARY

TABLE F-1

STRAIN GAGE INSTRUMENTATION INSTALLATION SUMMARY

Slot Number	Blade Serial Number	System Type	Blade-Disk Leadwire: Wire Material	Gage	Insulation	Strain Gage Number	Strain Gage Location	Installer and Comments
FIRST STAGE ROTOR								
1	20	6	Chromel/Alumel	28	Duplex Fiberglas/Asbestos	120	A	NASA
2	6	7	Stranded Nickel-Plated Copper	32	Kapton/Teflon	106	B	NASA
3	5	6	Chromel/Alumel	28	Duplex Fiberglas/Asbestos	105	A	NASA
4	19	7	Stranded Nickel-Plated Copper	32	Kapton/Teflon	119	B	NASA
5	14	6	Chromel/Alumel	28	Duplex Fiberglas/Asbestos	114	A	NASA
6	17	5	Stranded Nickel-Plated Copper	32	Kapton/Teflon	117	B	P&WA EP on cc side
7	23	EP						NASA
8	33	EP						NASA
9	26	EP						NASA
10	36	EP						NASA
11	8	EP						NASA
12	38	EP						NASA
13	28	2	Chromel/Alumel	28	Duplex Fiberglas/Asbestos	128	B	P&WA EP on cc side
14	3	5	Stranded Nickel-Plated Copper	32	Kapton/Teflon	103	A	P&WA
15	32	7	Stranded Nickel-Plated Copper	32	Kapton/Teflon	132	B	NASA
16	16	2	Chromel/Alumel	28	Duplex Fiberglas/Asbestos	116	A	P&WA
17	25	EP						NASA
18	18	4	Chromel/Alumel	28	Duplex Fiberglas/Asbestos	118	A	P&WA
19	30	3	Stranded Nickel-Plated Copper	32	Kapton/Teflon	130	B	P&WA EP on cc side
20	1	5	Stranded Nickel-Plated Copper	32	Kapton/Teflon	101	A	P&WA
21	9	EP						NASA
22	35	EP						NASA
23	37	EP						NASA
24	11	EP						NASA
25	21	EP						NASA
26	12	EP						NASA
27	31	6	Chromel/Alumel	28	Duplex Fiberglas/Asbestos	131	A	NASA
28	2	1	Stranded Nickel-Plated Copper	32	Kapton/Teflon	102	B	P&WA EP on cc side
29	27	1	Stranded Nickel-Plated Copper	32	Kapton/Teflon	127	A	P&WA
30	4	4	Chromel/Alumel	28	Duplex Fiberglas/Asbestos	104	B	P&WA EP on cc side
31	29	3	Stranded Nickel-Plated Copper	32	Kapton/Teflon	129	A	P&WA
32	15	1	Stranded Nickel-Plated Copper	32	Kapton/Teflon	115	B	P&WA EP on cc side
33	24	EP						NASA
34	22	EP						NASA
35	10	EP						NASA
36	13	7	Chromel/Alumel	28	Duplex Fiberglas/Asbestos	113	B	NASA
37	34	EP						NASA
38	7	EP						NASA

System type numbers are defined in Table IV.
Location A = Above shroud, trailing edge, concave side
Location B = Above shroud, maximum thickness, convex side
EP = Erosion Patch

TABLE F-1 (Continued)

Slot Number	Blade Serial Number	System Type	Blade-Disk Leadwire: Wire Material	Gage	Insulation	Strain Gage Number	Strain Gage Location	Installer and Comments
THIRD STAGE ROTOR								
1	19	2	Chromel P	36	Uninsulated	319	A	P&WA
2	20	3	Chromel/Alumel	28	Duplex Fiberglas/Asbestos	320	B	P&WA EP on cc side
3	27	4	Chromel P	36	Uninsulated	327	B	P&WA
4	7	1	Chromel/Alumel	28	Duplex Fiberglas/Asbestos	307	B	P&WA EP on cc side
5	11	6	Chromel/Alumel	28	Duplex Fiberglas/Asbestos	311	B	NASA
6	22	6	Chromel/Alumel	28	Duplex Fiberglas/Asbestos	322	B	NASA
7	35	5	Chromel/Alumel	28	Duplex Fiberglas/Asbestos	335	A	P&WA
8	24	1	Chromel/Alumel	28	Duplex Fiberglas/Asbestos	324	A	P&WA
9	38	5	Chromel/Alumel	28	Duplex Fiberglas/Asbestos	338	B	P&WA
10	36	5	Chromel/Alumel	28	Duplex Fiberglas/Asbestos	336	B	P&WA
11	39	6	Chromel/Alumel	28	Duplex Fiberglas/Asbestos	339	B	NASA
12	12	7	Chromel P	36	Uninsulated	312	A	NASA
13	4	4	Chromel P	36	Uninsulated	304	B	P&WA EP on cc side
14	15	3	Chromel/Alumel	28	Duplex Fiberglas/Asbestos	315	A	P&WA
15	16	4	Chromel P	36	Uninsulated	316	B	P&WA EP on cc side
16	30	5	Chromel/Alumel	28	Duplex Fiberglas/Asbestos	330	B	P&WA
17	23	7	Chromel P	36	Uninsulated	323	A	NASA
18	32	3	Chromel/Alumel	28	Duplex Fiberglas/Asbestos	332	B	P&WA EP on cc side
19	25	2	Chromel P	36	Uninsulated	325	B	P&WA
20	2	2	Chromel P	36	Uninsulated	302	B	P&WA EP on cc side
21	37	5	Chromel/Alumel	28	Duplex Fiberglas/Asbestos	337	A	P&WA
22	17	6	Chromel/Alumel	28	Duplex Fiberglas/Asbestos	317	A	NASA
23	5	6	Chromel/Alumel	28	Duplex Fiberglas/Asbestos	305	A	NASA
24	9	3	Chromel/Alumel	28	Duplex Fiberglas/Asbestos	309	B	P&WA EP on cc side
25	1	1	Chromel/Alumel	28	Duplex Fiberglas/Asbestos	301	A	P&WA
26	33	4	Chromel P	36	Uninsulated	333	A	P&WA
27	8	2	Chromel P	36	Uninsulated	308	A	P&WA
28	40	7	Chromel P	36	Uninsulated	340	A	NASA
29	29	7	Chromel P	36	Uninsulated	329	B	NASA
30	13	1	Chromel/Alumel	28	Duplex Fiberglas/Asbestos	313	A	P&WA
31	3	3	Chromel/Alumel	28	Duplex Fiberglas/Asbestos	303	A	P&WA
32	18	1	Chromel/Alumel	28	Duplex Fiberglas/Asbestos	318	B	P&WA EP on cc side
33	31	2	Chromel P	36	Uninsulated	331	A	P&WA
34	6	7	Chromel P	36	Uninsulated	306	B	NASA
35	14	2	Chromel P	36	Uninsulated	314	B	P&WA EP on cc side
36	26	3	Chromel/Alumel	28	Duplex Fiberglas/Asbestos	326	A	P&WA
37	21	4	Chromel P	36	Uninsulated	321	A	P&WA
38	10	4	Chromel P	36	Uninsulated	310	A	P&WA
39	34	7	Chromel P	36	Uninsulated	334	B	NASA
40	28	6	Chromel/Alumel	28	Duplex Fiberglas/Asbestos	328	A	NASA

System type numbers are defined in Table IV.
Location A = Above shroud, trailing edge, concave side
Location B = Above shroud, maximum thickness, convex side
EP = Erosion Patch

APPENDIX G

MANUFACTURERS SUMMARY

BLH Electronics
42 Fourth Avenue
Waltham, Massachusetts 02154

PLD - Single component polyimide adhesive

CER 1000 - Two-component ceramic phosphate cement

CER 1200 - Same as CER 1000 but provides greater mechanical strength and higher operating temperature

Barrier H protective coating

Claude S. Gordon Co.
5710 Kenosha Street
Richmond, Illinois 60071

28-gage Chromel/Alumel duplex wire with Fiberglas-asbestos insulation

Flame Spray Industries
152 Haven Avenue
Port Washington, New York 11050

Powder flame spray equipment

Hitec Corp
Nardone Industrial Park
Westford, Massachusetts 01886

Rokide HT Rod - Ceramic spray rod for strain gage application manufactured by the Norton Company to Hitec specifications

Bean H ceramic cement used in high temperature instrumentation

Powder flame spray equipment

E. I. duPont deNemours & Co (Inc.)
Pigments Department
Wilmington, Delaware 19898

Fybex - Inorganic reinforcing titanate

Hoskins Mfg. Co.
4445 Lawton Avenue
Detroit, Michigan 48208

36-gage uninsulated Chromel P wire

Metco, Inc.
1101 Prospect Avenue
Westbury, New York 11590

Metco 443 - Nickel-chromium-aluminum composite bondcoat for flame sprayed ceramics

Metco 450 - Nickel-aluminum composite bondcoat for flame sprayed ceramics

Metco 105 - White aluminum oxide ceramic powder for erosion patch installations

Micro-Measurements Division
Vishay Intertechnology Inc.
PO Box 306
38905 Chase Road
Romulus, Michigan

RTV - General purpose silicone rubber coating

GA-60 - Epoxy cement for leadwire attachment in high G fields

GA-100 - Ceramic cement for overcoating splice areas

M-600, M-610 - Epoxy cements used to apply strain gages

Mithra Engineering Company
14734 Arminta Street
Van Nuys, California

Mithra 200 - Epoxy cement for leadwire attachment in high G fields

Norton Company
Industrial Ceramics Division
Worcester, Massachusetts 01606

Rokide H, S Rods - Ceramic spray rods for strain gage application

Plasmadyne
Division of Geotel, Inc.
PO Box 1559
Santa Ana, California 92702

Plasmalloy 331-M Powder - Aluminum oxide flame spray powder for strain gage application

Secon Metals Corporation
7 Intervale Street
White Plains, New York 10606

Nichrome V Wire (trademark of Driver Harris)

TeleFlex Incorporated
SermeTel Division
PO Box 187
North Wales, Pennsylvania 19454

SP-1, PBX - Ceramic cements used in high temperature instrumentation

W. B. Driver Co.
PO Box 1467, Hwy 33
Orangeburg, South Carolina 29115

Evanohm Wire

W. L. Gore Associates, Inc.
555 Paper Mill Road
Newark, Delaware 19711

Stranded nickel-plated copper alloy 32-gage wire with Kapton/Teflon insulation

DISTRIBUTION LIST

NASA Lewis Research Center
Attn Raymond Holanda MS 77-1
21000 Brookpark Road
Cleveland, OH 44135 25

NASA Lewis Research Center
Attn John E. Dilley MS 500-305
21000 Brookpark Road
Cleveland, OH 44135 1

NASA Scientific and Technical
Information Facility
Attn Acquisitions Branch
P.O. Box 33

College Park, MD 20740 22

NASA Lewis Research Center
Attn: Library MS 60-3
21000 Brookpark Road
Cleveland, OH 44135 2

NASA Lewis Research Center
Attn: Report Control Off.
MS 5-5
21000 Brookpark Road

Cleveland, OH 44135 1

General Electric Company
Aircraft Engine Group
Attn. Wayne Shaffernocker MSH-78
1 Newman Way

Evendale, OH 45215 1

Air Force Aero Propulsion Lab.
Attn: Joseph Batka/TBC
Wright Patterson Air Force Base
Dayton, OH 45433 1

Air Force Aero Propulsion Lab.
Attn: Everett E. Bailey
Wright Patterson Air Force Base
Dayton, OH 45433 1

Air Force Aero Propulsion Lab.
Attn. Terry M. Trumble/TFI
Chief, Instrument Group
Wright Patterson Air Force Base

Dayton, OH 45433 1

Air Force Aero Propulsion Lab.
Attn: John Horner/TFA
Wright Patterson Air Force Base
Dayton, OH 45433 1

Pratt & Whitney Aircraft
Palm Beach Gardens Facility
Attn: John T. Carroll
Bldg 30 MS R-23

West Palm Beach, FL 33402 1

Pratt & Whitney Aircraft
Palm Beach Gardens Facility
Attn: William Deskin MS R-13
P.O. Box 2691

West Palm Beach, FL 33402 1

General Electric Company
Attn: Richard Handel
Bldg. 262 - Room 209
1 River Road

Schenectady, NY 12345 1

Kulite Semiconductor Products
Attn: John C Kicks
1039 Hoyt Avenue
Ridgefield, NJ 07657 1

Arnold Engineering Development
Center
Attn: Marshall Kingery
Arnold Air Force Station, TN

37389 1

Hitec Corporation
Attn: Steve Wnuk
Nardone Industrial Park
Westford, Mass 01886 1

General Electric Company
Aircraft Engine Group
Attn: George Lapercne A129kD
1000 Western Avenue

Lynn, MASS 01910 1

Teledyne CAE
Attn: R. Hugh Gaylord
1330 Lasked Road
Toledo, OH 43612

Garrett - AiResearch
Attn Robert Olive
P.O. Box 5217
Phoenix, AZ 85010

Battelle Columbus Laboratories
Attn: M. M. Lencoe
505 King Avenue
Columbus, OH 43201

Peter K. Stein
5602 E. Monterosa
Phoenix, AZ 85018

Pratt & Whitney Aircraft
Main Plant
Attn John Prosser MS C-04
P.O Box 2691

West Palm Beach, FL 33402